

INTEGRAL EQUATION METHODS IN THE NUMERICAL SOLUTION OF
BOUNDARY-VALUE PROBLEMS FOR LAPLACE'S EQUATION FOR TWO-DIMENSIONAL
REGIONS BOUNDED BY POLYGONS.

A thesis for the degree of
Master of Philosophy
of the
University of London
by
M.J. HAMSON

(Senior Lecturer in Mathematics, Thames Polytechnic, London S.E.18.)

(Registered at Imperial College of Science and Technology)

September 1978

Abstract

M.J. HAMSON - "Integral equation methods in the numerical solution of boundary-value problems for Laplace's equation for two-dimensional regions bounded by polygons"

Although considerable research has been carried out on the application of integral equation methods in solving two-dimensional Laplace boundary problems, often the occurrence and effect of corner points on the boundary contour is not treated. Accordingly and also with regard to practical problems, this thesis concentrates on the case in which the boundary is polygonal.

In Chapter I it is shown how the interior Dirichlet, Neumann and mixed boundary-value problems may be formulated in terms of integral equations. Use is made of 'single' and 'double' layer potentials, Green's boundary formulae and complex variable methods in the formulations presented, thus allowing for comparisons and relations to be made between these various methods. The systematic treatment given is a particular feature of Chapter I.

The main investigatory work in the thesis is concerned with obtaining the solution of the interior Dirichlet problem through the use of the double layer potential and resulting boundary density function. In Chapter II reference is made in detail to the classical work of Radon in order that the existence of this density and hence the solution of the Dirichlet problem is justified when the boundary of the region possesses corner points. It is recognised that in practice an approximate solution will be necessary and in Chapter III the author proposes three alternatives leading to approximate values of the density based on its replacement as a piecewise constant, linear or quadratic function over some boundary interval. When the polygon is convex it is shown that the calculated density and hence the resulting approximate solution of the problem will converge to their theoretical values for all three of the proposals as the size of the boundary interval decreases to zero.

These methods have been tested on a rectangular region and the results are given in Chapter IV. Comment is made on the suitability of the methods and the accuracy of the results.

Acknowledgements

I would like to express my sincere thanks to my supervisor, Dr.K.E.Pitman of Imperial College of Science and Technology, for his help and guidance during all the many stages of my research work. I much appreciate also his advice concerning the presentation of the material in this thesis.

I would further like to acknowledge the facilities provided by Thames Polytechnic which encouraged the research to be undertaken and also the support of the college Computer Centre in processing the many computer programs.

The thesis was typed by Mrs.E.B. McFall of the School of Mathematics, Statistics and Computing at Thames Polytechnic and I would like to record my thanks to her for this work, particularly in dealing with the many mathematical expressions.

CONTENTS

	Page
Chapter I	
Introduction	5
§ 1.1 The Single Layer Potential	8
§ 1.2 The Potential of the Double Layer	20
§ 1.3 Green's Boundary Formula	38
§ 1.4 Complex Variable methods	44
Summary of integral equation formulations	59
 Chapter II	
Existence Theory for Polygonal Regions	60
 Chapter III	
§ 3.1 Introduction to the numerical analysis	77
§ 3.2 Approximations proposed for the Double Layer Density	80
§ 3.3 Investigation of the Linear Algebra	87
§ 3.4 Convergence	100
§ 3.5 Error in the calculation of the potential function	111
 Chapter IV	
Details of computer programs and comments on the formulation	116
Results Section	122
References	141

Chapter I

Introduction

Many authors have worked successfully to obtain a numerical solution of Laplace's equation in two dimensions by integral equation methods and full references will be acknowledged as appropriate. However the possibility of the boundary not being smooth has sometimes been avoided and thus the particular difficulties associated with corner points not treated. Hence at the outset the following polygonal boundary shape is posed (Fig.1) and the aim of this thesis will be to concentrate on the possible solution of Laplace's equation in the region interior to this boundary.

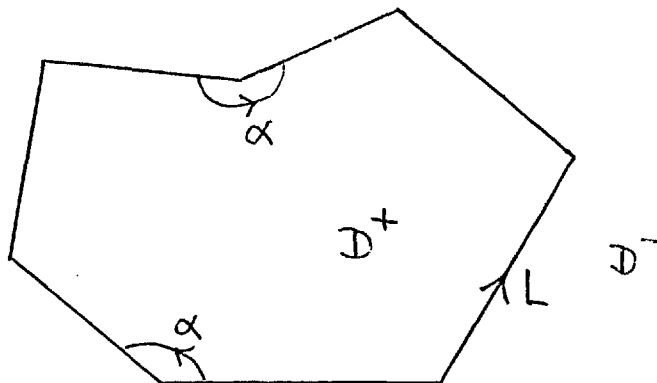
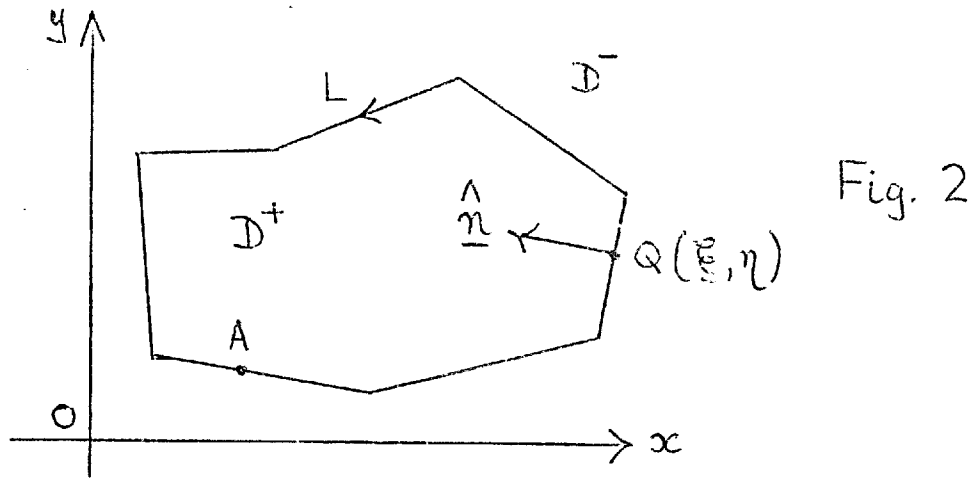


Fig. 1

The possibility of a re-entrant corner at which the interior angle α exceeds π is included so that the polygon can be convex or non-convex. No rounding of corners will be undertaken and so the polygon will always be entirely made up of straight edges. Further, cusp points will be automatically excluded so that $0 < \alpha < 2\pi$.

Along the boundary contour L , s will be used to measure length, beginning from some convenient initial point A which may or may not be a corner point. Denoting the total length of the boundary by S , then $0 \leq s \leq S$. Also the region interior to L will be denoted by D^+ and that exterior by D^- (Fig.2),

the direction of description of L being such that D^+ lies to the left and D^- to the right.



Any point Q on L will have cartesian coordinates $\{\xi(s), \eta(s)\}$, the functions $\xi(s)$ and $\eta(s)$ being piecewise linear due to the polygonal boundary. A normal unit vector $\hat{n} = \hat{n}(s)$ will be taken into D^+ ; \hat{n} will be piecewise constant with a finite discontinuity at each corner point.

With this notation the fundamental potential theory problems in two dimensions for the interior region may be stated:

To find a function u , harmonic within D^+ (i.e. satisfying Laplace's equation $\frac{\partial^2 u}{\partial x^2} + \frac{\partial^2 u}{\partial y^2} = 0$) and continuous in $D^+ + L$ such that either

- (a) $u(s)$ takes prescribed values $f(s)$ on L , (Dirichlet problem);
- or (b) $\frac{\partial u(s)}{\partial n}$ takes prescribed values $g(s)$ on L , (Neumann problem);
- or (c) at each point on L , either $u(s)$ or $\frac{\partial u(s)}{\partial n}$ takes a prescribed value $h(s)$, (mixed boundary value problem)

Throughout, $f(s)$ will be assumed continuous, $g(s)$ and $h(s)$ piecewise continuous (it being impossible to associate $g(s)$ and $h(s)$ with a value of $\frac{\partial u}{\partial n}$ at a corner point).

Each of the problems (a), (b) and (c) will be re-formulated as an integral equation. The question of existence of solutions will be discussed in Chapter II. The corresponding external problems will be referred to only where necessary.

As stated in the Abstract, an effort will be made to give all the integral equation formulations for (a), (b) and (c). Thus 'single' and 'double' layer potentials are discussed as well as the application of Green's formula and complex variable theory.

§1.1 Single Layer Potential

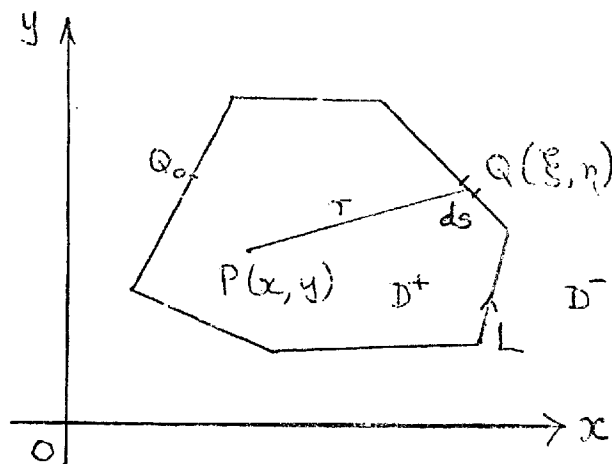


Fig. 3

The electrostatic background to the single layer potential may be found in [1] (page 83). It is shown there that the electrostatic potential at $P(x, y)$ (Fig. 3) due to a line charge at Q is proportional to $\ln(\frac{1}{r})$, where $r = |PQ|$. We require a 'single layer' of such line charges to be placed around L with density $\sigma(s)$ so that the potential at P due to the charge over boundary increment ds can be taken as $\sigma \times (ds) \times \ln(\frac{1}{r})$.

Hence using the principle of superposition, the total potential u at P , u_p , is

$$u_p = u(x, y) = \oint_L \sigma(s) \ln(\frac{1}{r}) ds, \quad P \in D^+ \quad (1.1)$$

Since $P \in D^+$, $\ln(\frac{1}{r})$ is bounded. Hence (1.1) will exist if σ is integrable, and will define a continuous function of position as P moves in D^+ . If σ is allowed to become unbounded the integral will exist as an improper integral provided each $\int_{s_i}^{s_{i+1}} |\sigma(s)| ds$ exists, where $s_i \leq s \leq s_{i+1}$ denotes some interval within which σ is unbounded.

In either case we may differentiate under the integral with

respect to x and y to show that u is harmonic:

$$\begin{aligned}\nabla^2 u_P &= \left(\frac{\partial^2}{\partial x^2} + \frac{\partial^2}{\partial y^2} \right) \oint_L \sigma(s) \ell_n \left(\frac{1}{r} \right) ds \\ &= - \oint_L \frac{\sigma(s)}{2} \left(\frac{\partial^2}{\partial x^2} + \frac{\partial^2}{\partial y^2} \right) \ell_n r^2 ds\end{aligned}$$

But $r^2 = (x - \xi)^2 + (y - \eta)^2$

$$\begin{aligned}\frac{\partial^2}{\partial x^2} (\ell_n r^2) &= \frac{\partial}{\partial x} \cdot \frac{\partial}{\partial x} \ell_n \{ (x - \xi)^2 + (y - \eta)^2 \} \\ &= \frac{\partial}{\partial x} \frac{2(x - \xi)}{(x - \xi)^2 + (y - \eta)^2} \\ &= \frac{\{ (x - \xi)^2 + (y - \eta)^2 \}^2 - 2(x - \xi) \cdot 2(x - \xi)}{\{ (x - \xi)^2 + (y - \eta)^2 \}^2} \\ &= \frac{2(y - \eta)^2 - 2(x - \xi)^2}{r^4}\end{aligned}$$

Hence $\left(\frac{\partial^2}{\partial x^2} + \frac{\partial^2}{\partial y^2} \right) \ell_n r^2 = \frac{2(y - \eta)^2 - 2(x - \xi)^2 + 2(x - \xi)^2 - 2(y - \eta)^2}{r^4} = 0$

so that $\nabla^2 u_P = 0$ as required.

To solve any of the boundary value problems (a), (b) or (c) it is necessary to consider the value of this potential as P approaches a boundary point Q_0 of L at which $s = s_0$. (Fig.3) When P coincides with Q_0 , (1.1) becomes an improper integral since $r \rightarrow 0$ as $Q \rightarrow Q_0$. It is therefore necessary to find whether u_P has a value when $P = Q_0 \in L$ and also whether the limiting value of u_P as $P \rightarrow Q_0$ from D^+ coincides with this value.

Firstly place P at a point Q_0 of L : then clearly the existence or otherwise of the integral (1.1) is determined by the

contribution to the integral given from the neighbourhood of Q_0 .

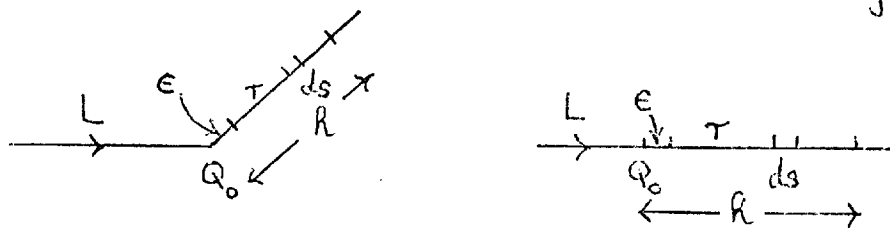


Fig. 4

It is sufficient to consider one side of Q_0 and investigate the value of $I = \lim_{\epsilon \rightarrow 0} \int_{\epsilon}^h \sigma(s) \ln\left(\frac{1}{r}\right) ds$ where without loss s may be measured from Q_0 and h is a suitable small distance (Fig.4). It is clear that Q_0 being a corner point has no effect on the integral I , which can be thought of conveniently as taken along the x axis (Fig.5),

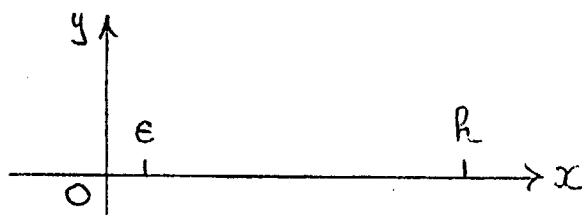


Fig. 5

so that
$$I = \lim_{\epsilon \rightarrow 0} \int_{\epsilon}^h \sigma(x) \ln\left(\frac{1}{x}\right) dx \tag{1.2}$$

Now this integral exists when $\sigma(x)$ is bounded in $[0, h]$ because $\int_0^h \ln\left(\frac{1}{x}\right) dx$ exists.

If $\sigma(x)$ is unbounded, e.g. suppose $\sigma(x)$ behaves as x^α when $x \rightarrow 0^+$, for some constant α , then we may use

$$\int_{\epsilon}^h x^\alpha \ln\left(\frac{1}{x}\right) dx = \left[\frac{x^{\alpha+1}}{\alpha+1} \ln\left(\frac{1}{x}\right) + \frac{x^{\alpha+1}}{(\alpha+1)^2} \right]_{\epsilon}^h$$

and this has a limit when $\epsilon \rightarrow 0$ provided $\alpha > -1$. In both

these situations, the value of I can also be made as small as we please by letting $h \rightarrow 0$.

Returning now to the polygonal contour representation, it follows that when P is placed at some Q_0 on L , where Q_0 may be a corner, then the single layer potential (1.1) possesses a value, notwithstanding a possible singularity at Q_0 in $\sigma(s)$ of the form s^α , $\alpha > -1$. We note also that u_{Q_0} is convergent in the ordinary sense and no 'Principal Value' integrals are necessary.

To complete the investigation on the single layer potential as $P \rightarrow Q_0 \in L$, let P be placed not on L but close to it in D^+ (Fig.6). Then we are interested in $\lim_{P \rightarrow Q_0} u_P$.

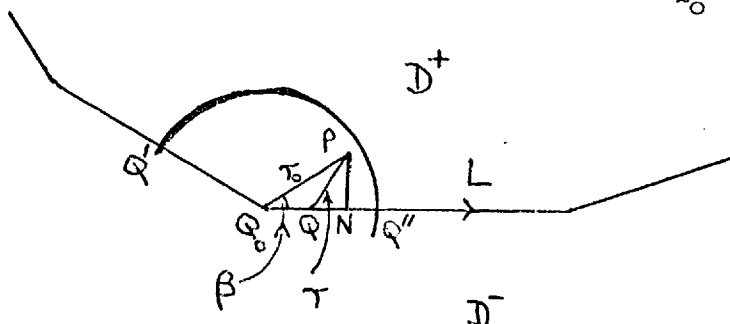


Fig. 6

Construct a circular arc centre Q_0 , radius h , intersecting L at Q' and Q'' and containing P as shown. This divides the boundary L into two parts: $Q'Q_0Q''$ denoted by l , say, and the rest of the boundary denoted by $L - l$. Now take u_P , as defined by (1.1),

$$= \int_L \sigma(s) \ell_n \left(\frac{1}{r} \right) ds \equiv u_P(L) = u_P(l) + u_P(L-l).$$

In Fig.6, Q_0 is placed at a corner point and the boundary l includes a length h to either side of Q_0 . However it is evident that we need only consider the contribution to $u_P(l)$ from Q_0Q''

and there is no need of special considerations for Q_0 at a corner or otherwise.

$$\text{Thus } u_P(Q_0 Q'') = \int_{Q_0 Q''} \sigma(s) \ell_n\left(\frac{1}{r}\right) ds \text{ where } r = PQ.$$

Letting $\rho = |QN|$, then $\rho \leq r$ as Q moves along $Q_0 Q''$

$\therefore \frac{1}{r} \leq \frac{1}{\rho}$ and, assuming that the dimensions of the region are such that $r, \rho, h < 1$ then $\left| \ell_n\left(\frac{1}{r}\right) \right| = \ell_n\left(\frac{1}{r}\right) \leq \ell_n\left(\frac{1}{\rho}\right)$.

$$\text{Hence } \left| u_P(Q_0 Q'') \right| \leq \int_{Q_0 Q''} |\sigma(s)| \left| \ell_n\left(\frac{1}{r}\right) \right| ds \leq \int_{Q_0 Q''} |\sigma(s)| \ell_n\left(\frac{1}{\rho}\right) ds.$$

If $|\sigma(s)| \leq M$ on $Q_0 Q''$ then

$$\begin{aligned} \left| u_P(Q_0 Q'') \right| &\leq M \int_{Q_0 Q''} \ell_n\left(\frac{1}{\rho}\right) ds \leq M \int_0^h \ell_n\left(\frac{1}{x}\right) dx \\ &= M(h - h \ell_n h) \end{aligned}$$

which expression tends to zero as $h \rightarrow 0$.

Further if $\sigma(s)$ has a singularity on $Q_0 Q''$ of type s^α , $-1 < \alpha < 0$ then we can again show that $\left| u_P(Q_0 Q'') \right| \rightarrow 0$ as $h \rightarrow 0$.

Hence we have that $\lim_{h \rightarrow 0} u_P(\ell) = 0$ and, since P always lies within the circular region described, then

$$\lim_{P \rightarrow Q_0} u_P(\ell) = 0. \quad (1.3)$$

But, writing $u_{Q_0} \equiv u_{Q_0}(L) = u_{Q_0}(\ell) + u_{Q_0}(L-\ell)$ then

$$\begin{aligned} u_P(L) - u_{Q_0}(L) &= u_P(\ell) + u_P(L-\ell) - u_{Q_0}(\ell) - u_{Q_0}(L-\ell) \\ &= \{u_P(\ell) - u_{Q_0}(\ell)\} + \{u_P(L-\ell) - u_{Q_0}(L-\ell)\} \\ \left| u_P(L) - u_{Q_0}(L) \right| &\leq \left| u_P(\ell) - u_{Q_0}(\ell) \right| + \left| u_P(L-\ell) - u_{Q_0}(L-\ell) \right| \quad (1.4) \end{aligned}$$

Now from (1.2) and (1.3) we have that $|u_P(\ell)|$ and $|u_{Q_0}(\ell)|$ can both be made arbitrarily small as $h \rightarrow 0$. Hence there is a small positive quantity ϵ such that for $h \leq h_1$, sufficiently small, then $|u_P(\ell) - u_{Q_0}(\ell)| < \frac{1}{2}\epsilon$.

Also $u_P(L-\ell)$ and $u_{Q_0}(L-\ell)$ are proper integrals since $P, Q_0 \notin L-\ell$. Further $u_P(L-\ell) = \int_{L-\ell} \sigma(s) \ell_n(\frac{1}{r}) ds$ is a continuous function of position as P varies and so for $h \leq h_2$, sufficiently small, we have

$$|u_P(L-\ell) - u_{Q_0}(L-\ell)| < \frac{1}{2}\epsilon.$$

Combining these results and substituting into (1.4) gives that for $h \leq \min(h_1, h_2)$ then $|u_P(L) - u_{Q_0}(L)| \leq \frac{1}{2}\epsilon + \frac{1}{2}\epsilon = \epsilon$.

Thus we have that $u_P \rightarrow u_{Q_0}$ as P moves to the boundary point Q_0 on L .

Further analysis can be undertaken to show that in fact u_P , as defined in (1.1), is continuous throughout the entire region $D^+ \cup L \cup D^-$. To summarise in particular, the harmonic function u defined by (1.1) at an internal point P of D^+ by

$$u_P = \oint_L \sigma(s) \ell_n(\frac{1}{r}) ds \tag{1.5}$$

is continuous up to the boundary L , and

$$\lim_{P \rightarrow Q_0} u_P = u_{Q_0} = \oint_L \sigma(s) \ell_n(\frac{1}{r}) ds \tag{1.6}$$

Hence problem (a), the Dirichlet problem, can be solved by treating (1.6) as an integral equation for the unknown boundary density $\sigma(s)$, since for (a), u_{Q_0} will be given equal to $f(s_0)$.

Having evaluated $\sigma(s)$, we return to (1.5) and insert $\sigma(s)$ to generate u_p for any required position of P .

The integral equation formulation of the Neumann problem using the potential of the single layer will now be considered.

As given in (1.1) and (1.5), $u_p = u(x,y)$ is a function of position and so may be differentiated with respect to some direction \hat{n}_o (Fig.7). We choose the direction \hat{n}_o deliberately to be that of the normal at some boundary point N (not a corner point). The differentiation could be undertaken with respect to any direction, but \hat{n}_o is selected so that the result may be used to solve the Neumann problem.

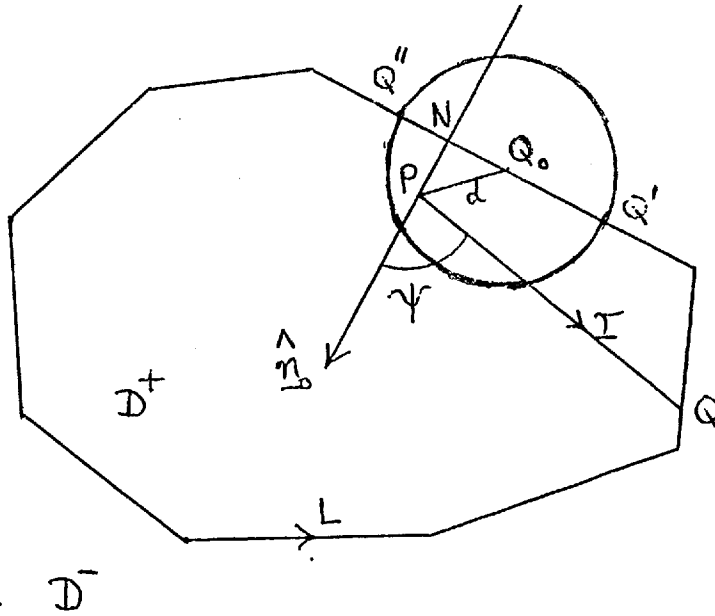


Fig. 7

$$\begin{aligned} \frac{\partial u_p}{\partial n_o} &= \frac{\partial}{\partial n_o} \oint_L \sigma(s) \ell_n\left(\frac{1}{r}\right) ds \\ &= \oint_L \sigma(s) \frac{\partial}{\partial n_o} \ell_n\left(\frac{1}{r}\right) ds . \end{aligned}$$

$$\text{But } \frac{\partial}{\partial n_0} \ell_n\left(\frac{1}{r}\right) = \frac{d}{dr} \ell_n\left(\frac{1}{r}\right) \frac{\partial r}{\partial n_0} = -\frac{1}{r} \frac{\partial r}{\partial n_0} = \frac{1}{r} \cos \psi ,$$

where $\psi = (\hat{r}, \hat{n}_0)$ is the angle made by the vectors \hat{n}_0 and \hat{r} ,
 $0 \leq \psi \leq \pi$. (By studying infinitesimals we obtain $\frac{\partial r}{\partial n_0} = -\cos \psi$)

$$\therefore \frac{\partial u}{\partial n_0} = \oint_L \sigma(s) \frac{\cos \psi}{r} ds \quad (1.7)$$

Now we want to find the value of $\frac{\partial u}{\partial n_0}$ as P approaches the boundary point Q_0 , Q_0 being taken distinct from N so that P does not approach along a normal (Fig.7). In order to investigate the limit construct a circle centre Q_0 radius h and place P inside this circle at distance d from Q_0 . Suppose that the circle intersects the straight edge of L that contains Q_0 in two points Q', Q'' along a diameter, assuming the circle is small enough for this to be the case. As before we denote that part of L between Q' and Q'' (including the points Q', Q'' themselves) by ℓ and denote the rest of the contour by $L-\ell$.

$$\begin{aligned} \text{Then } \lim_{P \rightarrow Q_0} \frac{\partial u}{\partial n_0} &= \lim_{P \rightarrow Q_0} \oint_L \sigma(s) \frac{\cos \psi}{r} ds \quad \text{from (1.7)} \\ &= \lim_{P \rightarrow Q_0} \int_{\ell} + \lim_{P \rightarrow Q_0} \int_{L-\ell} \equiv A + B . \end{aligned}$$

Consider A : this integral is taken over $Q'Q''$ and can be put in the form $\int \sigma(s_0 + d \cos \alpha + x) \frac{\cos \psi}{r} dx$,

where $s = s_0$ at Q_0 , $x = NQ$ measured from origin N and

$$\alpha = \widehat{PQ_0Q''}.$$

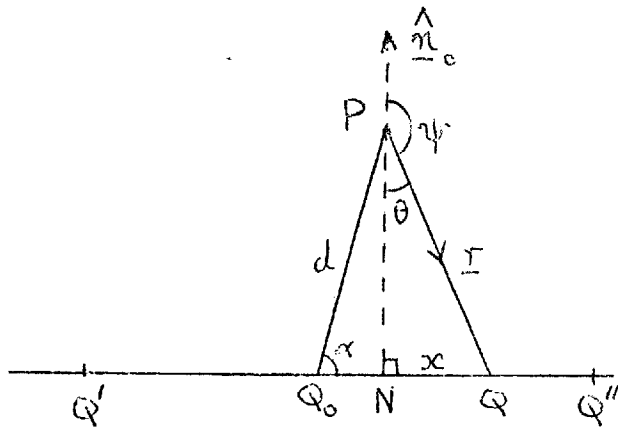


Fig 8

With $\theta = \widehat{NPQ} = \pi - \psi$ then the contribution to the integral from NQ'' over which $x, \theta \geq 0$ can be evaluated:-

$$\cos \psi = -\cos \theta = -\frac{d \sin \alpha}{r}$$

and $x = d \sin \alpha \tan \theta$

$$dx = d \sin \alpha \sec^2 \theta d\theta$$

$$\therefore \int_N^{Q''} \equiv \int \sigma(s_0 + d \cos \alpha + d \sin \alpha \tan \theta) \cdot -\frac{d \sin \alpha}{r^2} d \sin \alpha \sec^2 \theta d\theta$$

But from $r \cos \theta = d \sin \alpha$ we have $\frac{d^2 \sin^2 \alpha \sec^2 \theta}{r^2} = 1$

$$\therefore \int_N^{Q''} \equiv -\int \sigma(s_0 + d \cos \alpha + d \sin \alpha \tan \theta) d\theta \quad (1.8)$$

If we assume now that σ can be expanded about Q_0 so that

$$\sigma(s_0 + d \cos \alpha + d \sin \alpha \tan \theta) = \sigma(s_0) + d(\cos \alpha + \sin \alpha \tan \theta) \sigma'(s_0 + s_1),$$

$$d \cos \alpha < s_1 < Q_0 Q''$$

then (1.8) becomes $-\sigma(s_0) \widehat{NPQ''} - O(d)$.

Similar analysis gives the contribution $\int_{Q'}^N = -\sigma(s_0) \widehat{Q'PN} - O(d)$

Hence A becomes $-\sigma(s_0) \widehat{Q'PQ''} - O(d)$ so that as

$$P \rightarrow Q_0, d \rightarrow 0, \widehat{Q'PQ''} \rightarrow \pi \quad \text{and we are left with} \quad -\pi \sigma(s_0).$$

$$\text{Consider B : } \int_{L-l} \sigma(s) \frac{\cos \psi}{r} ds.$$

This time r is never zero; also as $P \rightarrow Q_0$ it can be seen that for that part of $L-\ell$ which is made up of the straight edge containing Q_0 , $\psi \rightarrow \pi/2$ and so $\cos\psi \rightarrow 0$.

i.e. $\int_{L-\ell}$ only has a contribution from the contour distant

from Q_0 and so it is well defined and finite.

Hence we have the result as follows:-

$$\lim_{P \rightarrow Q_0} \frac{\partial u_P}{\partial n_0} = \frac{\partial u_{Q_0}}{\partial n_0} = -\pi \sigma(s_0) + \int_{L-\ell} \frac{\sigma(s) \cos \psi ds}{r}$$

$$\text{i.e. } \frac{\partial u_{Q_0}}{\partial n_0} = -\pi \sigma(s_0) + \oint_L \frac{\sigma(s) \cos(\hat{r}, \hat{n}_0) ds}{r} \quad (1.9)$$

the latter integral now known to exist in the ordinary sense. This result provides a method for solving the internal Neumann problem in which the normal derivative of a harmonic function is given on L with the corners excepted. The equation (1.9) is an integral equation for the determination of $\sigma(s)$ given values for

$\frac{\partial u_{Q_0}}{\partial n_0} = g(s)$ on L at points Q_0 which are not corners. Having

obtained its solution, then $\sigma(s)$ would be substituted back into the single layer potential $u_P = \oint_L \sigma(s) \ln\left(\frac{1}{r}\right) ds$ and values of

u_P generated accordingly.

As the normal derivative of u would have two differing limiting values either side of a corner point and would be undefined at a corner then (1.9) would be applied only at non-corner points Q_0 .

The limiting value of $\oint_L \frac{\sigma(s) \cos \psi ds}{r}$ could be investigated as

P approaches a corner point but the value would depend on the way P approached Q_0 .

Finally to solve the mixed boundary value problem, the single layer potential can be used in conjunction with its normal derivative to form a pair of coupled integral equations:-

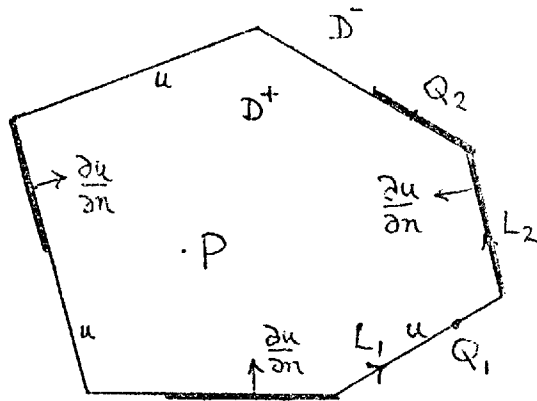


Fig. 9

The boundary L will now be divided into two parts L_1 and L_2 where on L_1 values of u are prescribed and on L_2 values of $\frac{\partial u}{\partial n}$ prescribed, (except at corners of L_2).

On L_1 , at a typical point Q_1 we take the boundary value of the single layer potential

$$u_{Q_1} = \oint_{L_1 + L_2} \sigma(s) \ell_n\left(\frac{1}{r}\right) ds ; \quad (1.10)$$

while on L_2 at a typical point Q_2 we take the boundary value of the internal normal derivative of the single layer

$$\frac{\partial u_{Q_2}}{\partial n} = \oint_{L_1 + L_2} \frac{\sigma(s) \cos(\underline{r}, \underline{n}) ds}{r} - \pi \sigma(s_{Q_2}) \quad (1.11)$$

Now as Q describes L it becomes in turn a point of type Q_1 , then Q_2 then Q_1 again etc. so that the left hand sides of (1.10) and (1.11) will be known taking up values of the prescribed boundary function $h(s)$. The above equations are integral equations for the determination of the density function $\sigma(s)$ and may be taken together and solved numerically for $\sigma(s)$.

Discussion of the numerical methods is given in Chapter III but suffice here to state that an approximate solution of (1.10), (1.11) would be possible by replacing them by a set of linear equations for $\sigma(s_i)$ where s_i are suitable node points around L placed on both L_1 and L_2 . The 'right hand side' of these linear equations would be alternatively u_{Q_1} then $\frac{\partial u_{Q_2}}{\partial n}$ and would take up the prescribed boundary value $h(s)$. Having obtained a solution $\sigma(s_i)$ then the potential function would be generated in D^+ by numerical evaluation of

$$u_p = \int_L \sigma(s) \ln\left(\frac{1}{r}\right) ds .$$

The three fundamental boundary problems having been posed as integral equations in terms of the potential of the single layer, we pass now to a similar investigation in terms of the potential of the double layer.

§ 1.2 The Potential of the Double Layer

As in the case of the single layer, consider first the electrostatic potential at a point due to two equal and opposite parallel line charges. When these line charges are brought into proximity they will constitute the two-dimensional dipole:

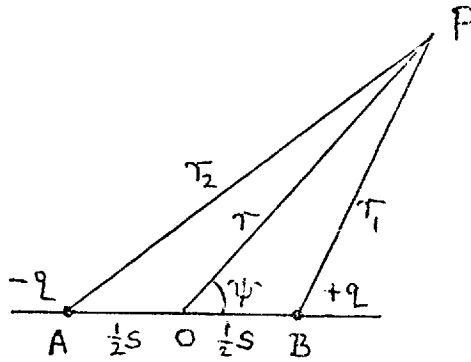


Fig. 10

The potential due to a single line charge +q at distance r is given by $-2q \ell_n r$. Hence in the system displayed in Fig.10, the potential at P

$$\begin{aligned} u_P &= -2q \ell_n r_1 + 2q \ell_n r_2 \\ &= q \ell_n \left(\frac{r_2}{r_1} \right) \\ &= q \ell_n \left\{ \frac{r^2 + \left(\frac{1}{2}s\right)^2 + 2r\left(\frac{s}{2}\right) \cos \psi}{r^2 + \left(\frac{1}{2}s\right)^2 - 2r\left(\frac{s}{2}\right) \cos \psi} \right\} \end{aligned}$$

Now remembering that the line charges at A and B are to be brought close together, this expression is expanded in powers of s

$$\begin{aligned} u_P &= q \ell_n \left\{ \left(r^2 + \frac{1}{4}s^2 + rs \cos \psi \right) \cdot \frac{1}{r^2} \cdot \left(1 + \frac{s^2 - 4rs \cos \psi}{4r^2} \right)^{-1} \right\} \\ &= q \ell_n \left\{ \left(r^2 + \frac{1}{4}s^2 + rs \cos \psi \right) \cdot \frac{1}{r^2} \cdot \left(1 - \frac{s^2 - 4rs \cos \psi}{4r^2} + O(s^2) \right) \right\} \\ &= q \ell_n \left\{ \left(1 + \frac{s \cos \psi}{r} + O(s^2) \right) \left(1 + \frac{s \cos \psi}{r} + O(s^2) \right) \right\} \end{aligned}$$

Retaining only first degree terms in s , this reduces to

$$u_p = 2q \ln\left(1 + \frac{s \cos \psi}{r}\right) = 2q \left\{ \frac{s \cos \psi}{r} + O(s^2) \right\}.$$

Now to obtain the mathematical dipole potential let $s \rightarrow 0$ and $q \rightarrow \infty$ in such a way that the quantity $2qs$ tends to a finite quantity μ , called the dipole moment.

$$u_p = \frac{\mu \cos \psi}{r}.$$

Further, the potential of any number of dipoles is obtained by adding. Hence for a distribution of dipoles along some contour L , the direction of the dipoles always being normal to the contour, we can take

$$u_p = \oint_L \frac{\mu(s) \cos \psi}{r} ds \quad (1.12)$$

where $\mu = \mu(s)$ is now the moment density and $\psi = (\hat{r}, \hat{n})$ is the angle between the vector \underline{r} and the inward normal \hat{n} as before (Fig.11).

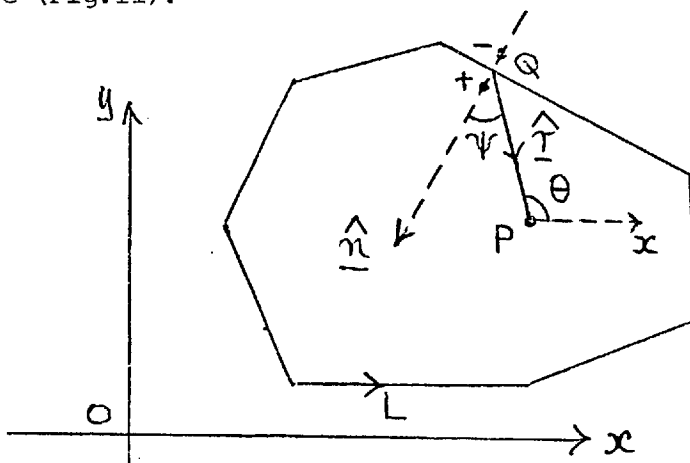


Fig. 11

The expression (1.12) may also be stated in terms of $\ln(\frac{1}{r})$ since

$$\frac{\partial}{\partial n} \ln\left(\frac{1}{r}\right) = \frac{d}{dr} \ln\left(\frac{1}{r}\right) \frac{\partial r}{\partial n} = \frac{1}{r} \cos \psi. \quad (1.13)$$

$$u_p = \oint_L \frac{\mu(s) \cos \psi}{r} ds = \oint_L \mu(s) \frac{\partial}{\partial n} \left(\ln \frac{1}{r} \right) ds \quad (1.14)$$

We may also verify directly that u_p is a potential function.

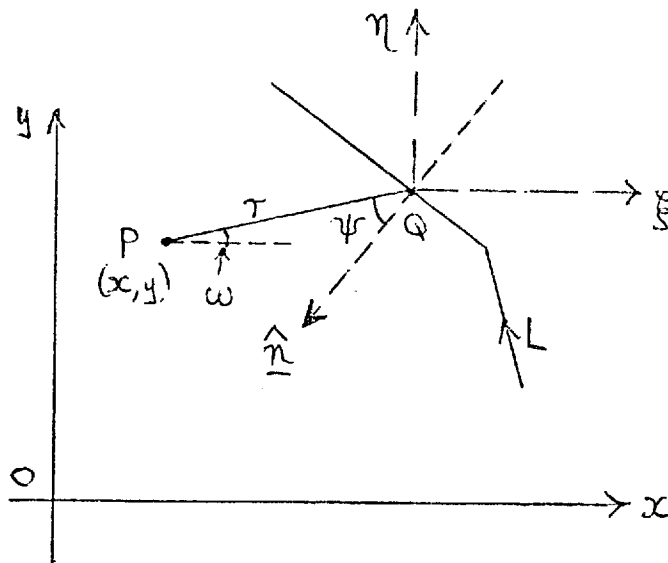


Fig. 12

Consider $\nabla^2 = \frac{\partial^2}{\partial x^2} + \frac{\partial^2}{\partial y^2}$ operating on

$$\ell_n \frac{1}{r} = -\frac{1}{2} \ell_n \left\{ (x-\xi)^2 + (y-\eta)^2 \right\}. \text{ Then we easily get}$$

$\nabla^2 \ell_n \frac{1}{r} = 0$. But the partial derivative of $\ell_n \frac{1}{r}$ with respect to the direction ξ will also be harmonic i.e. $\nabla^2 \frac{\partial}{\partial \xi} \ell_n \left(\frac{1}{r} \right) = 0$ since the order of differential operators may be interchanged to give

$$\frac{\partial}{\partial \xi} \nabla^2 \ell_n \frac{1}{r} = 0.$$

Similarly $\frac{\partial}{\partial \eta} \ell_n \left(\frac{1}{r} \right)$ is also harmonic.

Now consider the expression $\frac{\partial}{\partial n} \ell_n \frac{1}{r}$:-

First $\frac{\partial}{\partial n} = \frac{\partial}{\partial \xi} \frac{\partial \xi}{\partial n} + \frac{\partial}{\partial \eta} \frac{\partial \eta}{\partial n}$ so that $\frac{\partial}{\partial n} \ell_n \frac{1}{r}$ is the sum of two known harmonic terms, $\frac{\partial \xi}{\partial n}$ and $\frac{\partial \eta}{\partial n}$ being constants for a particular \hat{n} .

Hence by (1.13) $\frac{\partial}{\partial n} \left(\ell_n \frac{1}{r} \right) = \frac{\cos \psi}{r}$ is a harmonic function of the variables (x, y) .

Now introduce an arbitrary function $\mu(s)$ defined on L where s is a measurement of arc length along L and consider

the expression

$$u_P = \oint_L \mu(s) \frac{\partial}{\partial n} \left(\ell_n \frac{1}{r} \right) ds = \oint_L \frac{\mu(s) \cos \psi}{r} ds ,$$

where $\mu(s)$ is chosen so that the integral exists.

$$\text{Then } \nabla^2 u_P = \nabla^2 \oint_L \mu(s) \frac{\partial}{\partial n} \left(\ell_n \frac{1}{r} \right) ds = \oint_L \mu(s) \cdot \nabla^2 \frac{\partial}{\partial n} \left(\ell_n \frac{1}{r} \right) ds = 0$$

$$\therefore u_P = \oint_L \frac{\mu(s) \cos \psi}{r} ds \quad \text{defines a function harmonic in } D^+ .$$

Further we may write $ds \cos \psi = r d\theta$ where θ is the angle made by QP with some fixed direction.

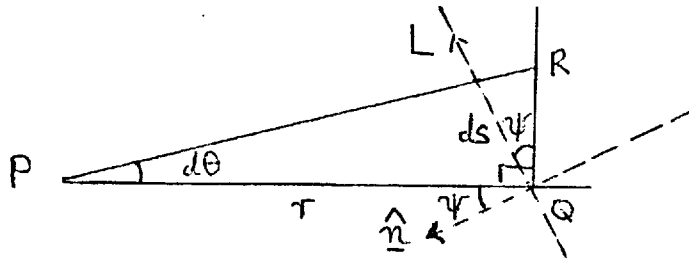


Fig. 13

(For in Fig.13, to the first order smallness $QR = r d\theta = ds \cos \psi$).

$$\therefore u_P = \oint_L \mu(s) d\theta \quad \text{which is often more convenient than the two}$$

earlier forms.

Thus we have, for P not on L, that

$$u_P = \oint_L \frac{\mu(s) \cos \psi}{r} ds \tag{1.15}$$

$$= \oint_L \mu(s) \frac{\partial}{\partial n} \ell_n \left(\frac{1}{r} \right) ds \tag{1.16}$$

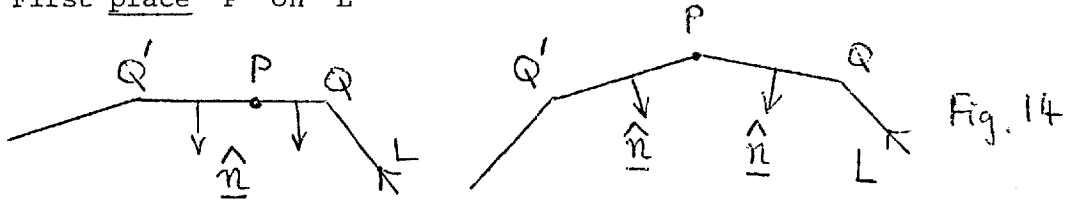
$$= \oint_L \mu(s) d\theta \tag{1.17}$$

gives the value at P of a function harmonic throughout D^+ .

The notation and sign conventions are in line with those of the single layer potential.

Now u_p is defined for all $P \notin L$ but if P lies on L or approaches L from D^+ then the value of u_p must be investigated.

First place P on L



Then with reference to the diagrams in which P may be on a straight edge or at a corner, we consider the contributions to u_p as Q describes the complete polygon. Clearly only those edges of L which contain P will need investigation since for the rest of the polygonal contour Q is distant from P and thus the integrand is well behaved.

Hence we examine $\int_{QPQ'} \frac{\mu(s) \cos \psi}{r} ds$ with QPQ' as shown in

the above diagrams.

Now in fact, the integral $\int_{QPQ'}$ will be zero in both cases

from examination of either (1.15) or (1.17). In the first instance as Q moves towards P along the straight line we have $\psi = \frac{\pi}{2}$

and so $\cos \psi \equiv 0$; and in the second instance $d\theta \equiv 0$ as Q moves towards P since no change will occur in $\angle QP_x$. (Fig.11)

Hence u_p exists when P is situated on L either on a straight edge or at a corner.

However this will not imply that u_p is necessarily continuous as P passes through L from D^+ into D^- . This is now discussed:-

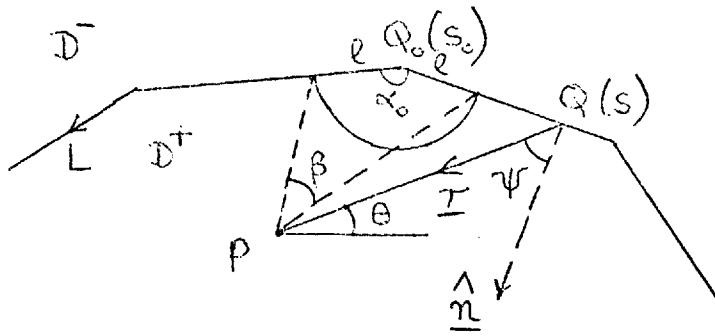


Fig. 15

Let $P \rightarrow Q_0$ on L where Q_0 will be taken at a corner.

Instead of investigating u_P given by (1.15) (1.16) (1.17) directly, it is convenient to consider the limiting value of the modified double layer potential w_P , where

$$w_P = \oint_L \{ \mu(s) - \mu(s_0) \} d\theta = \oint_L \{ \mu(s) - \mu(s_0) \} \frac{\cos \psi}{r} ds .$$

Suppose $\mu(s)$ is continuous on L so that there exists a part e of L around Q_0 upon which

$$| \mu(s) - \mu(s_0) | \leq \epsilon \quad \text{for an arbitrarily chosen } \epsilon .$$

Then consider $w_P = \oint_L \equiv \oint_e + \int_{L-e} = w_1(P) + w_2(P) .$

Then $w_1(P) = \int_e \{ \mu(s) - \mu(s_0) \} d\theta .$

$$\therefore |w_1| \leq \int_e | \mu(s) - \mu(s_0) | d\theta \leq \epsilon \int_e d\theta = \epsilon \beta . \text{ (see Fig. 15)}$$

$$\begin{aligned} \text{Now } w_P - w_{Q_0} &= w_1(P) + w_2(P) - w_1(Q_0) - w_2(Q_0) \\ &= w_1(P) - w_1(Q_0) + w_2(P) - w_2(Q_0) . \end{aligned}$$

$$\therefore |w_P - w_{Q_0}| \leq |w_1(P)| + |w_1(Q_0)| + |w_2(P) - w_2(Q_0)| .$$

But $|w_1(P)| \leq \epsilon \beta$ and $w_1(Q_0)$ is zero .

$$\therefore |w_P - w_{Q_0}| \leq \epsilon \beta + |w_2(P) - w_2(Q_0)| .$$

Now $W_2(P)$ and $W_2(Q_0)$ are integrals taken over $L-\ell$ and so do not possess a singularity since P and Q_0 do not lie on $L-\ell$.

Also w_P will be a continuous harmonic function for any "arc" such as $L-\ell$ and so we may make

$|W_2(P) - W_2(Q_0)| \leq \epsilon'$, for any arbitrarily chosen positive ϵ' , by taking P sufficiently close to Q_0 .

Finally $|w_P - w_{Q_0}| \leq \epsilon\beta + \epsilon' = \epsilon''$ say, so that for all P sufficiently close to Q_0 , $|w_P - w_{Q_0}| \leq \epsilon''$ and w_P is continuous as P passes through the corner point Q_0 . Similarly w_P will be continuous across the boundary at Q_0 when Q_0 is not a corner point, the only change to the above being that β is replaced by π .

However to return now to the potential of the double layer given in

the form $u_P = \oint_L \mu(s) d\theta$:-

We have $w_P = \oint_L \{\mu(s) - \mu(s_0)\} d\theta$ is continuous across L .

Now write $w_P = \oint_L \mu(s) d\theta - \oint_L \mu(s_0) d\theta = u_P - \oint_L \mu(s_0) d\theta$

and suppose that P is placed at Q on L ; then

$$w_Q = u_Q - \oint_L \mu(s_0) d\theta(Q) \text{ where it is already known}$$

that u_Q exists. But $\oint_L \mu(s_0) d\theta = \mu(s_0) \oint_L d\theta = \pi \mu(s_0)$ in

this case assuming that Q is not a corner point.

$$w_Q = u_Q - \pi \mu(s_0). \tag{1.18}$$

Suppose, further, that P is now placed at Q_0 on L , a corner

point, then

$$w_{Q_0} = u_{Q_0} - \oint_L \mu(s_0) d\theta(Q_0) \text{ where again } u_{Q_0} \text{ is known}$$

to exist.

But this time $\oint_L \mu(s_0) d\theta = \alpha_0 \mu(s_0)$ where α_0 is the internal

angle at the corner Q_0 (see Fig.15)

$$w_{Q_0} = u_{Q_0} - \alpha_0 \mu(s_0) \quad (1.19)$$

Let $Q \rightarrow Q_0$ along L . We know that w is continuous everywhere so as $Q \rightarrow Q_0$, $w_Q \rightarrow w_{Q_0}$.

$$u_Q - \pi \mu(s) \rightarrow u_{Q_0} - \alpha_0 \mu(s_0)$$

$\therefore u_Q$ possesses a discontinuity of amount $(\pi - \alpha_0) \mu(s_0)$

as it passes along L through a corner point; otherwise it will be continuous along L .

But when $P \in D^+$, $w_P = u_P - \mu(s_0) \oint_L d\theta(P) = u_P - 2\pi \mu(s_0)$.

Now let $P \rightarrow Q_0$ (from within D^+), then $w_P \rightarrow w_{Q_0}$ since w is continuous everywhere.

$$\text{Using (1.19) this gives } u_{Q_0}^+ - 2\pi \mu(s_0) = u_{Q_0} - \alpha_0 \mu(s_0)$$

$$\text{or } u_{Q_0}^+ = (2\pi - \alpha_0) \mu(s_0) + u_{Q_0} \quad (1.20)$$

where $u_{Q_0}^+$ is the limiting value of u_P as $P \rightarrow Q_0$ from the

interior D^+ and u_{Q_0} is the value of u_P when P is placed on

the boundary at Q_0 which may or may not be a corner. Hence we have the solution of the Dirichlet problem (a), by means of the double layer potential:

Given $f(s_0) = u_{Q_0}^+$ on the boundary, (1.20) is an integral

equation for the determination of the double layer density $\mu(s)$.

Having obtained its value, the required potential may be generated

at any internal point P from the equations (1.15), (1.16) or (1.17).

The Neumann Problem by Double Layer Potentials will now be considered.

Although certain authors, [2] and [3] refer to the normal derivative of the potential of the double layer close to a boundary of a region, the resulting integral equation and its use in solving the Neumann problem seem to have been neglected. An investigation is given below:-

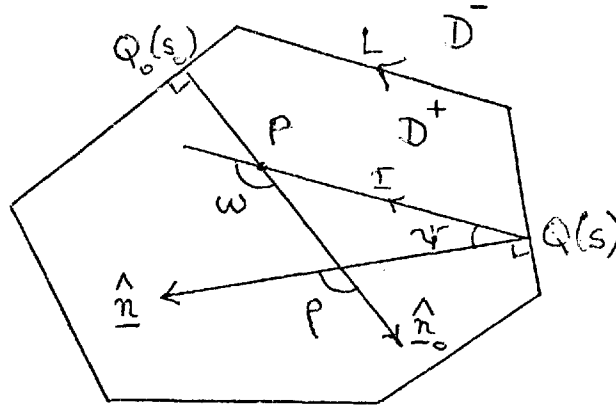


Fig. 16

We have, as above, from (1.15)

$$u_P = \oint_L \frac{\mu(s) \cos \psi}{r} ds .$$

Consider the derivative with respect to the direction \hat{n}_0 , this being the normal at $Q_0(s_0)$ (Fig.16). Then we shall be interested in the value of the derivative as $P \rightarrow Q_0$ in order that the Neumann problem can be treated.

$$\frac{\partial u_P}{\partial n_0} = \frac{\partial}{\partial n_0} \oint_L \frac{\mu(s) \cos \psi}{r} ds = \oint_L \mu(s) \frac{\partial}{\partial n_0} \left(\frac{\cos \psi}{r} \right) ds .$$

Whereas on taking the derivative of the single layer a term

$\frac{\partial}{\partial n_0} \left(\frac{1}{r} \right)$ is encountered ; on this occasion a function of two

(plane) variables r, ψ is to be differentiated.

As the relative positions of P, Q, Q_0 can obscure the result it is convenient to proceed using vector methods:

$$\begin{aligned}
 \frac{\partial}{\partial n_0} \left(\frac{\cos \psi}{r} \right) &= \hat{n}_0 \cdot \nabla \left(\frac{r \cos \psi}{r^2} \right) = \hat{n}_0 \cdot \nabla \left(\frac{\underline{r} \cdot \hat{n}}{r^2} \right) \\
 &= \hat{n}_0 \cdot \left\{ -\frac{2}{r^3} \underline{r} (\underline{r} \cdot \hat{n}) + \frac{1}{r^2} \text{grad} (\underline{r} \cdot \hat{n}) \right\} \\
 &= \frac{-2(\hat{n}_0 \cdot \underline{r})(\hat{n} \cdot \underline{r})}{r^2} + \frac{\hat{n}_0 \cdot \hat{n}}{r^2} \\
 &= \frac{\hat{n} \cdot \hat{n}_0}{r^2} - \frac{2(\hat{n}_0 \cdot \underline{r})(\hat{n} \cdot \underline{r})}{r^2} \\
 &= \frac{\cos \rho - 2 \cos \omega \cos \psi}{r^2} \tag{1.21}
 \end{aligned}$$

where $\rho = (\hat{n}, \hat{n}_0)$, $\omega = (\underline{r}, \hat{n}_0)$ and $\psi = (\underline{r}, \hat{n})$.

In order to investigate the limiting value of $\frac{\partial^{u_P}}{\partial n_0}$ as P approaches the contour edge, it is convenient to consider, as in the case of the ordinary double layer potential, the modified potential.

$$w_P = \oint_L \{ \mu(s) - \mu(s_0) \} \frac{\cos \psi}{r} ds \text{ where } s_0 \text{ is the}$$

arc parameter of Q_0 , the point to which P is approaching.

Provided that $P \in D^+$, the derivative with respect to n_0 direction may be taken so that

$$\frac{\partial w_P}{\partial n_0} = \oint_L \{ \mu(s) - \mu(s_0) \} \frac{\partial}{\partial n_0} \left(\frac{\cos \psi}{r} \right) ds$$

Now consider

$$\lim_{P \rightarrow Q_0} \left(\frac{\partial w_P}{\partial n_0} \right) = \lim_{P \rightarrow Q_0} \oint_L \{ \mu(s) - \mu(s_0) \} \frac{\partial}{\partial n_0} \left(\frac{\cos \psi}{r} \right) ds \tag{1.22}$$

Care is necessary as these limits are investigated, for it will be shown that where as the limit of the composite term on the RHS exists and is equal to its value when P is placed at Q_0 , the

limits of the separate parts do not have this property :-

when P is placed at Q_0 both $\oint_L \mu(s) \frac{\partial}{\partial n_0} \left(\frac{\cos \psi}{r} \right) \Big|_{Q_0} ds$ and

$$\oint_L \mu(s_0) \frac{\partial}{\partial n_0} \left(\frac{\cos \psi}{r} \right) \Big|_{Q_0} ds \text{ diverge.}$$

Provided the limits exist,

$$\begin{aligned} & \lim_{P \rightarrow Q_0} \oint_L \{ \mu(s) - \mu(s_0) \} \frac{\partial}{\partial n_0} \left(\frac{\cos \psi}{r} \right) ds \\ &= \lim_{P \rightarrow Q_0} \oint_L \mu(s) \frac{\partial}{\partial n_0} \left(\frac{\cos \psi}{r} \right) ds - \lim_{P \rightarrow Q_0} \oint_L \mu(s_0) \frac{\partial}{\partial n_0} \left(\frac{\cos \psi}{r} \right) ds \quad (1.23) \end{aligned}$$

$$\text{But } \lim_{P \rightarrow Q_0} \oint_L \mu(s_0) \frac{\partial}{\partial n_0} \left(\frac{\cos \psi}{r} \right) ds, \quad P \in D^+,$$

$$= \lim_{P \rightarrow Q_0} \mu(s_0) \oint_L \frac{\partial}{\partial n_0} \left(\frac{\cos \psi}{r} \right) ds = \lim_{P \rightarrow Q_0} \mu(s_0) \frac{\partial}{\partial n_0} \oint_L \frac{\cos \psi}{r} ds$$

and $\oint_L \frac{\cos \psi}{r} ds = 2\pi$ since this integral is the "two dimensional

solid angle" obtained from the relation $\frac{\cos \psi}{r} ds \equiv d\theta$

$$\therefore \frac{\partial}{\partial n_0} \oint_L \frac{\cos \psi}{r} ds = 0 \text{ for all } P \in D^+ \text{ so (1.23) reduces to}$$

$$\lim_{P \rightarrow Q_0} \oint_L \mu(s) \frac{\partial}{\partial n_0} \left(\frac{\cos \psi}{r} \right) ds = \lim_{P \rightarrow Q_0} \oint_L \{ \mu(s) - \mu(s_0) \} \frac{\partial}{\partial n_0} \left(\frac{\cos \psi}{r} \right) ds \quad (1.24)$$

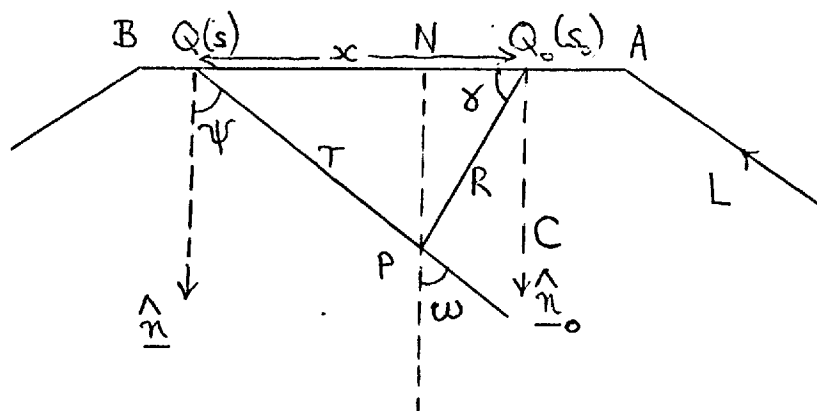
We show that the limit of the term on the right hand side as P approaches Q_0 exists and takes the value obtained if P were merely placed at Q_0 .

Let P approach $Q_0(s_0)$ along a line inclined at angle δ to the boundary edge on which Q_0 lies (Fig.17), as was attempted

for the single layer Neumann problem. Although the limit may exist when Q_0 is a corner, the normal derivative of u does not and so the limiting value would be of no help in solving the problem. The angles $\rho = (\hat{n}, \hat{n}_0)$, $\psi = (\hat{r}, \hat{n})$ and $\omega = (\hat{r}, \hat{n}_0)$ (Fig.16) are related by elementary triangle geometry such that $\omega = \rho + \psi$ for any position of P, Q, Q_0 when the polygon is convex. However to maintain the generality of the results it is more convenient to work with $\frac{\partial}{\partial n_0} \left(\frac{\cos \psi}{r} \right)$.

Now from (1.24), we are interested in

$$\begin{aligned} \lim_{P \rightarrow Q_0} \frac{\partial u_P}{\partial n_0} &= \lim_{P \rightarrow Q_0} \oint_L \mu(s) \frac{\partial}{\partial n_0} \left(\frac{\cos \psi}{r} \right) ds = \lim_{P \rightarrow Q_0} \oint_L \{ \mu(s) - \mu(s_0) \} \frac{\partial}{\partial n_0} \left(\frac{\cos \psi}{r} \right) ds \\ &= \lim_{P \rightarrow Q_0} \left\{ \int_{AB} + \int_{L \setminus AB} \right\} = \lim_{P \rightarrow Q_0} \int_{AB} + \lim_{P \rightarrow Q_0} \int_{L \setminus AB}. \end{aligned} \quad (1.25)$$



There is no difficulty encountered in evaluating from (1.25)

$$\lim_{P \rightarrow Q_0} \int_{L \setminus AB} \{ \mu(s) - \mu(s_0) \} \frac{\partial}{\partial n_0} \left(\frac{\cos \psi}{r} \right) ds = \int_{L \setminus AB} \{ \mu(s) - \mu(s_0) \} \frac{\partial}{\partial n_0} \left(\frac{\cos \psi}{r} \right) \Big|_{P=Q_0} ds$$

since $r \neq 0$ and all terms in the integrand are finite.

For $\lim_{P \rightarrow Q_0} \int_{AB} \{ \mu(s) - \mu(s_0) \} \frac{\partial}{\partial n_0} \left(\frac{\cos \psi}{r} \right) ds$, we have first from (1.21)

$$\text{that } \frac{\partial}{\partial n_0} \left(\frac{\cos \psi}{r} \right) = \frac{\cos \rho - 2 \cos \omega \cos \psi}{r^2} = \frac{1 - 2 \cos^2 \omega}{r^2} = \frac{-\cos 2\omega}{r^2} \text{ since}$$

$$\rho = (\hat{n}, \hat{n}) = 0 \text{ and } \psi = (\hat{r}, \hat{n}) = \omega = (\hat{r}, \hat{n}). \text{ (Fig.17). It is}$$

convenient to set up local axes with origin at $Q_0(s_0)$ where

$\vec{Q_0 B}$ is the x axis and $\vec{Q_0 C}$ the y axis. With $PQ_0 = R$,

$$s = s_0 + x, \quad r^2 = (x - R \cos \delta)^2 + R^2 \sin^2 \delta \quad \text{and}$$

$$\tan \omega = \frac{x - R \cos \delta}{R \sin \delta} \quad \text{i.e.} \quad \frac{\cos 2\omega}{r^2} = \frac{1}{r^2} \left(\frac{1 - \tan^2 \omega}{1 + \tan^2 \omega} \right) \\ = \frac{R^2 \sin^2 \delta - (x - R \cos \delta)^2}{\{R^2 \sin^2 \delta + (x - R \cos \delta)^2\}^2}$$

Hence consider

$$\lim_{R \rightarrow 0} \int_A^B \{ \mu(s_0) - \mu(s_0 + x) \} \cdot \frac{R^2 \sin^2 \delta - (x - R \cos \delta)^2}{\{R^2 \sin^2 \delta + (x - R \cos \delta)^2\}^2} dx \quad (1.26)$$

The limits of integration may be taken from $x = -a$ at A, say, to $x = +b$ at B so that if μ and μ' are continuous in $-a < x < b$ and μ'' exists in $-a < x < b$, Taylor's theorem gives

$$\mu(s_0 + x) = \mu(s_0) + x \mu'(s_0) + \frac{1}{2} x^2 \mu''(\eta) \quad (1.27)$$

where η is some point in $s_0 < x < s_0 + x$ whose exact position will depend on x . See Chapter III, p. 102 on derivative of μ .

Hence (1.26) becomes

$$\lim_{R \rightarrow 0} \int_{-a}^b \frac{[x \mu'(s_0) + \frac{1}{2} x^2 \mu''(\eta)] \{ (x - R \cos \delta)^2 - R^2 \sin^2 \delta \}}{\{ (x - R \cos \delta)^2 + R^2 \sin^2 \delta \}^2} dx$$

[Note that $\mu''\{\eta(x)\}$ is defined by (1.27) for $x \neq 0$ and is continuous. For $\mu''\{\eta(0)\}$ we have $\lim_{x \rightarrow 0} \frac{\mu(s_0 + x) - \mu(s_0) - x\mu'(s_0)}{\frac{1}{2}x^2}$

$$= \lim_{x \rightarrow 0} \left\{ \frac{\mu'(s_0 + x) - \mu'(s_0)}{\frac{1}{2} \cdot 2x} \right\} = \lim_{x \rightarrow 0} \mu''(s_0 + x) = \mu''(s_0)$$

provided that $\mu''(x)$ is continuous at s_0]

Now before examining this limit further, suppose we insert $R = 0$ so that the case where P is placed at Q_0 is considered. The contribution is

$$\int_{-a}^b \left[x\mu'(s_0) + \frac{1}{2}x^2\mu''(\eta) \right] \cdot \frac{1}{x^2} dx = \int_{-a}^b \frac{\mu'(s_0)}{x} dx + \frac{1}{2} \int_{-a}^b \mu''(\eta) dx. \quad (1.28)$$

But from the above discussion on the behaviour of $\mu(x)$ and also provided that the singular integral is taken as the Cauchy Principal Value we have the existence as a finite quantity the right hand side of (1.28).

Now consider the quantity I , defined by the subtraction

$$\begin{aligned} & \int_{-a}^b \frac{\mu'(s_0)}{x} dx + \frac{1}{2} \int_{-a}^b \mu''\{\eta(x)\} dx - \\ & \int_{-a}^b \left[x\mu'(s_0) + \frac{1}{2}x^2\mu''(\eta) \right] \frac{(x - R\cos\delta)^2 - R^2\sin^2\delta}{\{(x - R\cos\delta)^2 + R^2\sin^2\delta\}^2} dx \\ & = \mu'(s_0) \int_{-a}^b \left(\frac{1}{x} - x \frac{\{(x - R\cos\delta)^2 - R^2\sin^2\delta\}}{\{(x - R\cos\delta)^2 + R^2\sin^2\delta\}^2} \right) dx + \\ & \quad \frac{1}{2} \int_{-a}^b \mu''(\eta) \left[1 - x^2 \frac{\{(x - R\cos\delta)^2 - R^2\sin^2\delta\}}{\{(x - R\cos\delta)^2 + R^2\sin^2\delta\}^2} \right] dx \quad (1.29) \end{aligned}$$

The first integral I_1 may be shown to tend to zero as $R \rightarrow 0$, for

considering
$$\int_{-a}^b x \frac{\{(x - R \cos \gamma)^2 - R^2 \sin^2 \gamma\}}{\{(x - R \cos \gamma)^2 + R^2 \sin^2 \gamma\}^2} dx \quad (1.30)$$

and making the substitution $x - R \cos \gamma = R \sin \gamma \tan \theta$, we obtain after completing the integrations
$$\left[\frac{\sin(\gamma - 2\theta)}{2 \sin \gamma} - \ell_n \cos \theta \right]_{\theta_1}^{\theta_2}$$

where θ_1 lies in $-\frac{\pi}{2} < \theta_1 < 0$ such that $\tan \theta_1 = \frac{-(a + R \cos \gamma)}{R \sin \gamma}$

and θ_2 lies in $0 < \theta_2 < \frac{\pi}{2}$ such that $\tan \theta_2 = \frac{b - R \cos \gamma}{R \sin \gamma}$

Hence (1.30) takes the value

$$\begin{aligned} & \frac{\sin(\gamma - 2\theta_2) - \sin(\gamma - 2\theta_1)}{2 \sin \gamma} - \ell_n \left(\frac{\cos \theta_2}{\cos \theta_1} \right) \\ &= \frac{\cos \{\gamma - (\theta_1 + \theta_2)\} \sin(\theta_1 - \theta_2)}{\sin \gamma} - \ell_n \left(\frac{\cos \theta_2}{\cos \theta_1} \right) \end{aligned}$$

But as $R \rightarrow 0$, $\theta_1 \rightarrow -\frac{\pi}{2}$ and $\theta_2 \rightarrow +\frac{\pi}{2}$ so that

$$\begin{aligned} & \frac{\cos \{\gamma - (\theta_1 + \theta_2)\} \sin(\theta_1 - \theta_2)}{\sin \gamma} \rightarrow 0 \quad \text{whilst} \\ & \ell_n \left(\frac{\cos \theta_2}{\cos \theta_1} \right) = \ell_n \left\{ \frac{R \sin \gamma}{\sqrt{b^2 - 2bR \cos \gamma + R^2}} \times \frac{\sqrt{a^2 + 2aR \cos \gamma + R^2}}{R \sin \gamma} \right\} \\ &= \frac{1}{2} \ell_n \left\{ \frac{a^2 + 2aR \cos \gamma + R^2}{b^2 - 2bR \cos \gamma + R^2} \right\} \rightarrow \frac{1}{2} \ell_n \frac{a^2}{b^2} = \ell_n \left(\frac{a}{b} \right) \quad \text{as } R \rightarrow 0. \end{aligned}$$

Thus the first integral of (1.29), I_1 , tends to

$$\mu'(s_0) \int_{-a}^b \frac{1}{x} dx + \mu'(s_0) \ell_n \left(\frac{a}{b} \right) = 0 \quad \text{provided the}$$

Cauchy Principal Value is taken.

The second integral can be treated by the same substitution

to give $\frac{1}{2} \int_{\theta_1}^{\theta_2} \mu'' \{ \xi(\theta) \} \{ 1 + \tan \theta \sin 2(\gamma - \theta) \} \frac{R}{\sin \gamma} d\theta$ after

some simplification where $\eta(x) = \eta(R \cos \gamma + R \sin \gamma \tan \theta) \equiv \xi(\theta)$.

We require to show that this integral also tends to zero as $R \rightarrow 0$.

$$\begin{aligned} \text{Write } & \frac{1}{2} \int_{\theta_1}^{\theta_2} \mu'' \{ \xi(\theta) \} \{ 1 + \tan \theta \sin 2(\gamma - \theta) \} \frac{R}{\sin \gamma} d\theta = I_2, \text{ say,} \\ & = \frac{R}{2 \sin \gamma} \int_{\theta_1}^0 \mu'' \{ \xi(\theta) \} \{ 1 + \tan \theta \sin 2(\gamma - \theta) \} d\theta \\ & \quad + \frac{R}{2 \sin \gamma} \int_0^{\theta_2} \mu'' \{ \xi(\theta) \} \{ 1 + \tan \theta \sin 2(\gamma - \theta) \} d\theta. \end{aligned}$$

Then if $M_1'' = \max_{-a \leq x < 0} | \mu''(x) |$ and $M_2'' = \max_{0 \leq x \leq b} | \mu''(x) |$,

$$\begin{aligned} |I_2| & \leq \frac{RM_1''}{2 \sin \gamma} \int_{\theta_1}^0 (1 - \tan \theta) d\theta + \frac{RM_2''}{2 \sin \gamma} \int_0^{\theta_2} (1 + \tan \theta) d\theta \\ & = \frac{RM_1''}{2 \sin \gamma} (-\theta_1 - \ell_n \cos \theta_1) + \frac{RM_2''}{2 \sin \gamma} (\theta_2 - \ell_n \cos \theta_2) \\ & = \frac{RM_1''}{2 \sin \gamma} \left(-\theta_1 - \ell_n \frac{R \sin \gamma}{a^2 + 2aR \cos \gamma + R^2} \right) + \frac{RM_2''}{2 \sin \gamma} \left(\theta_2 - \ell_n \frac{R \sin \gamma}{b^2 - 2bR \cos \gamma + R^2} \right) \end{aligned}$$

But as $R \rightarrow 0$, $\theta_1 \rightarrow -\frac{\pi}{2}$, $\theta_2 \rightarrow \frac{\pi}{2}$ and since $\lim_{R \rightarrow 0} (R \ell_n R) = 0$

we see that $|I_2| \rightarrow 0$ as $R \rightarrow 0$.

Thus returning to (1.29) we have shown that the quantity I tends to zero as the point P approaches the boundary point Q_0 .

Thus we have established that

$$\lim_{P \rightarrow Q_0} \int_{AB} \{ \mu(s) - \mu(s_0) \} \frac{\partial}{\partial n_0} \left(\frac{\cos \psi}{r} \right) ds \text{ exists equal to the value}$$

of the integral obtained by placing P at Q_0 to give

$$\int_{AB} \{ \mu(s) - \mu(s_0) \} \frac{\partial}{\partial n_0} \left(\frac{\cos \psi}{r} \right) \Big|_{P=Q_0} ds \text{ provided that the latter integral}$$

is treated as a Principal Value Integral.

On the other hand it is relatively easy to show that

both $\int_{AB} \mu(s) \frac{\partial}{\partial n_0} \left(\frac{\cos \psi}{r} \right) \Big|_{P=Q_0} ds$ and $\int_{AB} \mu(s_0) \frac{\partial}{\partial n_0} \left(\frac{\cos \psi}{r} \right) \Big|_{P=Q_0} ds$ diverge. For instance in the latter case we get $\mu(s_0) \int_{AB} \frac{-\cos 2\omega}{r^2} \Big|_{\omega = \frac{\pi}{2}} ds$ which reduces to an integral of the form $\mu(s_0) \int_{-a}^a \frac{dx}{x^2}$ which ^{does} not exist.

Hence the investigation of the limiting value of the derivative of the modified potential w_P as P approaches $Q_0 \in L$ leads finally to the result, from (1.25)

$$\lim_{P \rightarrow Q_0} \frac{\partial u_P}{\partial n_0} = \oint_L \{ \mu(s) - \mu(s_0) \} \frac{\partial}{\partial n_0} \left(\frac{\cos \psi}{r} \right) \Big|_{P=Q_0} ds \quad (1.31)$$

Thus given values of $\frac{\partial u}{\partial n}$ on L , the equation becomes an integral equation for the determination of the density function $\mu(s)$. Note that it was necessary to stipulate that μ and μ' be continuous on L and that μ'' existed.

Having obtained the solution $\mu(s)$, a return would then be made to (1.17) so that u_P could be generated throughout D^+ as required.

Finally by making use of the previous section it is possible to pose the solution of the Mixed Problem in terms of double layer potentials.

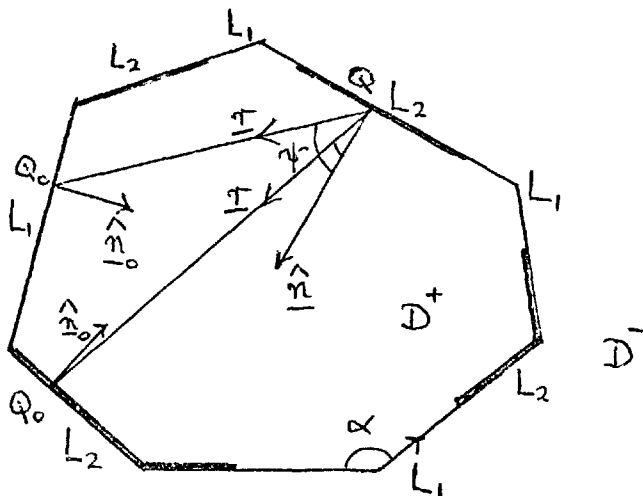


Fig. 18

As in the case of using single layer potentials we take $L = L_1 + L_2$ where on L_1 values of u are specified while on L_2 , values of $\frac{\partial u}{\partial n}$ are specified.

With a double layer density $\mu(s)$ defined everywhere on L , we already have that $u_p = \oint \frac{\mu(s) \cos \psi}{r} ds$ defines a harmonic function u_p , $P \in D^+$.

With P carried onto the boundary L from D^+ , we may write

$$h(s) = \begin{cases} u_{Q_0} = (2\pi - \alpha) \cdot u_{Q_0} + \oint_L \mu(s) d\theta, & Q_0 \in L_1 \\ \frac{\partial u}{\partial n_0}(Q_0) = \oint_L \{ \mu(s) - \mu(s_0) \} \frac{\partial}{\partial n_0} \left[\frac{\cos \psi}{r} \right] ds, & Q_0 \in L_2 \end{cases} \quad (1.32)$$

These equations provide a pair of coupled integral equations for the determination of $\mu(s)$, which would then be substituted back into (1.17) so that u_p may be generated.

§ 1.3 Green's Boundary Formula

We now turn to the third method of formulating the three fundamental boundary problems, namely that making use of Green's formulas. The results needed are based on 'Green's theorem in the plane' expressed as

$$\oint_L (M dx + N dy) = \iint_{D^+} \left(\frac{\partial N}{\partial x} - \frac{\partial M}{\partial y} \right) dx dy \quad (1.33)$$

in relation to the polygon (Fig.3), where $M(x,y)$ and $N(x,y)$ are defined and continuous in $D^+ \cup L$ such that the integrals in (1.33) exist. The validity of the result is generally established in [4] pp.284 - 292, including the case here where the region is polygonal.

The formula (1.33) is now converted into appropriate form by using vectors:-

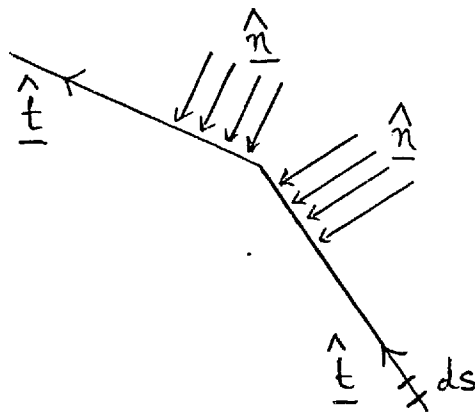


Fig. 19

With the usual cartesian vector notation $M dx + N dy = (M_i + N_j) \cdot (dx_i + dy_j) = (M_i + N_j) \cdot dr$. But we may write $dr = \frac{dr}{ds} ds = \underline{\hat{t}} ds$, $\underline{\hat{t}}$ piecewise constant and $\underline{\hat{t}} = \underline{\hat{n}} \wedge \underline{k}$ where as usual $\underline{\hat{n}}$ is the inward normal possessing two limiting values as a corner point is approached from either side.

$$\begin{aligned} \text{Thus } \oint_L (M dx + N dy) &= \oint_L (M_i + N_j) \cdot \hat{n} \wedge \underline{k} ds = \oint_L \underline{k} \wedge (M_i + N_j) \cdot \hat{n} ds \\ &= \oint_L (-N_i + M_j) \cdot \hat{n} ds \end{aligned}$$

$$\text{Also } \iint_{D^+} \left(\frac{\partial N}{\partial x} - \frac{\partial M}{\partial y} \right) dx dy = - \iint_{D^+} \left(\frac{\partial}{\partial x} \underline{i} + \frac{\partial}{\partial y} \underline{j} \right) \cdot (-N_i + M_j) dx dy .$$

Writing, say, $\underline{B} = -N_i + M_j$ and writing the symbol ∇ in a two dimensional sense gives

$$\oint_L \underline{B} \cdot \hat{n} ds = - \iint_{D^+} \nabla \cdot \underline{B} dx dy .$$

Now introduce two further functions of position $u(x,y)$ and $v(x,y)$ having continuous derivatives up to the second order at least in D^+ and substitute $\underline{B} = u \nabla v$ and $v \nabla u$ in turn and subtract

the results. This gives $\oint_L (u \nabla v - v \nabla u) \cdot \hat{n} ds = \iint_{D^+} (v \nabla^2 u - u \nabla^2 v) dx dy$

But $\nabla u \cdot \hat{n}$ is the 'directional' derivative $\frac{\partial u}{\partial n}$.

$$\oint_L \left(u \frac{\partial v}{\partial n} - v \frac{\partial u}{\partial n} \right) ds = \iint_{D^+} (v \nabla^2 u - u \nabla^2 v) dx dy \quad (1.34)$$

Note that since both u and v are considered to have continuous first derivatives in $D^+ \cup L$ it follows that $\frac{\partial u}{\partial n}$ is a piecewise continuous function having a finite discontinuity at each corner of L .

Now suppose that u is continuous with continuous first derivatives in $L \cup D^+$ and is a plane harmonic function in D^+ . Let v take the value $\ell_n \left(\frac{1}{r} \right)$ where r is the radial distance from the origin O to any point P in $D^+ \cup L$.

Then should O lie outside the polygon, $r \neq 0$ and (1.34) reduces to

$$\oint_L \left\{ u \frac{\partial}{\partial n} \left(\ell_n \frac{1}{r} \right) - \frac{\partial u}{\partial n} \ell_n \left(\frac{1}{r} \right) \right\} ds = 0. \quad (1.35)$$

Now place the axes so that O lies at a corner point of L . Then v is no longer defined at this point and so in order to apply (1.35) we surround O by a circular arc radius ϵ .

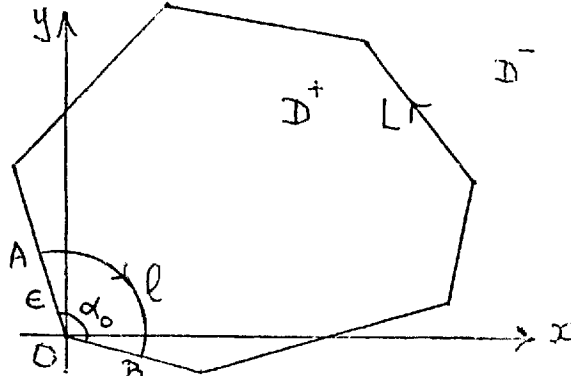


Fig. 20

Then (1.35) may be applied to the indented contour $L' + l$, L' being that part of the original polygon from B round to A (Fig.20)

$$\text{i.e. } \oint_{L'+l} \left\{ u \frac{\partial}{\partial n} \left(\ln \frac{1}{r} \right) - \frac{\partial u}{\partial n} \ln \frac{1}{r} \right\} ds = 0 .$$

$$\text{But } \int_l u \frac{\partial}{\partial n} \left(\ln \frac{1}{r} \right) ds = \int_A^B u \frac{\partial}{\partial r} \left(\ln \frac{1}{r} \right) ds = \int_A^B u \cdot \frac{-1}{\epsilon} \cdot ds = \int_A^B \frac{u}{\epsilon} \cdot \epsilon d\omega$$

where $d\omega$ is the angle subtended by ds so that as $\epsilon \rightarrow 0$, this tends to $-u_0 \times \alpha_0$, where $u_0 = u(x,y)$ at O .

$$\text{Also } \int_l \frac{\partial u}{\partial n} \ln \frac{1}{r} ds = \int_A^B \frac{\partial u}{\partial r} \cdot \ln \epsilon \cdot \epsilon d\omega = -\epsilon \ln \epsilon \int_A^B \frac{\partial u}{\partial r} d\omega$$

tends to zero as $\epsilon \rightarrow 0$.

We already have that $\frac{\partial}{\partial n} \left(\ln \frac{1}{r} \right)$ is zero along straight edges OA

and OB , while $\int_A^O \ln \frac{1}{r} ds$ is finite. Hence we may make $\epsilon \rightarrow 0$ to give

$$\oint_L \left\{ u \frac{\partial}{\partial n} \left(\ln \frac{1}{r} \right) - \frac{\partial u}{\partial n} \ln \frac{1}{r} \right\} ds - \alpha_0 u_0 = 0 \quad (1.36)$$

knowing the line integral to exist in the ordinary sense.

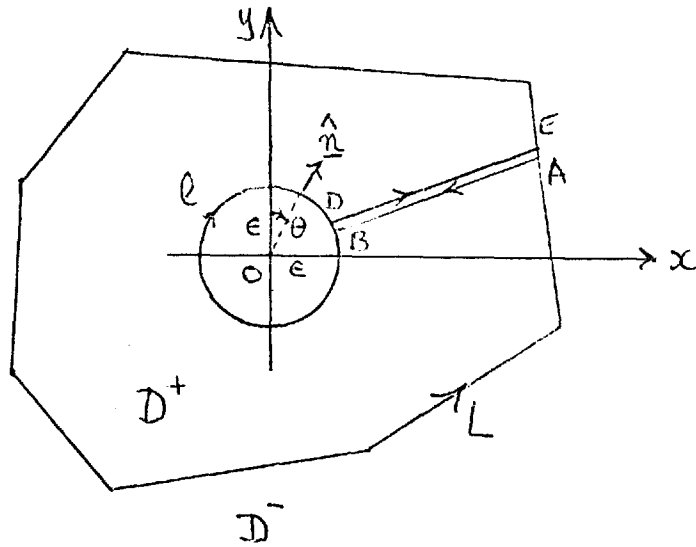


Fig. 21

Finally should the origin O lie in D^+ , describe a circle l about O with radius ϵ and join l to L by two parallel cuts AB and DE such that a new contour $L + AB + l + DE$ is formed for which O , the singularity lies entirely outside. Then for this contour, called L' say, we can apply

$$\oint_{L'} \left\{ u \frac{\partial}{\partial n} \left(\ln \frac{1}{r} \right) - \frac{\partial u}{\partial n} \ln \frac{1}{r} \right\} ds = 0.$$

Breaking this into constituent parts, $\int_L + \int_{AB} + \int_l + \int_{DE} = 0$

When the gap between AB and DE is closed up, we assume

$$\int_{AB} + \int_{DE} = 0$$

Also $\int_l \left\{ u \frac{\partial}{\partial n} \left(\ln \frac{1}{r} \right) - \frac{\partial u}{\partial n} \ln \frac{1}{r} \right\} ds = \int_l \left\{ u \frac{d}{d\epsilon} \left(\ln \epsilon \right) - \frac{\partial u}{\partial \epsilon} \ln \frac{1}{\epsilon} \right\} \epsilon \cdot d\theta$

$$= \int_l \left\{ -u + \frac{du}{d\epsilon} \cdot \epsilon \ln \epsilon \right\} d\theta \quad \text{and as } \epsilon \rightarrow 0, u \rightarrow u_0, \frac{\partial u}{\partial \epsilon} \text{ is undefined.}$$

As $\epsilon \log \epsilon \rightarrow 0$ as $\epsilon \rightarrow 0$, \int_l reduces to $-2\pi u_0$

$$\therefore \oint_L \left\{ u \frac{\partial}{\partial n} \left(\ln \frac{1}{r} \right) - \frac{\partial u}{\partial n} \ln \frac{1}{r} \right\} ds - 2\pi u_0 = 0 \quad (1.37)$$

The three equations (1.35) (1.36) and (1.37) can now be used as a framework for the solution of the three fundamental boundary problems by integral equation methods:-

Firstly the Dirichlet problem in which u takes the value $f(s)$ on L , may be solved by considering either (1.35) or (1.36) as integral equations for the determination of $\frac{\partial u}{\partial n}$ on L

$$\text{i.e. } \oint_L \frac{\partial u}{\partial n} \ell_n \frac{1}{r} ds = \oint_L f(s) \frac{\partial}{\partial n} \left(\ell_n \frac{1}{r} \right) ds, \quad o \in D^-$$

$$\text{or } \oint_L \frac{\partial u}{\partial n} \ell_n \frac{1}{r} ds = \oint_L f(s) \frac{\partial}{\partial n} \left(\ell_n \frac{1}{r} \right) ds - \alpha_o f(s_o), \quad o \in L$$

Making use of the Cauchy-Riemann relation $\frac{\partial}{\partial n} \left(\ell_n \frac{1}{r} \right) = + \frac{\partial \theta}{\partial s}$,

these integral equations may be simply stated as

$$\oint_L \frac{\partial u}{\partial n} \ell_n \frac{1}{r} ds = \oint_L f(s) d\theta, \quad o \in D^-, \quad (1.38)$$

$$\text{and } \oint_L \frac{\partial u}{\partial n} \ell_n \frac{1}{r} ds = -\alpha_o f(s_o) + \oint_L f(s) d\theta, \quad o \in L. \quad (1.39)$$

In each case here the righthand side expressions will be known.

Having solved for $\frac{\partial u}{\partial n}$, (1.37) is used to generate u throughout D^+ by writing it explicitly as

$$u = \frac{1}{2\pi} \oint_L \left\{ -\frac{\partial u}{\partial n} \ell_n \frac{1}{r} + f(s) \frac{\partial}{\partial n} \left(\ell_n \frac{1}{r} \right) \right\} ds = \frac{1}{2\pi} \oint_L \frac{\partial u}{\partial n} \ell_n r ds + \frac{1}{2\pi} \oint_L f(s) d\theta, \quad o \in D^+.$$

For the Neumann problem, the roles of u and $\frac{\partial u}{\partial n}$ are reversed since this time it is $\frac{\partial u}{\partial n}$ that is prescribed on $L = g(s)$.

Hence we have alternate integral equations for the determination of u on L :-

$$\oint_L u d\theta = \oint_L g(s) \ell_n \frac{1}{r} ds, \quad o \in D^- \quad (1.40)$$

$$\text{and } -\alpha_o u_o + \oint_L u d\theta = \oint_L g(s) \ell_n \frac{1}{r} ds, \quad o \in L \quad (1.41)$$

Having obtained u from either of these integral equations

(1.37) would be used as before to generate u throughout D^+ .

For the mixed problem as before let L be divided into two parts

L_1 and L_2 and let u be given on L_1 and $\frac{\partial u}{\partial n}$ on L_2 . Again

either (1.35) or (1.36) may be used to set up coupled integral

equations for the determination of $\frac{\partial u}{\partial n}$ on L_1 and u on L_2 .

In the case of (1.35) write

$$-\int_{L_1} \frac{\partial u}{\partial n} e_n \frac{1}{r} ds + \int_{L_2} u d\theta = + \int_{L_2} h(s) \cdot e_n \frac{1}{r} ds - \int_{L_1} h(s) d\theta, \quad o \in D^-$$

and for (1.36) we write

$$-\int_{L_1} \frac{\partial u}{\partial n} e_n \frac{1}{r} ds + \int_{L_2} u d\theta - \alpha_o u_o \Big|_{L_2} = + \int_{L_2} h(s) \cdot e_n \frac{1}{r} ds - \int_{L_1} h(s) d\theta + \alpha_o h(s_o) \Big|_{L_1}$$

$o \in L$.

With suitable discretisation on the boundary either of these

integral equations will yield discrete data values for u on L_2

and $\frac{\partial u}{\partial n}$ on L_1 .

Finally again return to (1.37) and generate u throughout D^+ .

§ 1.4 Complex Variable methods.

The representation of the fundamental boundary value problems in two dimensions by integral equations through the means of complex variable theory will now be discussed. Use of complex variable methods is particularly suited to the Laplace problem in two dimensions, but does not carry over into three dimensions; the representations given above are relatively easily extended into spatial situations.

Most emphasis on complex variable methods has been provided by Russian authors [5] and [6]. Also Milne Thomson [7] presents the key results in a concise manner.

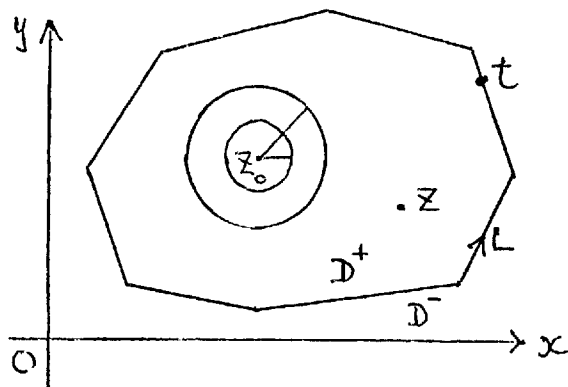


Fig. 22

As before suppose L is a polygonal contour (Fig.22). Let $\psi(t)$ be a complex function of the complex variable t , which is defined

at all points $t \in L$ such that $\oint_L |\psi(t)| ds$ is bounded. Then

$$\Phi(z) = \frac{1}{2\pi i} \oint_L \frac{\psi(t)}{t-z} dt$$

is called a Cauchy integral where

$z \notin L$. Often $\psi(t)$ is called the 'density' function; later the value of $\Phi(z)$ will be discussed in the case of $z \in L$.

We first show that $\Phi(z)$ is holomorphic, $z \in D^+$:-

Take $z_0 \in D^+$ and describe two concentric circles about

z_0 with radii $\frac{1}{2}\delta$ and δ (δ real), δ chosen so that neither circle intersects L . Then when z lies within the smaller circle we have $|t - z| > \frac{1}{2}\delta$.

$$\begin{aligned} \text{Consider } \Phi(z) - \Phi(z_0) &= \frac{1}{2\pi i} \oint_L \frac{\psi(t) dt}{t - z} - \frac{1}{2\pi i} \oint_L \frac{\psi(t) dt}{t - z_0} \\ &= \frac{(z - z_0)}{2\pi i} \oint_L \frac{\psi(t) dt}{(t - z)(t - z_0)}. \end{aligned}$$

$$\begin{aligned} \therefore |\Phi(z) - \Phi(z_0)| &< \frac{|z - z_0|}{2\pi} \oint_L \frac{|\psi(t)| ds}{\frac{1}{2}\delta \cdot \frac{1}{2}\delta} \\ &= |z - z_0| \cdot \frac{2}{\pi\delta^2} \oint_L |\psi(t)| ds \end{aligned}$$

when z lies inside smaller circle as stated.

Hence letting $z \rightarrow z_0$ (independent of δ) and noting the use of the boundedness of $\oint_L |\psi(t)| dt$, we obtain $\Phi(z) \rightarrow \Phi(z_0)$

so that $\Phi(z)$ is continuous at each $z_0 \in D^+$.

$$\text{Further consider } \frac{\Phi(z) - \Phi(z_0)}{z - z_0} = \frac{1}{2\pi i} \oint_L \frac{\psi(t) dt}{(t - z)(t - z_0)} = E(z), \text{ say.}$$

$$\begin{aligned} \text{Then } E(z) - E(z_0) &= \frac{1}{2\pi i} \oint_L \left\{ \frac{\psi(t)}{(t - z)(t - z_0)} - \frac{\psi(t)}{(t - z_0)^2} \right\} dt \\ &= \frac{(z - z_0)}{2\pi i} \oint_L \frac{\psi(t) dt}{(t - z)(t - z_0)^2}. \end{aligned}$$

$$\begin{aligned} \text{Again, } |E(z) - E(z_0)| &< \frac{|z - z_0|}{2\pi} \oint_L \frac{|\psi(t)| ds}{\frac{1}{2}\delta \cdot (\frac{1}{2}\delta)^2} \\ &= |z - z_0| \frac{4}{\pi\delta^3} \oint_L |\psi(t)| ds, \quad z \in |z - z_0| < \frac{1}{2}\delta. \end{aligned}$$

Hence letting $z \rightarrow z_0$ as before gives $E(z) \rightarrow E(z_0)$.

$$\text{But } E(z_0) = \frac{1}{2\pi i} \oint_L \frac{\psi(t) dt}{(t-z_0)^2} = \frac{d}{dz} \cdot \left[\frac{1}{2\pi i} \oint_L \frac{\psi(t) dt}{t-z} \right]_{z=z_0}$$

i.e. $E(z)$ is a continuous function of z and represents the derivative of $\Phi(z)$.

Hence $\Phi(z)$ is continuous and possesses a continuous derivative.

Similarly we may demonstrate that $E(z)$ also possesses a continuous derivative and so on.

Thus $\Phi(z)$ is holomorphic (or analytic) for $z \in D^+$. It may be shown similarly that $\Phi(z)$ is holomorphic for $z \in D^-$.

Now thus far, the investigation of $\Phi(z)$ has concentrated upon $z \notin L$. We must now consider the effect of (i) placing z on L at some point t_0 , say, and (ii) evaluating $\Phi(z)$ as $z \rightarrow t_0$, $z \in D^+$ (or $z \in D^-$).

First (i) : place z at t_0 , deliberately taken as a corner point of L .

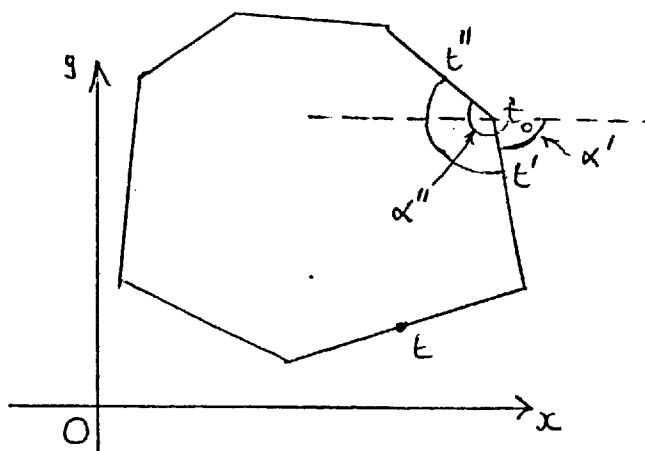


Fig. 23

We show that the integral $\Phi(t_0) = \frac{1}{2\pi i} \oint_L \frac{\psi(t) dt}{t-t_0}$ exists as

a Cauchy principal value. Describe a circular arc about t_0 , radius ϵ , to cut L at points t' and t'' as shown.

Denote by ℓ that portion of the polygon $t't_0t''$ so that $L-\ell$ may denote the remainder of the polygon.

Then $\frac{1}{2\pi i} \int_{L-\ell} \frac{\psi(t) dt}{t-t_0}$ possesses a limit as $\ell \rightarrow 0$, subject to

certain conditions on $\psi(t)$:-

Write
$$\frac{1}{2\pi i} \int_{L-\ell} \frac{\psi(t) dt}{t-t_0} = \frac{1}{2\pi i} \int_{L-\ell} \frac{\psi(t) - \psi(t_0) dt}{t-t_0} + \frac{1}{2\pi i} \int_{L-\ell} \frac{\psi(t_0) dt}{t-t_0} \quad (1.42)$$

The latter integral becomes
$$\frac{\psi(t_0)}{2\pi i} \int_{L-\ell} \frac{dt}{t-t_0} = \frac{\psi(t_0)}{2\pi i} \left[\ell_n(t-t_0) \right]_{t''}^{t'}$$

$$= \frac{\psi(t_0)}{2\pi i} \ell_n \left(\frac{t'-t_0}{t''-t_0} \right).$$

To close the contour again so that $\ell \rightarrow 0$, we need to find the limit of this term as $t', t'' \rightarrow t_0$.

But $t'-t_0 = e e^{-i\alpha'}$ and $t''-t_0 = e e^{-i\alpha''}$ (Fig.23)

i.e.
$$\frac{\psi(t_0)}{2\pi i} \ell_n \left(\frac{t'-t_0}{t''-t_0} \right) = \frac{\psi(t_0)}{2\pi i} \ell_n \left(\frac{e e^{-i\alpha'}}{e e^{-i\alpha''}} \right) = \frac{\psi(t_0)}{2\pi i} \cdot i(\alpha'' - \alpha')$$

$$= \psi(t_0) \cdot \frac{\alpha_0}{2\pi} \text{ where } \alpha_0 \text{ is the local}$$

interior angle at t_0 .

$$\therefore \lim_{\ell \rightarrow 0} \frac{1}{2\pi i} \int_{L-\ell} \frac{\psi(t_0) dt}{t-t_0} = \frac{\alpha_0}{2\pi} \psi(t_0).$$

Returning to the former integral of (1.42),
$$\frac{1}{2\pi i} \int_{L-\ell} \frac{\psi(t) - \psi(t_0) dt}{t-t_0} \quad :- \quad (1.43)$$

Suppose the condition $|\psi(t) - \psi(t_0)| \leq A|t-t_0|^\mu$, $A > 0$, $0 < \mu \leq 1$ (1.44)

is imposed on $\psi(t)$ near t_0 , i.e. for $|t-t_0| \leq R$, say, this

being referred to as the Holder condition by Muskhelishvili.

Denoting the contribution to (1.43) for this region by I ,

then
$$|I| \leq 2 \frac{1}{\pi} \int_{\epsilon}^R \left| \frac{\psi(t) - \psi(t_0)}{t-t_0} \right| ds.$$

Writing $t-t_0 = re^{-i\alpha'}$ or $re^{-i\alpha''}$ depending on which side of the corner t lies, we have

$$|\psi(t) - \psi(t_0)| \leq Ar^\mu \quad \text{from (1.44)}$$

$\therefore |I| \leq \frac{1}{2\pi} \int_{\epsilon}^R Ar^{\mu-1} dr = \frac{A}{2\pi\mu} (R^\mu - \epsilon^\mu)$ which is finite since $\mu > 0$. Hence subject to the Holder condition,

$$\lim_{\epsilon \rightarrow 0} \frac{1}{2\pi i} \int_{L-\epsilon} \frac{\psi(t) - \psi(t_0)}{t - t_0} dt \quad \text{exists.}$$

Thus to summarise the results, having placed z at a corner point t_0 of L we have shown that $\Phi(t_0)$ exists as a principal value and

$$\Phi(t_0) = \frac{1}{2\pi i} \oint_L \frac{\psi(t) - \psi(t_0)}{t - t_0} dt + \frac{\alpha_0 \psi(t_0)}{2\pi} \quad (1.45)$$

Second (ii) Consider the limiting value of $\Phi(z)$ as $z \rightarrow t_0, z \in D^+$ and t_0 is a corner point.

$$\text{From } \Phi(z) = \frac{1}{2\pi i} \oint_L \frac{\psi(t)}{t-z} dt, \quad \text{write}$$

$$\begin{aligned} \Phi(z) &= \frac{1}{2\pi i} \oint_L \frac{\psi(t) - \psi(t_0)}{t-z} dt + \frac{1}{2\pi i} \oint_L \frac{\psi(t_0)}{t-z} dt \\ &= \psi(t_0) + \frac{1}{2\pi i} \oint_L \frac{\psi(t) - \psi(t_0)}{t-z} dt, \quad z \in D^+, \end{aligned}$$

$$\text{since } \frac{1}{2\pi i} \oint_L \frac{dt}{t-z} = 1, \quad z \in D^+.$$

Now let $z \rightarrow t_0$ where t_0 is a corner point of $L, z \in D^+$.

$$\lim_{z \rightarrow t_0} \Phi(z) = \psi(t_0) + \lim_{z \rightarrow t_0} \frac{1}{2\pi i} \oint_L \frac{\psi(t) - \psi(t_0)}{t-z} dt \quad (1.46)$$

$$\text{Write } M(z, t_0) = \frac{1}{2\pi i} \oint_L \frac{\psi(t) - \psi(t_0)}{t-z} dt$$

Then $M(t_0, t_0) = \frac{1}{2\pi i} \oint_L \frac{\psi(t) - \psi(t_0)}{t - t_0} dt$ and is known to exist

by previous discussion.

Then $M(z, t_0) - M(t_0, t_0) = \frac{1}{2\pi i} \oint_L \frac{\{\psi(t) - \psi(t_0)\}(z - t_0)}{(t - z)(t - t_0)} dt$

and $|M(z, t_0) - M(t_0, t_0)| < \frac{1}{2\pi} \oint_L \frac{|\psi(t) - \psi(t_0)| |t_0 - z|}{|t - z| |t - t_0|} ds$.

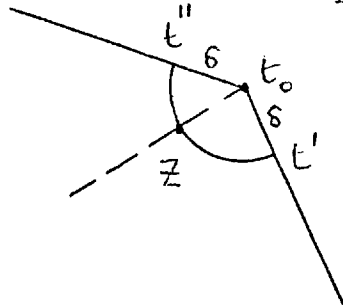


Fig. 24

Now describe a circular arc radius δ centre t_0 and let $z \rightarrow t_0$ along the vector $(t_0 - z)$ where $\alpha = \arg \left(\frac{t_0 - z}{t_0 - t_0} \right)$.

It is again convenient to split L into two parts for the purposes of the analysis:-

That part lying inside the circle denoted by ℓ and the remainder by $L - \ell$. Then we may write

$$\lim_{z \rightarrow t_0} |M(z, t_0) - M(t_0, t_0)| \leq \lim_{z \rightarrow t_0} \frac{1}{2\pi} \int_{\ell} \frac{|\psi(t) - \psi(t_0)| |t_0 - z|}{|t - z| |t - t_0|} ds + \lim_{z \rightarrow t_0} \frac{1}{2\pi} \int_{L - \ell} \frac{|\psi(t) - \psi(t_0)| |t_0 - z|}{|t - z| |t - t_0|} ds.$$

But the second right hand side term here is zero since the integrand tends to zero as $z \rightarrow t_0$, for all $t = z, t_0$.

In considering the first right hand side term, substitute

$$|t_0 - z| = \delta \quad \text{and also note that } |t - z| \geq \delta \sin \alpha.$$

$$\text{Thus } \lim_{z \rightarrow t_0} \frac{1}{2\pi} \int_{\ell} \leq \lim_{z \rightarrow t_0} \frac{1}{2\pi} \int_{t'}^{t_0} \frac{|\psi(t) - \psi(t_0)|}{\delta \sin \alpha |t - t_0|} ds$$

$$+ \lim_{z \rightarrow t_0} \frac{1}{2\pi} \int_{t_0}^{t''} \frac{|\psi(t) - \psi(t_0)| \delta}{\delta \sin \beta |t - t_0|} ds$$

where $\alpha + \beta = \alpha_0$, $\alpha, \beta > 0$.

But with the Hölder condition on $\psi(t)$, near t_0 ,

$$|\psi(t) - \psi(t_0)| \leq A |t - t_0|^\mu, \quad 0 < \mu \leq 1 \quad (\text{for sufficiently small } \delta, t \in \ell).$$

$$\text{Thus } \lim_{z \rightarrow t_0} \frac{1}{2\pi} \int_{\ell} \leq \lim_{z \rightarrow t_0} \frac{A}{2\pi \sin \alpha} \int_{t'}^{t_0} |t - t_0|^{\mu-1} ds + a$$

similar term

$$= \frac{A}{2\pi \sin \alpha} \cdot \frac{|t' - t_0|^\mu}{\mu} + \text{a similar term}$$

$$= \frac{A \delta^\mu}{2\pi \mu \sin \alpha} + \frac{A \delta^\mu}{2\pi \mu \sin \beta}, \quad \mu > 0.$$

Since as $z \rightarrow t_0$, $\delta \rightarrow 0$, this term will tend to zero.

Hence we have that $M(z, t_0) \rightarrow M(t_0, t_0)$ as $z \rightarrow t_0$ so that

$M(z, t_0)$ is continuous onto the boundary as $z \in D^+$ approaches the corner point t_0 .

Thus returning to (1.46), we may write now

$$\lim_{z \rightarrow t_0} \text{from } D^+ \Phi(z) = \psi(t_0) + \frac{1}{2\pi i} \oint_L \frac{\psi(t) - \psi(t_0)}{t - t_0} dt, \quad z \in D^+ \quad (1.47)$$

But from (1.45) we have that

$$\frac{1}{2\pi i} \oint_L \frac{\psi(t) - \psi(t_0)}{t - t_0} dt = \Phi(t_0) - \frac{\alpha_0 \psi(t_0)}{2\pi}.$$

$$\lim_{z \rightarrow t_0} \Phi(z) = \psi(t_0) + \Phi(t_0) - \frac{\alpha_0 \psi(t_0)}{2\pi}$$

$$\text{or } \Phi^+(z) = \left(1 - \frac{\alpha_0}{2\pi}\right) \psi(t_0) + \Phi(t_0)$$

$$\Phi^+(z) = \left(1 - \frac{\alpha_0}{2\pi}\right) \psi(t_0) + \frac{1}{2\pi i} \oint_L \frac{\psi(t)}{t - t_0} dt, \quad (1.48)$$

$z \rightarrow t_0, z \in D^+$

This result is known as a Plemelj formula, and a counterpart is similarly derived when $z \rightarrow t_0$, $z \in D^-$ giving

$$\Phi^-(z) = -\frac{\alpha_0}{2\pi} \Psi(t_0) + \frac{1}{2\pi i} \oint_L \frac{\Psi(t) dt}{t - t_0}$$

These results are for the case $z \rightarrow t_0$, where t_0 is a corner point having interior angle α_0 , $0 < \alpha_0 < 2\pi$. Of course t_0 need not be a corner point of L , in which situation α_0 is merely replaced by π .

Further results concerning the nature of $\Phi^+(z)$ may be obtained by [6] page 45 notably that this limiting value $\Phi^+(z) = \Phi^+(t_0)$ is a continuous function of t_0 , notwithstanding the lack of a smooth contour.

The application of the above results to two dimensional potential theory problems follows because the real and imaginary parts of any holomorphic function are harmonic functions.

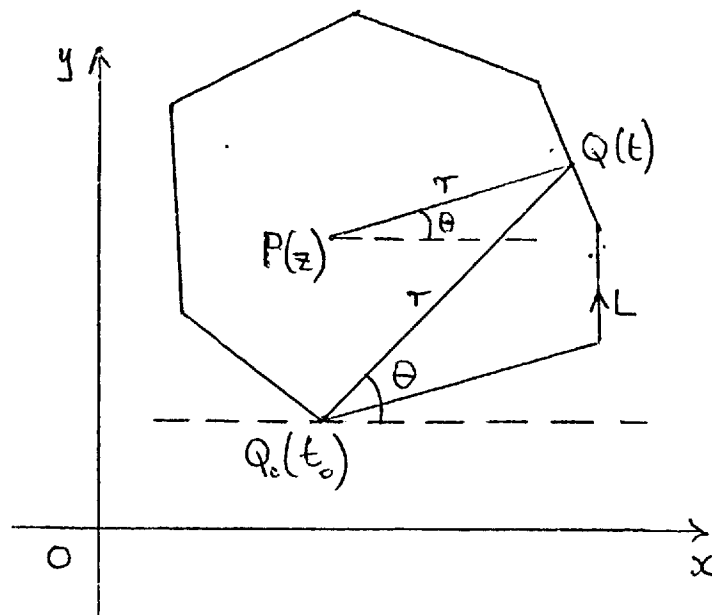


Fig. 25

Now $\Phi(z)$ was seen to be holomorphic in D^+ or D^- subject only to $\psi(t)$ being a complex function of the complex variable t satisfying

$$(i) \quad \oint_L |\psi(t)| ds \quad \text{exists}$$

and (ii) the Holder condition.

This freedom in $\psi(t)$ is now used by demanding that ψ be solely real.

Treating z or t_0 as a local fixed point we have

$$t - z = re^{i\theta} \quad \text{or} \quad t - t_0 = re^{i\theta} \quad (\text{Fig.25})$$

$$dt = dre^{i\theta} + ire^{i\theta} d\theta \quad \text{or} \quad dt = dre^{i\theta} + ire^{i\theta} d\theta$$

$$\frac{dt}{t-z} = \frac{dr}{r} + id\theta \quad \text{or} \quad \frac{dt}{t-t_0} = \frac{dr}{r} + id\theta$$

$$\text{Hence } \Phi(z) = \frac{1}{2\pi i} \oint_L \frac{\psi(t) dt}{t-z}, \quad z \in D^+ \quad \text{becomes}$$

$$u(x,y) + iv(x,y) = \frac{1}{2\pi i} \oint_L \psi(t) \left\{ \frac{dr}{r} + id\theta \right\}$$

$$\text{while } \Phi^+(z) = \left(1 - \frac{\alpha_0}{2\pi}\right) \psi(t_0) + \frac{1}{2\pi i} \oint_L \frac{\psi(t) dt}{t-t_0}, \quad z \rightarrow t_0 \in L$$

$$\text{becomes } u(t_0) + iv(t_0) = \left(1 - \frac{\alpha_0}{2\pi}\right) \psi(t_0) + \frac{1}{2\pi i} \oint_L \psi(t) \left\{ \frac{dr}{r} + id\theta \right\}.$$

Extracting the real part of these equations gives

$$u(x,y) = \frac{1}{2\pi} \oint_L \mu(t) d\theta, \quad (x,y) \in D^+ \quad (1.49)$$

$$u(t_0) = \left(1 - \frac{\alpha_0}{2\pi}\right) \mu(t_0) + \frac{1}{2\pi} \oint_L \mu(t) d\theta, \quad t_0 \in L \quad (1.50)$$

where we write μ in place of ψ to represent the now real

density defined on L . We note that the integral in (1.50) is no longer a principal value integral.

Extracting the imaginary part of the equations gives

$$v(x,y) = -\frac{1}{2\pi} \oint_L \frac{\mu(t) dr}{r}, \quad (x,y) \in D^+ \quad (1.51)$$

$$v(t_0) = -\frac{1}{2\pi} \oint_L \frac{\mu(t) dr}{r}, \quad t_0 \in L \quad (1.52)$$

where in (1.52) we now have a Cauchy principal value integral again.

Consider separately $\oint_L \frac{\mu(t) dr}{r} = \left[\mu(t) \ell_{nr} \right]_L - \oint_L \frac{d\{\mu(t)\}}{ds} \ell_{nr} ds$.

But $\mu \ell_{nr}$ being essentially real terms, we have that

$$\left[\mu(t) \ell_{nr} \right]_L = 0 \text{ no matter whether } \underline{r} = \overrightarrow{PQ} \text{ or } \underline{r} = \overrightarrow{Q_0Q} \text{ (Fig.25)}$$

If further $\frac{d\mu}{ds} = -\sigma(s)$ is inserted then (1.51) and (1.52) become

$$v(x,y) = \frac{1}{2\pi} \oint_L \sigma(s) \ell_n \frac{1}{r} ds, \quad (x,y) \in D^+ \quad (1.53)$$

$$v(t_0) = \frac{1}{2\pi} \oint_L \sigma(s) \ell_n \frac{1}{r} ds, \quad t_0 \in L \quad (1.54)$$

Thus two formulations of the Dirichlet problem in integral equation form are now obtained given by (1.50) and (1.54) where $u(t_0), v(t_0)$ take the prescribed boundary values $f(s_0)$. The results exactly reflect those obtained earlier by consideration of single and double layer potentials.

These formulations have been obtained by inserting $\psi(t)$ as an entirely real function defined on L . Clearly if $\psi(t)$ is taken as a completely imaginary function $i\mu(t)$ then precisely the same results as (1.49), (1.50), (1.53) and (1.54) will emerge, with the roles of u and v exchanged.

Before discussing the Neumann problem in the context of the complex variable, it is convenient to give an alternative version for the Dirichlet problem in which the choice available in the density $\psi(t)$ is exploited.

It has been seen that $\psi(t)$, originally a complex function defined on L and satisfying the Holder condition, may be taken as entirely real so that the integral equations (1.50) and (1.54) for the solution of the Dirichlet problem arise.

Returning now to the situation in which $\psi(t)$ is complex, we know that where $F(z)$ is a holomorphic function in $D^+ + L$, Cauchy's theorem gives $\oint_L F(t) dt = 0$. The conditions for this

may be weakened, see for instance [8]; it is sufficient that $F(t)$ is merely the boundary value of $F(z)$ holomorphic in D^+ and continuous in $D^+ + L$.

Thus in particular when $\psi(t)$ is the boundary value of $\psi(z)$ holomorphic in D^+ and continuous in $D^+ + L$ then Cauchy's theorem gives

$$\frac{1}{2\pi i} \oint_L \frac{\psi(t)}{t-z} dt = 0, \quad z \in D^-$$

the function $\frac{\psi(z)}{t-z}$ being holomorphic throughout D^+ in the case when $z \in D^-$.

However it was shown that $\Phi(z) = \frac{1}{2\pi i} \oint_L \frac{\psi(t)}{t-z} dt$ gave rise to

$\Phi(z)$ being holomorphic for $z \in D^+$ or D^- under very general conditions on $\psi(t)$.

Hence with the above choice for $\psi(t)$ we have that

$$\Phi(z) \equiv 0, \quad z \in D^-.$$

Now working from the general Cauchy integral and taking its limiting values as $z \rightarrow t_0$ we had from (1.48)

$$\Phi^+(t_0) = (1 - \frac{\alpha_0}{2\pi}) \psi(t_0) + \frac{1}{2\pi i} \oint_L \frac{\psi(t)}{t - t_0} dt, \quad z \in D^+$$

$$\Phi^-(t_0) = -\frac{\alpha_0}{2\pi} \psi(t_0) + \frac{1}{2\pi i} \oint_L \frac{\psi(t)}{t - t_0} dt, \quad z \in D^-$$

But in this situation $\Phi^-(t_0)$ being the limiting value of the holomorphic function "zero" must itself be zero.

$$\therefore \psi(t_0) = \frac{1}{i\alpha_0} \oint_L \frac{\psi(t)}{t - t_0} dt \quad (1.55)$$

Finally Cauchy's integral formula gives

$$\psi(z) = \frac{1}{2\pi i} \oint_L \frac{\psi(t)}{t - z} dt, \quad z \in D^+ \quad (1.56)$$

By taking real and imaginary parts of (1.55) we can display the required integral equations as follows.

Let $\psi(z) = u(x,y) + iv(x,y)$, u, v both harmonic and as $z \rightarrow t_0$ write $\psi(t_0) = u(t_0) + iv(t_0)$ where $u(t_0), v(t_0)$ are the limiting values of $u(x,y)$ and $v(x,y)$ respectively.

$$\therefore u(t_0) + iv(t_0) = \frac{1}{i\alpha_0} \oint_L \frac{u(t) + iv(t)}{t - t_0} dt$$

As before, put $t - t_0 = re^{i\theta}$,

$$\frac{dt}{t - t_0} = \frac{dr}{r} + id\theta$$

$$\begin{aligned} \therefore u(t_0) + iv(t_0) &= \frac{1}{i\alpha_0} \oint_L \{u(t) + iv(t)\} \left\{ \frac{dr}{r} + id\theta \right\} \\ &= -\frac{i}{\alpha_0} \oint_L \left\{ \frac{u dr}{r} - v d\theta + i \left(\frac{v dr}{r} + u d\theta \right) \right\} \end{aligned}$$

Taking the real part gives

$$u(t_0) = \frac{1}{\alpha_0} \oint_L \left(v \frac{dr}{r} + u d\theta \right) \quad (1.57)$$

and the imaginary part gives

$$v(t_0) = -\frac{1}{\alpha_0} \oint_L \left(u \frac{dr}{r} - v d\theta \right) \quad (1.58)$$

But the terms $\oint_L \frac{v dr}{r}$ and $\oint_L \frac{u dr}{r}$ may be integrated by parts

$$\text{i.e. } \oint_L v \frac{dr}{r} = \oint_L v \frac{d}{ds} (\ell_{nr}) ds = \left[v \ell_{nr} \right]_L - \oint_L \frac{\partial v}{\partial s} \ell_{nr} ds$$

$$\text{Now } \left[v \ell_{nr} \right]_L = \lim_{\delta \rightarrow 0} \left\{ v_b \ell_n |b - t_0| - v_a \ell_n |a - t_0| \right\}, \quad \text{Fig. 26.}$$

where $\delta = |b - t_0| = |a - t_0|$.

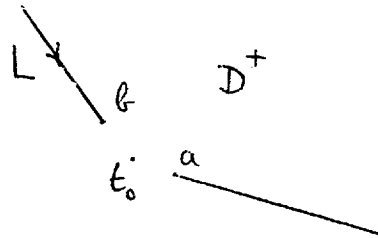


Fig. 26

and so assuming that $v(x,y)$ tends to a continuous boundary function $v(t_0)$, then $\left[v \ell_{nr} \right]_L = 0$.

Further $u(x,y)$ and $v(x,y)$ are conjugate harmonic functions for $z = x + iy \in D^+$. Thus the Cauchy Riemann equations hold between u' and v ,

$$\frac{\partial u}{\partial s} = \frac{\partial v}{\partial n} \quad \text{and} \quad \frac{\partial u}{\partial n} = -\frac{\partial v}{\partial s}$$

Again in the limit as $(x,y) \rightarrow t_0$ on L we have

$$\frac{\partial u(t)}{\partial s} = \frac{\partial v(t)}{\partial n} \quad \text{and} \quad \frac{\partial u(t)}{\partial n} = -\frac{\partial v(t)}{\partial s}$$

$$\oint_L \frac{v dr}{r} \equiv -\oint_L \frac{\partial u}{\partial n} \ell_{nr} ds = -\oint_L \frac{\partial u}{\partial n} \ell_n \left(\frac{1}{r} \right) ds$$

$$\text{Similarly } \oint_L \frac{u dr}{r} \equiv -\oint_L \frac{\partial v}{\partial n} \ell_{nr} ds = \oint_L \frac{\partial v}{\partial n} \ell_n \left(\frac{1}{r} \right) ds$$

Substituting into (1.57), (1.58) gives the identical pair of equations

$$u(t_0) = -\frac{1}{\alpha_0} \oint_L \frac{\partial u}{\partial n} \ell_n \frac{1}{r} ds + \frac{1}{\alpha_0} \oint_L u d\theta \quad (1.59)$$

$$\text{and } v(t_0) = -\frac{1}{\alpha_0} \oint_L \frac{\partial v}{\partial n} \ell_n \frac{1}{r} ds + \frac{1}{\alpha_0} \oint_L v d\theta \quad (1.60)$$

Further by taking real and imaginary parts of (1.56) we obtain in a similar manner the pair of equations

$$u(x,y) = \frac{1}{2\pi} \oint_L \left(-\frac{\partial u}{\partial n} \ell_n \frac{1}{r} ds + u d\theta \right)$$

$$v(x,y) = \frac{1}{2\pi} \oint_L \left(-\frac{\partial v}{\partial n} \ell_n \frac{1}{r} ds + v d\theta \right)$$

Thus this analysis yields an exact repetition of the equation obtained from Green's Boundary Formula. We return now to the situation in which the density $\psi(t)$ is a real valued function $\mu(t)$ and attempt a solution of the Neumann problem:

given $\frac{\partial u}{\partial n}(t_0) = g(s)$ at all $t_0 \in L$ except at corner points, to generate $u(x,y)$, harmonic in D^+ .

As $\nabla^2 u = 0$, (x,y) in D^+ , there exists a harmonic conjugate $v(x,y)$ and Cauchy-Riemann equations hold between them

$$\frac{\partial u}{\partial n} = -\frac{\partial v}{\partial s} \quad \text{and} \quad \frac{\partial u}{\partial s} = \frac{\partial v}{\partial n} \quad \text{on } L, \text{ except at}$$

corner points.

Now $\frac{\partial u}{\partial n} = g(s)$ along L

$$\therefore \frac{\partial v}{\partial s} = -g(s)$$

$$\therefore v(t_s) = -\int_a^s g(s) ds \quad \text{for some arbitrary initial}$$

arc point $s = a$, this being the sum of integrals along the straight boundary edges.

Note that since $v(t)$ is taken continuous, then on integrating circuitously we obtain the well-known Gauss condition

$$\oint_L g(s) ds = 0 .$$

Now from (1.48) we had

$$\Phi^+(t_0) = (1 - \frac{\alpha_0}{2\pi}) \mu(t_0) + \frac{1}{2\pi i} \oint_L \frac{\mu(t)}{t - t_0} dt$$

Taking the real and imaginary parts gives

$$u(t_0) = (1 - \frac{\alpha_0}{2\pi}) \mu(t_0) + \frac{1}{2\pi} \oint_L \mu(t) d\theta$$

$$v(t_0) = - \frac{1}{2\pi} \oint_L \frac{\mu(t)}{r} dr .$$

Hence we obtain $\frac{1}{2\pi} \oint_L \frac{\mu(t)}{r} dr = \int_a^{s_0} g(s) ds$ where s is

the arc length measurement at t_0 .

$$\begin{aligned} \text{Again } \oint_L \frac{\mu(t)}{r} dr &= \oint_L \mu(t) \frac{d}{ds} (\ln r) ds = [\mu(t) \ln r]_L - \oint_L \frac{d\mu}{ds} \ln r ds \\ &= - \oint_L \frac{d\mu}{ds} \ln r ds \quad \text{by above.} \end{aligned}$$

$$\text{Hence consider } \oint_L \sigma(s) \ln r ds = - 2\pi \int_a^{s_0} g(s) ds \quad (1.61)$$

where $\sigma(s)$ is written for $\frac{d\mu}{ds}$. This gives an integral equation for the determination of $\sigma(s)$.

To recover $u(x,y)$ within D^+ it is necessary to return to

$$u(x,y) = \frac{1}{2\pi} \oint_L \mu(s) d\theta \quad \text{as in equation (1.49) ; and the density}$$

$$\mu(s) \text{ here would be obtained from } \mu(s) = \int_b^s \sigma(s) ds .$$

Summary of integral equation formulations

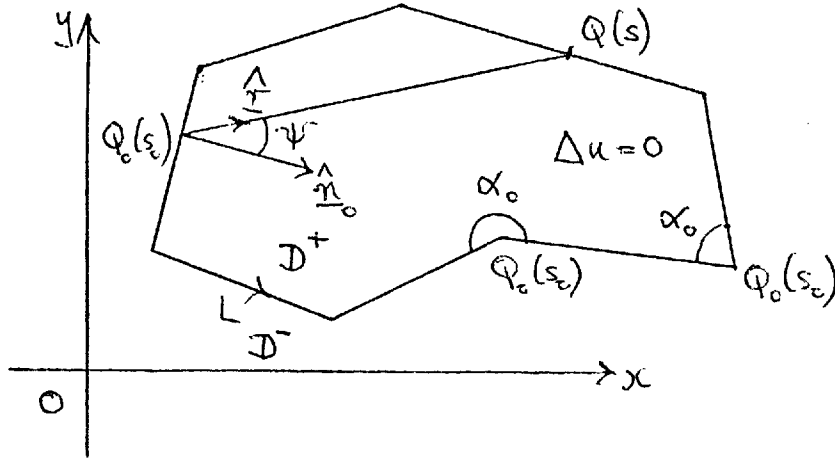


Fig. 27

Boundary conditions:

Dirichlet: $u(s) = f(s)$ Neumann: $\frac{\partial u}{\partial n}(s) = g(s)$.

Problem Formulation	Dirichlet integral equation	Neumann integral equation
SINGLE LAYER	$f(s_0) = \oint_L \sigma(s) \ell_n(\frac{1}{r}) ds$ (1.6)	$g(s_0) = -\pi\sigma(s_0) + \oint_L \frac{\sigma(s) \cos(\hat{r}, \hat{n}_0)}{r} ds$ (1.9) (s_0 not a corner point)
DOUBLE LAYER	$f(s_0) = (2\pi - \alpha_0)\mu(s_0) + \oint_L \mu(s) d\theta$ (1.20)	$g(s_0) = \oint_L \left\{ \mu(s) - \mu(s_0) \right\} \frac{\partial}{\partial n_0} \left(\frac{\cos \psi}{r} \right) ds$ (1.31)
GREEN'S FORMULA	$\oint_L \frac{\partial u}{\partial n} \ell_n(\frac{1}{r}) ds = \oint_L f(s) d\theta$ (1.38)	$\oint_L u(s) d\theta = \oint_L g(s) \ell_n(\frac{1}{r}) ds$ (1.40)
	$\oint_L \frac{\partial u}{\partial n} \ell_n(\frac{1}{r}) ds = -\alpha_0 f(s_0) + \oint_L f(s) d\theta$ (1.39)	$-\alpha_0 u(s_0) + \oint_L u(s) d\theta = \oint_L g(s) \ell_n(\frac{1}{r}) ds$ (1.41)
COMPLEX VARIABLE METHODS	$f(t_0) = (1 - \frac{\alpha_0}{2\pi})\mu(t_0) + \frac{1}{2\pi} \oint_L \mu(t) d\theta$ (1.50)	$\oint_L \sigma(s) \ell_n(\frac{1}{r}) ds = 2\pi \int_a^{s_0} g(s) ds$,
	$f(t_0) = \frac{1}{2\pi} \oint_L \sigma(s) \ell_n(\frac{1}{r}) ds$ (1.54)	$\sigma(s) = \frac{d\mu}{ds}$ (1.61)

Chapter II

Existence Theory for Polygonal Regions

In Chapter I the interior two dimensional boundary value problems for Laplace's equation were formulated as integral equations using various methods. The question must now be considered whether these equations, summarised for convenience of reference at the end of Chapter I, can be solved. This is a far reaching question for it concerns firstly the existence of a solution of these equations and secondly, when a theoretical solution is unobtainable in 'closed' form, whether an approximate solution can be obtained which will converge to the true solution in some sense.

We concentrate only on the formulations giving rise to the integral equations (1.20) or (1.50), which can be seen to be essentially the same, and investigate in detail the existence or otherwise of a (theoretical) exact solution, of an approximate solution and then the convergence of the approximate solution. The latter two are investigated in Chapter III; considerations of the existence of a solution given below in this Chapter. It should be remembered that we are concerned specifically with the case in which the boundary contour is polygonal, which makes a considerable effect on all these considerations.

With regard to the general theory of integral equations, there are many texts which describe in detail the occurrences and varieties of types of integral equation. Among the large literature available are the following references best known by the author: [5], [6], [9] and [10]. It will be apparent on reference that the integral equations derived here are all Fredholm integral equations of either the first or second kind. The Fredholm equations are usually displayed with respect to an integration along the real x - axis, viz

$$\int_a^b K(x,t)y(t)dt = h(x) , \quad x \in [a,b] \quad (2.1)$$

$$y(x) + \lambda \int_a^b K(x,t)y(t)dt = h(x) , \quad x \in [a,b] \quad (2.2)$$

where (2.1) is an equation of the first kind, and (2.2) that of the second kind, and $y(x)$ is to be determined. In this simple form (2.1) is known to be awkward to handle and in fact may have no solution for general $h(x)$ unless the kernel $K(x,t)$ is singular, [6]. For (2.2), we have at the outset for a wide variety of kernels $K(x,t)$ the well-known Fredholm Alternative which we state as follows:-

Either λ is a regular value and (2.2) possesses a unique solution for an arbitrary $h(x)$;

or λ is a characteristic value of (2.2) so that the homogeneous equation $y(x) + \lambda \int_a^b K(x,t)y(t)dt = 0$ possesses a denumerable number of linearly independent solutions $\phi_1(x), \phi_2(x), \dots$.

In this case the transposed homogeneous equation

$\psi(x) + \lambda \int_a^b K(t,x)\psi(t)dt = 0$ also possesses a denumerable set of solutions $\psi_1(x), \psi_2(x), \dots$ and (2.2) then has a solution if and only if $h(x)$ is orthogonal to all the $\{\psi_i(x)\}$.

The Fredholm Alternative is proved in [11] § 74 for $K(x,t)$ continuous on $a \leq x, t \leq b$ and is then carried over in [11] § 81 to demonstrate the existence of solution of the integral equation formulation of the interior Dirichlet problem. Double layer potentials are used and the integral equation produced is essentially (1.20) or (1.50). This discussion however requires that the kernel, in its equivalent form in the Dirichlet case,

(2.3) below, when a contour integral replaces the integration on the x - axis, be continuous for all points $s, s_0, 0 \leq s, s_0 \leq S$ on L . Provided that the contour L is smooth possessing a continuously turning tangent, then the kernel of the integral equation (1.20) or (1.50) is easily shown to be continuous. This kernel was displayed variously as

$$K(s, s_0) = \frac{\partial}{\partial n} \ell_n\left(\frac{1}{r}\right) = \frac{\cos(\hat{r}, \hat{n})}{r} = \frac{d\theta}{ds} \quad \text{in } \S 1.2. \quad (2.3)$$

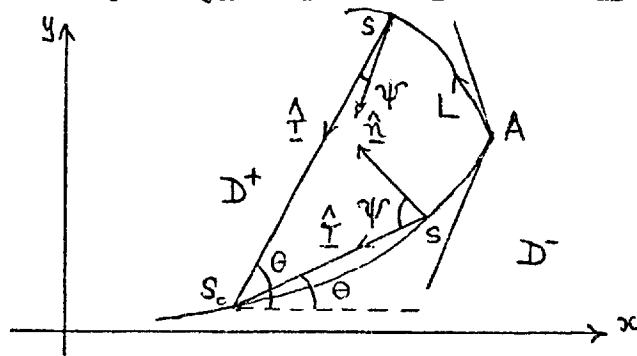


Fig 28

For given s_0 , $K(s, s_0)$ is continuous as s describes a smooth contour, continuity being maintained even when s passes through s_0 , [11] § 81, where it might appear that K becomes infinite. However this continuity is not maintained when s passes through any corner point of the contour, such as A in Fig.28. This arises due to the abrupt change in direction of \hat{n} . Moreover, the parameter λ in (2.2) is no longer a constant; an instantaneous change occurs at each corner point. Consequently we must first modify the demands of the Fredholm Alternative.

This requirement will be discussed in detail below. It will allow the application of (1.20) and (1.50) as a means of solving the Dirichlet problem, showing the existence of the density function $\mu(s)$ as the solution of (1.20) or (1.50). By examining the list given at the end of Chapter I, we see that the other formulations of the Dirichlet problem in terms of integral equations all fall into a different category; all are Fredholm equations of the first kind with logarithmic kernels,

i.e. $K(s, s_0) = \ell_n\left(\frac{1}{r}\right)$ where r is the distance between the points on L with arc parameter s and s_0 . Note that (1.38) is actually of a different, non singular, nature since in this case s_0 is always taken to lie outside the contour in D_- . The existence of a solution for these Fredholm equations of the first kind has

been considered by Jaswon and Symm [12]. They establish the existence of a solution for (1.6) (1.39) and (1.54) but only for smooth boundary contours. Convergence of approximate solutions to the solutions is not investigated.

With regard to the formulation (1.38), useful material appears in [13], p.253, in which the solution is shown to exist, but again the analysis refers to a smooth boundary contour. The author also gives details of the resulting approximate solution for (1.38) through linear algebraic methods. He is able to show that the approximate solution exists since, subject to a certain condition, the linear equations always have an invertible matrix. Some error analysis is given concerning the convergence of the approximate solution.

It is of course to be expected that all the integral equation formulations can be applied successfully to polygonal regions. We shall however concentrate completely on the double layer formulation and by referring to the methods of J.Radon [14] it will be possible to establish the existence of a unique continuous solution. It is probable that the ideas of Radon's work, which came to the attention of the author through the publication of J.Benveniste [15] can be extended to deal with other formulations of the two dimensional potential theory problem in terms of Fredholm equations of the first kind, but this is not investigated.

Thus we return now to the formulation of the interior Dirichlet problem through double layer potentials leading to (1.20) and effectively (1.50). As has been stated, the fundamental Fredholm theorem will deal with these equations only for continuous kernels.

Historically we have the analysis of Neumann, [16], which

is fully described in [17] p.201 and in [18] p.124. This gives the required result in the case of a region bounded by a convex contour having only a finite number of corner points. Neumann's work pre-dates Fredholm's but relies on certain geometrical constructions that apply only to convex regions, the boundary contours having non-zero curvature between the corner points.

Radon's aim was to establish existence of solution for a wide class of boundary curve, and to this end he considers L to be a curve of bounded rotation, this being a natural generalisation of smooth curves. A curve is said to be of bounded rotation when the angle $\Theta(s)$ (Fig.29) is of bounded variation as Q describes L , i.e. for $0 \leq s \leq S$.

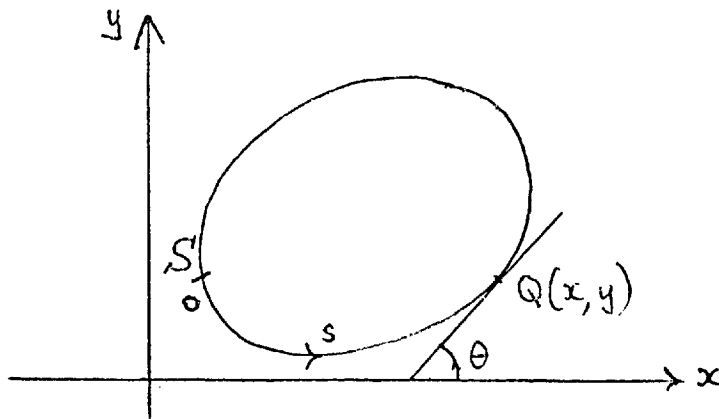


Fig. 29

The contour L , shown here as smooth for convenience, can be parameterised with respect to arc length s , $0 \leq s \leq S$ so that cartesian coordinates of a typical point Q on L are $\{x(s), y(s)\}$. When there is no chance of misunderstanding this point will be denoted by $Q(s)$.

We recall the standard definition of a function of bounded variation. Let g be a real function defined in $a \leq x \leq b$. Given a partition $\mathcal{P} = \{x_0, x_1, \dots, x_{n-1}, x_n\}$, $a = x_0$, $b = x_n$, $x_0 < x_1 < x_2 \dots < x_{n-1} < x_n$ possessing n intervals, write $\Delta g_k = g(x_k) - g(x_{k-1})$, $k = 1(1)n$. Then g is of bounded variation

on $[a, b]$ if there exists a positive real number M such that

$$\sum_{k=1}^n |\Delta g_k| \leq M \text{ for all possible partitions } \mathcal{P} \text{ (n finite). The}$$

total variation of g is further defined as $v_g[a, b] = \sup_{\mathcal{P}} \sum_{k=1}^n |\Delta g_k|$ taken over all possible partitions.

The angle θ made by the tangent at Q is defined by

$$\cos \theta(s) = x'(s) \text{ , } \sin \theta(s) = y'(s)$$

for points at which $x(s)$ and $y(s)$ are differentiable. For other points where $x'(s)$ and $y'(s)$ are not defined (i.e. corner points) then $\theta(s)$ is arbitrary.

$$\text{Hence } x(s) = x(0) + \int_0^s \cos \theta(s_0) ds_0 \tag{2.4}$$

$$\text{and } y(s) = y(0) + \int_0^s \sin \theta(s_0) ds_0$$

We note that when L is polygonal, $x(s)$ and $y(s)$ defined from (2.4) are piecewise linear. Now the major part of Radon's paper is concerned with the solution of the Dirichlet problem in terms of double layer potentials (cf. Chapter I, §1.2). This gives the harmonic function $u(x, y)$ at $P \in D^+$ expressed as $\oint_L \mu(s) dw_P$, (2.5) where $\mu(s)$ is continuous (Fig. 30) and of course an integral equation results when P passes onto the boundary of L at say Q_0 .

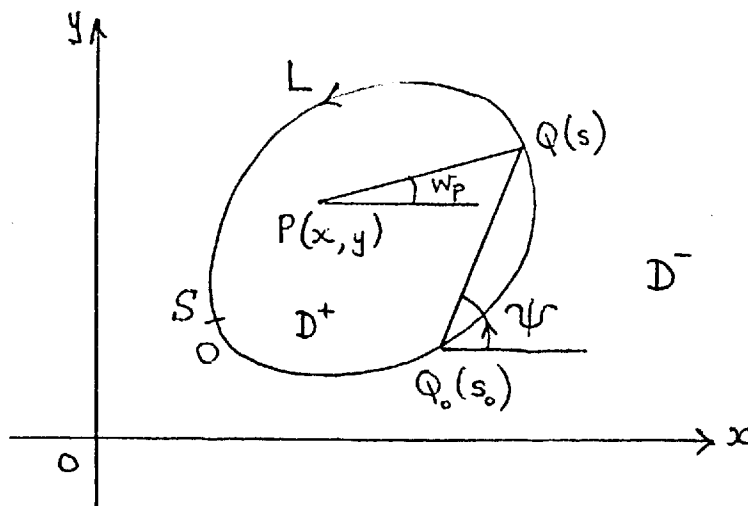


Fig. 30

In place of w_p when P is on L , Radon defines an angle

$\psi(s, s_0)$ as follows:-

(i) for $0 \leq s < s_0 \leq S$, define $\psi(s, s_0)$ by the relations

$$\begin{aligned} \cos \psi(s, s_0) &= K \{x(s) - x(s_0)\} \\ \sin \psi(s, s_0) &= K \{y(s) - y(s_0)\} \end{aligned} \quad , \quad K > 0 \quad (2.6)$$

(ii) for $0 \leq s_0 < s \leq S$, define $\psi(s, s_0) = \psi(s_0, s)$.

i.e. in this situation, using (2.5), $\psi(s_0, s)$ will be given by

$$\begin{aligned} \cos \psi(s_0, s) &= K' \{x(s_0) - x(s)\} \\ \sin \psi(s_0, s) &= K' \{y(s_0) - y(s)\} \end{aligned} \quad , \quad K' > 0 \quad (2.7)$$

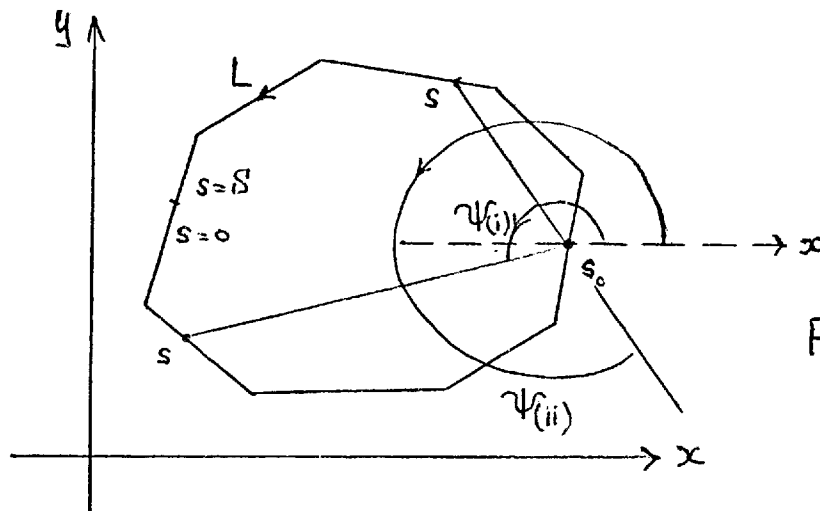


Fig. 31

(In the two situations drawn in Fig.31, $\psi = \psi_{(i)}$ lies in the third quadrant while $\psi = \psi_{(ii)}$ lies in the fourth quadrant). To keep the points s, s_0 distinct, the case $s = 0, s_0 = S$ is temporarily excluded.

Hence (2.6) and (2.7) define a symmetric expression $\psi(s, s_0)$, continuous at all its points of definition on the polygon L . We have not yet defined ψ for the cases $s = s_0; s = 0, s_0 = S; s_0 = 0, s = S$.

Now if the density $\mu(s)$ in (2.5) is set to unity, we obtain what Radon calls the order $O(x,y)$ of the point $P(x,y)$. (Fig.30) Clearly from (2.5), when $P \in D^+$, $O(x,y) = 2\pi$ and it is easy to show that $O(x,y) = 0$ for $P \in D^-$.

Suppose now that P lies on L at a corner point $Q_0(s_0)$ (Fig.32). Then we may write, formally,

$$\begin{aligned} O(x,y) &= O(x_{Q_0}, y_{Q_0}) = O(s_0) \text{ for brevity} \\ &= \oint_L d_s \psi(s, s_0), \end{aligned} \tag{2.8}$$

although $\psi(s_0, s_0)$ is not yet defined. (The notation d_s is used here to indicate that s is varying and that s_0 is a fixed point).

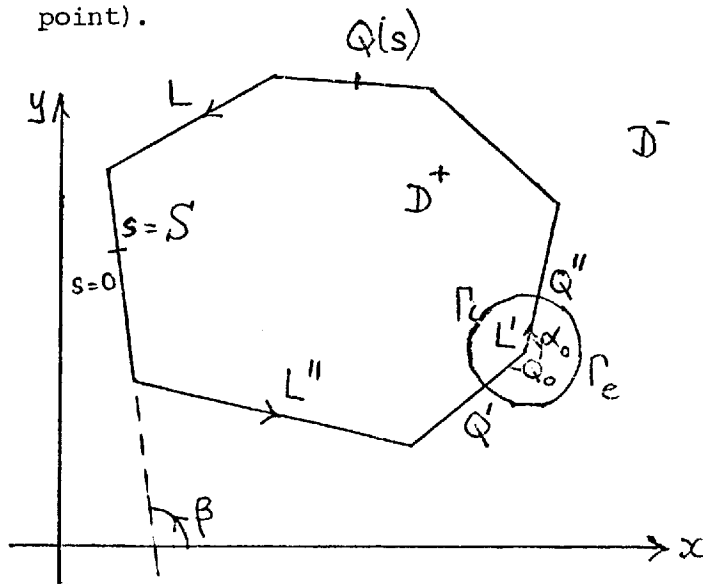


Fig. 32

Construct a circle centre Q_0 , radius δ , which cuts L in points Q', Q'' ($s = s', s''$ respectively, $s' < s_0 < s''$). Denote that part of L interior to the circle by L' and the remainder by L'' . Denote also two regions of the circumference of the circle: Γ_i that arc lying in D^+ and Γ_e the arc lying in D^- . It is assumed that δ is sufficiently small for the configuration of Fig.32 to hold.

Now we consider the value of the expression in (2.8). Taking $L = L'' + \Gamma_e$ then by (2.5) $O(s_0) = 2\pi$. But $\oint_{L'' + \Gamma_e} d_s \psi(s, s_0)$ can

be split into two parts: $\int_{L''} + \int_{\Gamma_e}$ and we have

$$\oint_{L'' + \Gamma_e} d_s \psi(s, s_0) = \int_0^{s'_0} d_s \psi(s, s_0) + \int_{\Gamma_e} d_s \psi(s, s_0) + \int_{s''_0}^S d_s \psi(s, s_0)$$

$$2\pi = \psi(s'_0, s_0) - \psi(0, s_0) + \int_{\Gamma_e} d_s \psi(s, s_0) + \psi(S, s_0) - \psi(s''_0, s_0),$$

recalling the symmetry of $\psi(s, s_0)$. Further, $\int_{\Gamma_e} d_s \psi(s, s_0)$ will

give the exterior angle at the vertex Q_0 . Denoting this by α_0

we have

$$\psi(s'_0, s_0) - \psi(0, s_0) + \psi(S, s_0) - \psi(s''_0, s_0) + \alpha_0 = 2\pi. \quad (2.9)$$

Now let $\delta \rightarrow 0$ and write $\lim_{\delta \rightarrow 0} \psi(s'_0, s_0) = \lim_{\delta \rightarrow 0} \psi(s_0, s'_0) = \psi(s_0, s_0^-)$.

Similarly take $\lim_{\delta \rightarrow 0} \psi(s''_0, s_0) = \psi(s_0, s_0^+)$ so that we have

$$\psi(s_0, s_0^+) = \theta(s_0^+) \quad \text{and} \quad \psi(s_0, s_0^-) = \theta(s_0^-)$$

where as before θ denotes the angle made by the tangent with Ox.

Also in the situation in which Q_0 were not to be a corner, then $\alpha_0 = \pi$ and $\psi(s'_0, s_0) \rightarrow \psi(s''_0, s_0) \rightarrow \theta(s_0)$ so that (2.9) would then reduce to

$$\psi(S, s_0) - \psi(0, s_0) = \pi \quad (2.10)$$

However (2.10) may be considered to hold generally for $0 < s_0 < S$ because of the continuity of $\psi(0, s_0)$ and $\psi(S, s_0)$ with respect to s_0 . Substituting (2.10) into (2.9) gives

$$\psi(s'_0, s_0) - \psi(s''_0, s_0) + \alpha_0 = \pi, \quad \text{or, as } \delta \rightarrow 0, \quad \psi(s_0, s_0^+) - \psi(s_0, s_0^-) = \alpha_0 - \pi \quad (2.11)$$

Thus in (2.11) we have a relation to indicate the discontinuity

in $\psi(s, s_0)$ as s passes through the corner s_0 . The understanding of $\psi(s, s_0)$ is completed by assigning appropriate limiting value meanings for $\psi(0, 0)$, $\psi(0, S)$, $\psi(S, 0)$ and $\psi(S, S)$. Without loss take the initial point for the measurement of s not at a corner. Denoting by β the angle made with Ox by the polygon edge upon which this point lies, then we have

$$\psi(0, 0) = \psi(0, 0+) = \psi(0+, 0) = \beta,$$

$$\psi(0, S) = \psi(0+, S) = \psi(0, S-) = \pi + \beta,$$

$$\text{and } \psi(S, 0) = \psi(S-, 0) = \psi(S, 0+) = \pi + \beta.$$

Since ψ is defined mod 2π then by taking $\psi(S, S) = \psi(S-, S) = \psi(S, S-) = 2\pi + \beta$ we have the relations

$$\psi(S, 0) - \psi(0, 0) = \pi \quad \text{and} \quad \psi(S, S) - \psi(0, S) = \pi.$$

This extends (2.10) to hold for the cases $s_0 = 0, S$. Finally since $\psi(0, S) = \psi(S, 0)$, adding the two latter results gives

$$\psi(S, S) - \psi(0, 0) = 2\pi.$$

Having explained Radon's definition of the angle $\psi(s, s_0)$, his treatment of the Dirichlet problem using double layer potentials now follows; the treatment is of course very similar to that used in obtaining (1.20).

From (2.5), $u(x, y) = \oint_L \mu(s) dw_P$ is harmonic for $P(x, y)$

$\in D^+$, and w_P as in Fig. 30. We put

$$\oint_L \mu(s) dw_P = \oint_L \{\mu(s) - \mu(s_0)\} dw_P + \oint_L \mu(s_0) dw_P, \quad 0 \leq s, s_0 \leq S,$$

where s is a variable and s_0 regarded as a particular value.

$$\therefore \oint_L \mu(s) dw_P = \oint_L \{\mu(s) - \mu(s_0)\} dw_P + 2\pi \mu(s_0), \quad P \in D^+. \quad (2.12)$$

Now with s_0 lying in, say, the interval $[s'_0, s''_0]$ (Fig.32), then given $\epsilon > 0$, there exists $\delta = s''_0 - s_0 = s_0 - s'_0$ such that $|\mu(s) - \mu(s_0)| < \epsilon$ for all $s \in [s'_0, s''_0]$, assuming $\mu(s)$ continuous for $0 \leq s \leq S$.

Thus (2.12) becomes

$$\oint_L \mu(s) dw_P = \int_0^{s'_0} \{\mu(s) - \mu(s_0)\} dw_P + \int_{s'_0}^{s''_0} \{\mu(s) - \mu(s_0)\} dw_P + \int_{s''_0}^S \{\mu(s) - \mu(s_0)\} dw_P + 2\pi \mu(s_0),$$

$$\text{where now } \int_{s'_0}^{s''_0} \{\mu(s) - \mu(s_0)\} dw_P \leq \int_{s'_0}^{s''_0} |\mu(s) - \mu(s_0)| dw_P < \epsilon \int_{s'_0}^{s''_0} dw_P \quad (2.13)$$

Labelling the point on L with arc parameter s_0 by Q_0 , as in Fig.32, we now let $P \rightarrow Q_0$ from within D^+ .

$$\text{Then } \int_0^{s'_0} \{\mu(s) - \mu(s_0)\} dw_P \rightarrow \int_0^{s'_0} \{\mu(s) - \mu(s_0)\} d_s \psi(s, s_0)$$

$$\text{and } \int_{s''_0}^S \{\mu(s) - \mu(s_0)\} dw_P \rightarrow \int_{s''_0}^S \{\mu(s) - \mu(s_0)\} d_s \psi(s, s_0)$$

Hence letting $\epsilon \rightarrow 0$ and using (2.13) we have

$$\begin{aligned} \lim_{P \rightarrow Q_0} u(x, y) &= u^+(Q_0) \quad (\text{see the notation in (1.20)}) \\ &= \int_0^{s_0^-} \{\mu(s) - \mu(s_0)\} d_s \psi(s, s_0) + \int_{s_0^+}^S \{\mu(s) - \mu(s_0)\} d_s \psi(s, s_0) + 2\pi \mu(s_0) \end{aligned}$$

But the two integrals can be combined together as $s_0^- \rightarrow s_0$ and $s_0^+ \rightarrow s_0$ so that

$$\begin{aligned} u^+(Q_0) &= \int_0^S \{\mu(s) - \mu(s_0)\} d_s \psi(s, s_0) + 2\pi \mu(s_0) \\ &= \int_0^S \mu(s) d_s \psi(s, s_0) - \mu(s_0) \int_0^S d_s \psi(s, s_0) + 2\pi \mu(s_0) \\ &= \int_0^S \mu(s) d_s \psi(s, s_0) - \mu(s_0) \{\psi(S, s_0) - \psi(0, s_0)\} + 2\pi \mu(s_0) \end{aligned}$$

By (2.10) this reduces to

$$u^+(s_0) = \pi \mu(s_0) + \int_0^S \mu(s) d_s \psi(s, s_0) \quad (2.14)$$

= the prescribed boundary function $f(s_0)$.

This latter equation is equivalent to (1.20): essentially (1.20) has been re-cast into the form (2.14) which is a more suitable integral equation because of the constant factor π .

When $f(s_0)$ is continuous with respect to different positions of s_0 on L we see that for the density function μ to be continuous on L , then it must be the case that

$$\int_0^S \mu(s) d_s \psi(s, s_0) \text{ is also a continuous function of } s_0.$$

Thus defining the transformation T by

$$(T\mu)(s_0) = \int_0^S \mu(s) d_s \psi(s, s_0) \quad (2.15)$$

then we see that T has to be a linear transformation of the space of continuous functions $\mu(s)$ on L into itself.

That this is so follows from the theorem given in [11] page 220 which may be expressed in a form suited to the current notation as follows:-

"Let $\psi(s, s_0)$ be a function of bounded variation defined for $0 \leq s, s_0 \leq S$ whose total variation with respect to s is less than some finite value independent of s_0 , for which $\psi(0, s_0) = 0$ and for which $\psi(s_0, S)$ and

$$\int_0^S \psi(s, s_0) ds \text{ are continuous functions of } s_0. \text{ Then } T$$

generated by (2.15) is a linear transformation of the space of continuous functions on $[0, S]$ into itself".

It is clear that for a polygonal contour possessing only a finite number of corner points, that ψ is of bounded variation (but not necessarily continuous). A detailed and general proof is

given in Radon that the total variation of ψ for a curve of bounded rotation (and hence for a polygon) is less than some finite value independent of s_0 .

We can arrange for $\psi(0, s_0)$ to be zero for any given s_0 by prior arrangement of L in relation to the position of the cartesian frame Oxy . By taking the initial point for arc measurement not at a corner point then $\psi(s_0, S)$ will be a continuous function of s_0 . With regard to the continuity of $\int_0^S \psi(s, s_0) ds$ regarded as a function of s_0 for given S , we denote the integral by $\Phi(S, s_0)$ and proceed as follows:-

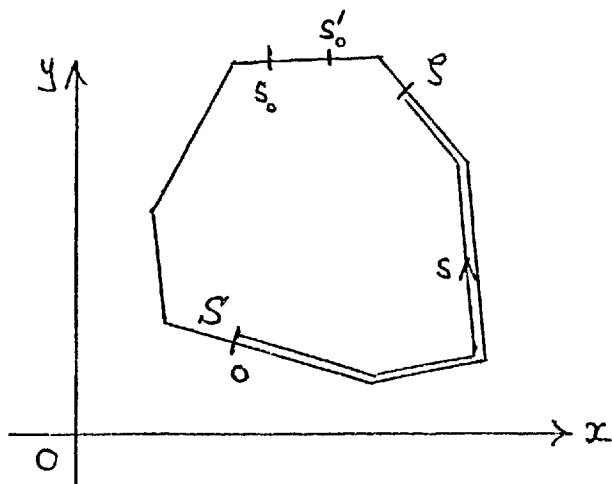


Fig. 33

Case 1 $s_0 > S$

This means $s_0 > s$ in the integrand and so $\psi(s, s_0)$ is continuous with respect to both variables s, s_0 . Hence $\Phi(S, s_0)$, being the integral of a continuous function is continuous in both S and s_0 .

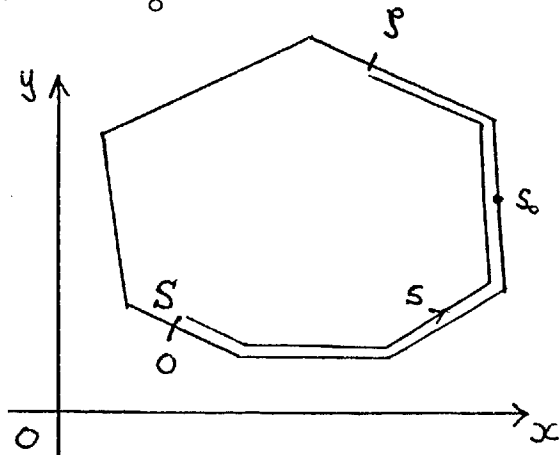


Fig. 34

Case 2 $s_0 < \xi$.

In this case $\Phi(\xi, s_0) = \int_0^\xi \psi(s, s_0) ds$, is such that s passes through s_0 .

Since $\psi(s, s_0)$ is a continuous function of s for s_0 not a corner point then it will be sufficient to consider the continuity at s_0 when s_0 is a corner point. The essence of the analysis can be seen by integrating across just the one corner point s_0 :-

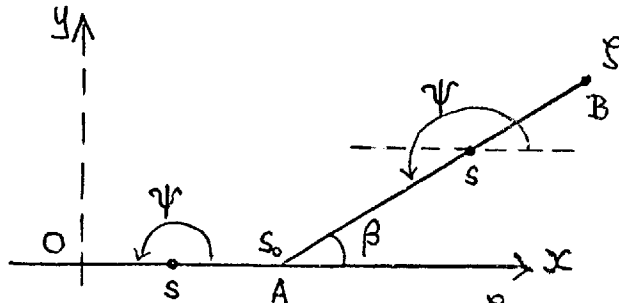


Fig. 35

Consider then $\Phi(\xi, s_0) = \int_0^\xi \psi(s, s_0) ds$ along the path OAB where without loss we take OA along the x axis, AB inclined to it at angle β , $0 < \beta < \pi/2$. Since we place s_0 at A then $OA = s_0$, $AB = \xi - s_0$.

From its definition, values for $\psi(s, s_0)$ are: $s < s_0$, $\psi = \pi$
 $s > s_0$, $\psi = \pi + \beta$
 $s = s_0$, is not defined.

$$\begin{aligned} \therefore \Phi(\xi, s_0) &= \int_0^{s_0} + \int_{s_0}^\xi \\ &= \int_0^{s_0} \pi ds + \int_{s_0}^\xi (\pi + \beta) ds \\ &= \pi s_0 + (\pi + \beta)(\xi - s_0) \\ &= \pi \xi + \beta(\xi - s_0) \end{aligned} \tag{2.16}$$

Now consider the evaluation for s_0 moved from the corner to say $s'_0 < \text{corner value}$. Again we evaluate $\Phi(\xi, s'_0) = \int_0^\xi \psi(s, s'_0) ds$

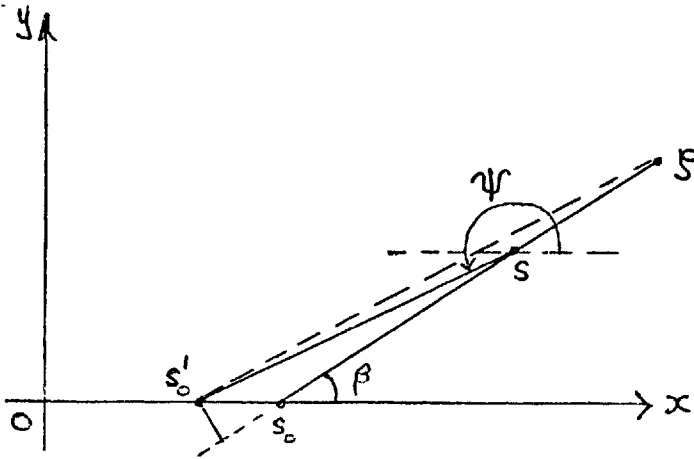


Fig. 36

Values for $\psi(s, s'_0)$: $0 \leq s \leq s'_0$, $\psi(s, s'_0) = \pi$ (as above),

$$s'_0 \leq s < s_0, \psi(s, s'_0) = \pi,$$

$$s_0 < s \leq s_1, \psi(s, s'_0) = \pi + \tan^{-1} \left[\frac{(s-s_0) \sin \beta}{(s_0-s'_0) + (s-s_0) \cos \beta} \right]$$

$$\begin{aligned} \text{Thus } \Phi(s_1, s'_0) &= \int_0^{s_1} \psi(s, s'_0) ds = \int_0^{s_0} + \int_{s_0}^{s_1} \\ &= \pi s_0 + \int_{s_0}^{s_1} \left\{ \pi + \tan^{-1} \left[\frac{(s-s_0) \sin \beta}{(s_0-s'_0) + (s-s_0) \cos \beta} \right] \right\} ds \end{aligned}$$

$$\text{i.e. } \Phi(s_1, s'_0) = \pi s_1 + \int_{s_0}^{s_1} \tan^{-1} \left[\frac{(s-s_0) \sin \beta}{(s_0-s'_0) + (s-s_0) \cos \beta} \right] ds \quad (2.17)$$

Now from (2.16) and (2.17),

$$\begin{aligned} \Phi(s_1, s_0) - \Phi(s_1, s'_0) &= \int_{s_0}^{s_1} \left\{ \beta - \tan^{-1} \left[\frac{(s-s_0) \sin \beta}{(s_0-s'_0) + (s-s_0) \cos \beta} \right] \right\} ds \\ &= \int_{s_0}^{s_1} \left\{ \tan^{-1}(\tan \beta) - \tan^{-1} \left[\frac{(s-s_0) \sin \beta}{(s_0-s'_0) + (s-s_0) \cos \beta} \right] \right\} ds \\ &= \int_{s_0}^{s_1} \tan^{-1} \left[\frac{(s_0 - s'_0) \sin \beta}{s-s_0 + (s_0-s'_0) \cos \beta} \right] ds \end{aligned}$$

But since $\frac{(s_0 - s'_0) \sin \beta}{(s-s_0) + (s_0 - s'_0) \cos \beta}$ is positive,

$$\text{then } \tan^{-1} \left[\frac{(s_0 - s'_0) \sin \beta}{(s-s_0) + (s_0 - s'_0) \cos \beta} \right] \leq \frac{(s_0 - s'_0) \sin \beta}{(s-s_0) + (s_0 - s'_0) \cos \beta}$$

$$|\Phi(\mathcal{P}, s_0) - \Phi(\mathcal{P}, s'_0)| \leq \int_{s_0}^{\mathcal{P}} \frac{(s_0 - s'_0) \sin \beta}{(s - s_0) + (s_0 - s'_0) \cos \beta} ds$$

Now $s - s_0 > (s - s_0) \cos \beta$ so $(s - s_0) + (s_0 - s'_0) \cos \beta > (s - s_0) \cos \beta + (s_0 - s'_0) \cos \beta$
 $= (s - s'_0) \cos \beta$

$$|\Phi(\mathcal{P}, s_0) - \Phi(\mathcal{P}, s'_0)| \leq \int_{s_0}^{\mathcal{P}} \frac{(s_0 - s'_0) \sin \beta}{(s - s'_0) \cos \beta} ds$$

$$= (s_0 - s'_0) \tan \beta \cdot \ln \frac{\mathcal{P} - s'_0}{s_0 - s'_0}$$

which tends to zero as $s'_0 \rightarrow s_0$.

Hence $\lim_{s'_0 \rightarrow s_0^-} \Phi(\mathcal{P}, s'_0) = \Phi(\mathcal{P}, s_0)$; and by a similar investigation

of $\Phi(\mathcal{P}, s'')$, $s'' > s_0$ we can show that $\lim_{s'' \rightarrow s_0^+} \Phi(\mathcal{P}, s'') = \Phi(\mathcal{P}, s_0)$.

This establishes the continuity of $\Phi(\mathcal{P}, s_0)$ with respect to varying s_0 as required.

Returning now to (2.14) we have

$$\pi \mu(s_0) + (T\mu)(s_0) = u^+(Q_0) \equiv f(s_0) \quad (\text{see 1.20})$$

$$(I + \frac{1}{\pi} T) \mu(s_0) = f(s_0) \quad (2.18)$$

where I is the identity transformation.

Thus we need to establish that the operator $I + \frac{1}{\pi} T$ has an inverse; more generally we consider the existence of $(I + \frac{\lambda}{\pi} T)^{-1}$ for various values of the scalar λ . The operator T is not completely continuous and so an extension of the Fredholm theory is needed.

Radon, [11], page 222 shows that for T defined on $C[0, S]$ by $(T\mu)(s_0) = \int_0^S \mu(s) d_s \psi(s, s_0)$ we may write $T = G + H$ where G is a linear transformation of integral type with degenerate kernel and H a linear transformation with norm $\|H\| \leq \epsilon$, where

$$w = \lim_{s_1 - s_2 \rightarrow 0} \sup_s \left| \psi(s_1, s) - \psi(s_2, s) \right| \quad (2.19)$$

and ϵ is an arbitrarily small positive quantity.

$$\text{Now } I + \frac{\lambda}{\pi} T = I + \frac{\lambda}{\pi} (G+H) = \left\{ I + \frac{\lambda}{\pi} H \right\} \left\{ I + \frac{\lambda}{\pi} (I + \frac{\lambda}{\pi} H)^{-1} G \right\}$$

For $I + \frac{\lambda H}{\pi}$ to possess an inverse we require that $\left| \frac{\lambda}{\pi} \right| \|H\| < 1$

But $\|H\| \leq w + \epsilon$ so that $\left| \frac{\lambda}{\pi} \right| \|H\| \leq \left| \frac{\lambda}{\pi} \right| (w + \epsilon)$.

$$\text{From (2.11) we have that } w = \lim_{s_1 - s_2 \rightarrow 0} \sup_s \left| \psi(s_1, s) - \psi(s_2, s) \right| = \alpha - \pi$$

where α is the magnitude of the greatest exterior angle at a corner point of the polygon and $s_1 - s_2 \rightarrow 0$ in such a manner that s_1 and s_2 are on either side of the corner.

$$\left| \frac{\lambda}{\pi} \right| \|H\| \leq \left| \frac{\lambda}{\pi} \right| (\alpha - \pi + \epsilon)$$

In the situation here in which $\lambda = 1$, then $\left| \frac{\lambda}{\pi} \right| \|H\| \leq \frac{\alpha - \pi}{\pi} + \frac{\epsilon}{\pi}$

But with the omission of cusp points the $\alpha < 2\pi$ so that $\frac{\alpha - \pi}{\pi} < 1$.

$\left| \frac{\lambda}{\pi} \right| \|H\| < 1$ is established since ϵ is arbitrarily small.

Hence $I + \frac{\lambda H}{\pi}$ possesses an inverse.

Further we must now consider $I + \frac{\lambda}{\pi} (I + \frac{\lambda}{\pi} H)^{-1} G$. But from [11] page 166 we have that $(I + \frac{\lambda}{\pi} H)^{-1} G$ is of finite rank since G is of finite rank (i.e. an integral operator corresponding to a degenerate kernel). From the establishment of the existence of $(I + \frac{\lambda}{\pi} H)^{-1}$ it can then be shown that $I + \frac{\lambda}{\pi} (I + \frac{\lambda}{\pi} H)^{-1} G$ possesses an inverse for the case $\lambda = 1$ since this is known not to be a singular value.

Hence on returning to (2.17), $I + \frac{1}{\pi} T$ can be inverted and a unique solution $\mu(s_0)$ exists.

This establishes the existence of the double layer density and hence the interior Dirichlet problem has a solution in the case of polygonal contours.

Chapter III

§3.1 Introduction to the numerical analysis

In this chapter we consider how to obtain the solution of an integral equation when applied to a specific boundary value problem. The reliability of the resulting numerical methods will be examined.

Although there is a full hand of integral-equation representations for each of the boundary problems at our disposal from Chapter I, attention will be concentrated on solving the interior Dirichlet problem represented as an integral equation through the use of the double-layer potential. Referring back to Chapter I we take the equations (1.49) and (1.50), which we repeat here for convenience:-

$$(1 - \frac{\alpha_0}{2\pi})\mu(t_0) + \frac{1}{2\pi} \text{Im} \oint_L \frac{\mu(t)}{t-t_0} dt = u(t_0) \quad (3.1)$$

$$u(x,y) = \frac{1}{2\pi} \oint_L \mu(t) d\theta \quad (3.2)$$

The notations used in (3.1) and (3.2) were fully described in § 1.4; t_0 represents the complex coordinate of the point Q_0 with arc coordinate s_0 on the polygon L at which the internal angle is α_0 , $0 < \alpha_0 < 2\pi$. Also the integral term in (3.1) is expressed in complex form for subsequent convenience. A specific Dirichlet problem is defined by declaring the shape of L and giving the values of $u(t_0) = f(t_0) \equiv f(s_0)$ for all positions of t_0 on L . We then attempt to solve (3.1) for the real-valued density function $\mu(t)$. From Chapter II it is known that a continuous solution $\mu(t)$ exists for any polygon L if $u(t)$ is continuous. Having obtained $\mu(t)$, the internal potential $u(x,y)$ is then generated using (3.2).

In general the determining of $\mu(t)$ and hence $u(x,y)$ in closed analytic form is usually impossible. In fact to obtain the exact solution for any integral equation presents difficulty in all but a few cases, for example when the kernel is degenerate ([9] pp 114).

Thus we seek an approximate solution of (3.1) for $\mu(t)$ using a numerical method. This gives rise to the following questions:

(i) Will the numerical method lead to a problem which can always be solved?

(ii) Subject to refinements in the numerical method, will the approximate solution, which will be denoted by $\tilde{\mu}(t)$, converge to the exact solution $\mu(t)$?

A number of methods are available for obtaining an approximate solution of an integral equation [19], not all necessarily suitable for application in (3.1). The method to be used here involves replacing the integral term $\frac{1}{2\pi} \text{Im} \oint_L \frac{\mu(t)}{t-t_0} dt$ in (3.1) by a quadrature formula,

say, $\sum_{j=1}^n w_j \mu_j$, where $\mu_j = \mu(t_j)$, the w_j are scalar weight

quantities and t_1, t_2, \dots, t_n are distinct points of L . Then if t_0 is taken to coincide with each of t_1, t_2, \dots, t_n in turn, a set of n simultaneous linear equations will be created whose solutions $\tilde{\mu}_j$, $j = 1(1)n$ hopefully approximate $\mu(t_j)$. We shall refer to the points t_j as node points.

An approximation to $u(x,y)$, denoted by $\tilde{u}(x,y)$, can then be calculated for various positions of $(x,y) \in D^+$ by replacing $\frac{1}{2\pi} \oint_L \mu(t) d\theta$ in (3.2) by $\sum_{j=1}^n w_j \tilde{\mu}_j$, w_j some weight quantity.

Hence L is to be partitioned into n intervals or segments. We shall now give some general details of how the nodes are fixed and numbered and also explain how the evident singularity in (3.1) disappears in the discretised problem. Since in (3.1), t_0 is to coincide with the t_j , $j = 1(1)n$ we will replace it by t_i , $i = 1(1)n$; further L is of course a contour so that node t_n must fall adjacent to node t_1 . In fact we shall number the nodes subsequently from 0 to $n-1$ so that $t_n = t_0$. This can be seen by reference to Fig. 37. We also always arrange

for corner points of L to occur as nodes in any partitioning undertaken. Consequently any segment $[t_j, t_{j+1}]$ will always be straight. Segments do not need to be of equal length.

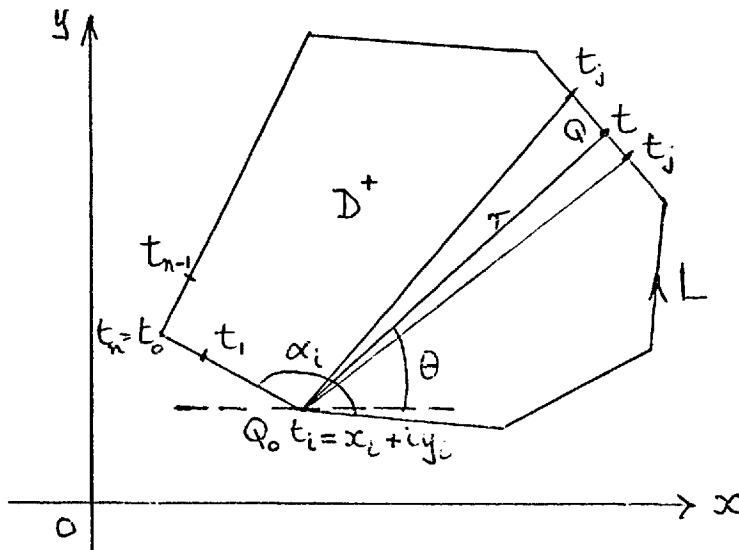


Fig. 37

Now in (3.1) the integral can be written as $\frac{1}{2\pi} \operatorname{Im} \sum_{j=0}^{n-1} \int_{t_j}^{t_{j+1}} \frac{\mu(t) dt}{t-t_i}$,

since the boundary of L is polygonal. The singular situation arises when $j = i-1, i$, the denominator of the integral becoming infinite at the end of the range $[t_{i-1}, t_i]$ and the beginning of the range $[t_i, t_{i+1}]$.

But we have $\operatorname{Im} \oint_L \frac{\mu(t)}{t-t_i} dt = \oint_L \mu(t) \operatorname{Im} \frac{dt}{t-t_i}$, since μ is

real, and as shown in Chapter I, pp. 52 if we write $t = t_i + re^{i\theta}$, $dt = dre^{i\theta} + ire^{i\theta} d\theta$, we have $\frac{dt}{t-t_i} = \frac{dr}{r} + id\theta$ so that

$$\operatorname{Im} \oint \frac{\mu(t)}{t-t_i} dt = \oint \mu(t) d\theta.$$

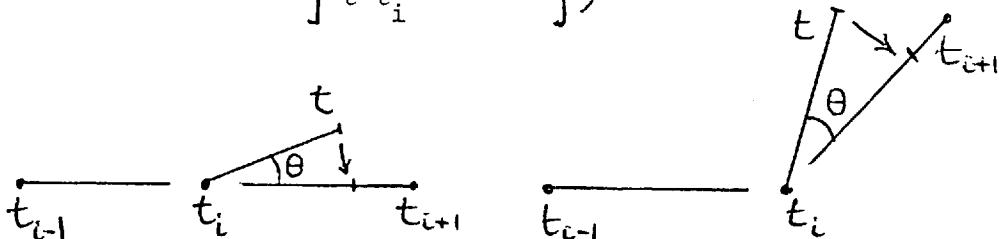


Fig. 38

Now as t moves along the straight segments $[t_{i-1}, t_i]$ and $[t_i, t_{i+1}]$,

the change in θ measured from t_i will be zero. This is the case whether or not t_i is a corner point. Thus the cases in the j count for which $j = i-1, i$ may be omitted altogether. As t passes through t_i , the term $(1 - \frac{\alpha_i}{2\pi})\mu(t_i)$ is "thrown-out" of the integral so that for any polygonal region the integral equation (3.1) is represented exactly by

$$(1 - \frac{\alpha_i}{2\pi})\mu(t_i) + \frac{1}{2\pi} \text{Im} \sum_{\substack{j=0 \\ (j \neq i-1, i)}}^{n-1} \int_{t_j}^{t_{j+1}} \frac{\mu(t)}{t-t_i} dt = f(t_i) \quad (3.3)$$

(Should $i=0, n$ then $i-1$ is interpreted as $n-1$).

We note also that other terms of the sum in (3.3) may also be zero depending on the geometry of L .

The stage is now reached at which quadrature methods must be applied to the integral in (3.3): $\int_{t_j}^{t_{j+1}} \frac{\mu(t)}{t-t_i} dt$.

The technique used in this thesis will be to substitute an approximation for $\mu(t)$ on $[t_j, t_{j+1}]$ and then to evaluate the resulting integral exactly. Three different approximations, denoted by A, B and C will be considered and the corresponding approximate solutions for $\mu(t)$

investigated in each case. In making the choice of an approximation for $\mu(t)$, we broadly follow the methods of G.T.Symm [20] and K.E.Atkinson [21].

Approximations proposed for the Double Layer Density

§ 3.2 Approximation A:

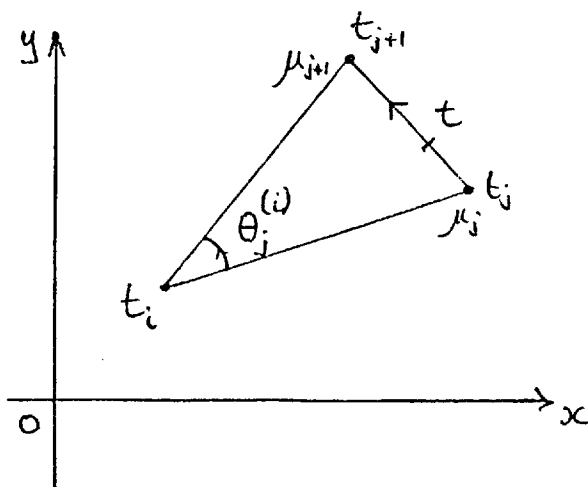


Fig. 39

In this, the simplest of the approximations we merely replace $\mu(t)$ on $[t_j, t_{j+1}]$ by the average of the end point node values, i.e. $\frac{1}{2}\{\mu(t_j) + \mu(t_{j+1})\} = \frac{1}{2}(\mu_j + \mu_{j+1})$.

$$\begin{aligned} \text{Hence } \frac{1}{2\pi} \operatorname{Im} \int_{t_j}^{t_{j+1}} \frac{\mu(t)}{t-t_i} dt &= \frac{1}{2\pi} \cdot \frac{1}{2}(\mu_j + \mu_{j+1}) \cdot \operatorname{Im} \int_{t_j}^{t_{j+1}} \frac{dt}{t-t_i} \\ &= \frac{1}{2\pi} \cdot \frac{1}{2}(\mu_j + \mu_{j+1}) \cdot \theta_j^{(i)}, \quad (\text{Fig. 39}) \end{aligned}$$

Thus (3.3) becomes

$$(2\pi - \alpha_i) \mu_i + \sum_{\substack{j=0 \\ (j+i-1, i)}}^{n-1} \frac{1}{2}(\mu_j + \mu_{j+1}) \theta_j^{(i)} = 2\pi f(t_i) \quad (3.4)$$

The angle $\theta_j^{(i)}$ will be the angle subtended at t_i by the boundary segment $[t_j, t_{j+1}]$, being positive anticlockwise as the point t moves round L .

Approximation B:

Here we take $\mu(t)$ to vary linearly in the interval $[t_j, t_{j+1}]$. The evaluation of $\int_{t_j}^{t_{j+1}} \frac{\mu(t)}{t-t_i} dt$ can then be completed and is best done by

a change of variable to the scalar λ where

$$t = (1-\lambda)t_j + \lambda t_{j+1}, \quad 0 \leq \lambda \leq 1 \quad (3.5)$$

Thus as $\mu(t)$ is linear over the interval,

$$\mu(t) = (1-\lambda)\mu_j + \lambda\mu_{j+1} \quad (3.6)$$

$$\begin{aligned} \text{Hence } \int_{t_j}^{t_{j+1}} \frac{\mu(t)}{t-t_i} dt &\equiv \int_0^1 \frac{(1-\lambda)\mu_j + \lambda\mu_{j+1}}{(1-\lambda)t_j + \lambda t_{j+1} - t_i} \cdot (t_{j+1} - t_j) d\lambda \\ &= (t_{j+1} - t_j) \int_0^1 \frac{\mu_j + \lambda(\mu_{j+1} - \mu_j)}{t_j - t_i + \lambda(t_{j+1} - t_j)} d\lambda. \end{aligned}$$

Putting $\frac{\mu_j + \lambda(\mu_{j+1} - \mu_j)}{t_j - t_i + \lambda(t_{j+1} - t_j)} = u + \frac{v}{t_j - t_i + \lambda(t_{j+1} - t_j)}$, say, gives

$$\mu_j + \lambda(\mu_{j+1} - \mu_j) \equiv u \{t_j - t_i + \lambda(t_{j+1} - t_j)\} + v$$

$$\therefore \mu_j = U(t_j - t_i) + v \quad \text{and} \quad \mu_{j+1} - \mu_j = U(t_{j+1} - t_j)$$

$$v = \mu_j - (t_j - t_i) \frac{(\mu_{j+1} - \mu_j)}{t_{j+1} - t_j} = \frac{\mu_j(t_{j+1} - t_j + t_j - t_i) - \mu_{j+1}(t_j - t_i)}{t_{j+1} - t_j}$$

$$\begin{aligned} \text{Hence} \quad \int_{t_j}^{t_{j+1}} \frac{\mu(t) dt}{t - t_i} &= (t_{j+1} - t_j) \int_0^1 \left\{ U + \frac{v}{(t_j - t_i) + \lambda(t_{j+1} - t_j)} \right\} d\lambda \\ &= (t_{j+1} - t_j)U + v \left[\ln \left\{ t_j - t_i + \lambda(t_{j+1} - t_j) \right\} \right]_0^1 \\ &= U(t_{j+1} - t_j) + v \cdot \ln \left(\frac{t_{j+1} - t_i}{t_j - t_i} \right) \\ &= \mu_{j+1} - \mu_j + \frac{\mu_j(t_{j+1} - t_i) - \mu_{j+1}(t_j - t_i)}{t_{j+1} - t_j} \cdot \ln \left(\frac{t_{j+1} - t_i}{t_j - t_i} \right) \end{aligned}$$

Thus as the approximation for $\frac{1}{2\pi} \text{Im} \int_{t_j}^{t_{j+1}} \frac{\mu(t)}{t-t_i} dt$ we have

$$\frac{1}{2\pi} \text{Im} \left[\frac{\mu_j(t_{j+1} - t_i) - \mu_{j+1}(t_j - t_i)}{t_{j+1} - t_j} \cdot \ln \left(\frac{t_{j+1} - t_i}{t_j - t_i} \right) \right] \quad (3.7)$$

Using (3.7) with (3.3) gives

$$\begin{aligned} (2\pi - \alpha_i) \mu_i + \sum_{\substack{j=0 \\ j+i-1, i}}^{n-1} \text{Im} \frac{\mu_j(t_{j+1} - t_i) - \mu_{j+1}(t_j - t_i)}{t_{j+1} - t_j} \times \ln \left(\frac{t_{j+1} - t_i}{t_j - t_i} \right) \\ = 2\pi f(t_i) \end{aligned} \quad (3.8)$$

Approximation C:

In this case we take $\mu(t)$ to be quadratic in the interval $[t_j, t_{j+1}]$.

The analysis here requires fitting a quadratic function through three consecutive node points. No difficulty is encountered in arranging the partitioning of the boundary providing corner points always lie at the end of a section of boundary over which $\mu(t)$ is to be quadratic. The partitioning is most conveniently achieved in fact by taking the same nodal points as before and merely fitting in an extra n nodes at the mid points of the intervals. Consequently three consecutive nodes are denoted by t_{j-1}, t_j, t_{j+1} where $t_{j-1} + t_{j+1} = 2t_j$ and we require to

fit a quadratic for $\mu(t)$ through the three points $\{t_{j-1}, \mu_{j-1}\}, \{t_j, \mu_j\}$ and $\{t_{j+1}, \mu_{j+1}\}$. We note in passing that this use of a piecewise quadratic $\mu(t)$ is slightly more specialised than that used by Atkinson [21].

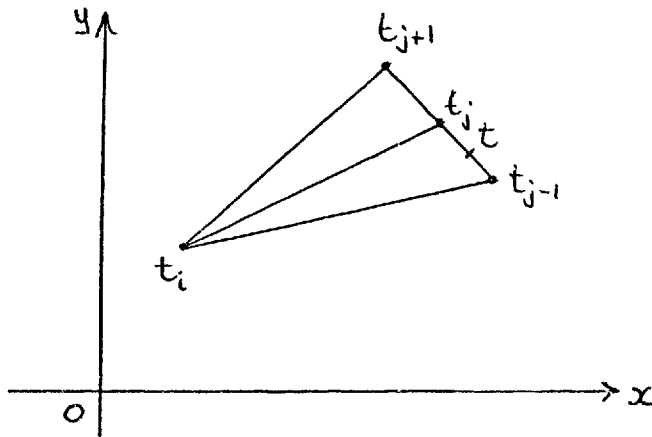


Fig. 40

For the evaluation of $\int_{t_{j-1}}^{t_{j+1}} \frac{\mu(t)}{t-t_i} dt$, we again introduce the scalar

λ and write

$$t = t_j + \lambda(t_{j+1} - t_j), \quad -1 \leq \lambda \leq 1. \quad (3.9)$$

Remembering that $t_{j-1} + t_{j+1} = 2t_j$ then for $\lambda = -1$, (3.9) gives

$$t = t_j - (t_{j+1} - t_j) = 2t_j - t_{j+1} = t_{j-1} \text{ as required.}$$

For $\mu(t)$ quadratic we may now write

$$\mu(t) = \frac{\lambda(\lambda-1)}{2} \mu_{j-1} + (1-\lambda^2) \mu_j + \frac{\lambda(\lambda+1)}{2} \mu_{j+1} \text{ so that we have (3.10)}$$

$$\text{collocation at } \lambda = -1, t = t_{j-1}, \mu = \mu_{j-1},$$

$$\lambda = 0, t = t_j, \mu = \mu_j,$$

$$\text{and } \lambda = 1, t = t_{j+1}, \mu = \mu_{j+1}.$$

$$\begin{aligned} \text{Hence } \int_{t_{j-1}}^{t_{j+1}} \frac{\mu(t)}{t-t_i} dt &= \int_{\lambda=-1}^{\lambda=+1} \left\{ \frac{\lambda(\lambda-1)}{2} \mu_{j-1} + (1-\lambda^2) \mu_j + \frac{\lambda(\lambda+1)}{2} \mu_{j+1} \right\} \cdot \frac{(t_{j+1}-t_j) d\lambda}{t_j - t_i + \lambda(t_{j+1}-t_j)} \\ &= (t_{j+1}-t_j) \int_{-1}^1 \frac{\lambda^2(\frac{1}{2}\mu_{j-1} - \mu_j + \frac{1}{2}\mu_{j+1}) + \frac{1}{2}\lambda(\mu_{j+1} - \mu_{j-1}) + \mu_j}{t_j - t_i + \lambda(t_{j+1}-t_j)} d\lambda \end{aligned} \quad (3.11)$$

Introducing for economy the notation $\delta\mu_j = \mu_{j+1} - \mu_{j-1}$,

$$\delta^2\mu_j = \mu_{j-1} - 2\mu_j + \mu_{j+1},$$

the integrand becomes

$$\frac{\frac{1}{2}\lambda^2 \delta^2\mu_j + \frac{1}{2}\lambda\delta\mu_j + \mu_j}{t_j - t_i + \lambda(t_{j+1} - t_j)} = U\lambda + V + \frac{W}{t_j - t_i + \lambda(t_{j+1} - t_j)}$$

where U, V and W are constants to be determined.

$$\frac{1}{2}\lambda^2 \delta^2\mu_j + \frac{1}{2}\lambda\delta\mu_j + \mu_j = U\lambda\{t_j - t_i + \lambda(t_{j+1} - t_j)\} + V\{t_j - t_i + \lambda(t_{j+1} - t_j)\} + W$$

Hence from the λ^2 coefficient, $\frac{1}{2}\delta^2\mu_j = U(t_{j+1} - t_j)$;

and from the λ coefficient, $\frac{1}{2}\delta\mu_j = U(t_j - t_i) + V(t_{j+1} - t_j)$.

$$V = \frac{\frac{1}{2}\delta\mu_j - (t_j - t_i) \frac{\frac{1}{2}\delta^2\mu_j}{t_{j+1} - t_j}}{t_{j+1} - t_j}$$

$$= \frac{\frac{1}{2}(t_{j+1} - t_j)\delta\mu_j - \frac{1}{2}(t_j - t_i)\delta^2\mu_j}{(t_{j+1} - t_j)^2}$$

Finally from the constant term,

$$\mu_j = V(t_j - t_i) + W,$$

$$W = \mu_j - (t_j - t_i) \left\{ \frac{\frac{1}{2}(t_{j+1} - t_j)\delta\mu_j - \frac{1}{2}(t_j - t_i)\delta^2\mu_j}{(t_{j+1} - t_j)^2} \right\}.$$

Returning to the integration at (3.11), we now have

$$\begin{aligned} \int_{t_{j-1}}^{t_{j+1}} \frac{\mu(t)}{t-t_i} dt &= (t_{j+1} - t_j) \int_{-1}^1 \left\{ U\lambda + V + \frac{W}{t_j - t_i + \lambda(t_{j+1} - t_j)} \right\} d\lambda \\ &= 2V(t_{j+1} - t_j) + W \left[\ln\{t_j - t_i + \lambda(t_{j+1} - t_j)\} \right]_{-1}^1 \\ &= 2V(t_{j+1} - t_j) + W \ln\left\{ \frac{t_{j+1} - t_i}{2t_j - t_{j+1} - t_i} \right\} \\ &= \frac{(t_{j+1} - t_j)\delta\mu_j - (t_j - t_i)\delta^2\mu_j}{t_{j+1} - t_j} + \left[\mu_j - \frac{(t_j - t_i)}{2(t_{j+1} - t_j)} \left\{ (t_{j+1} - t_j)\delta\mu_j - (t_j - t_i)\delta^2\mu_j \right\} \right] \\ &\quad \times \ln\left\{ \frac{t_{j+1} - t_i}{t_{j-1} - t_i} \right\} \end{aligned}$$

Replacing $\delta\mu_j$ and $\delta^2\mu_j$ and rearranging as coefficients of $\mu_{j-1}, \mu_j, \mu_{j+1}$ this becomes

$$\begin{aligned} & \mu_{j+1} - \mu_{j-1} - \frac{(t_j - t_i)}{t_{j+1} - t_j} (\mu_{j-1} - 2\mu_j + \mu_{j+1}) + \mu_j \ln \left(\frac{t_{j+1} - t_i}{t_{j-1} - t_i} \right) \\ & - \frac{(t_j - t_i)}{(t_{j+1} - t_j)} \left(\frac{\mu_{j+1} - \mu_{j-1}}{2} \right) \cdot \ln \left(\frac{t_{j+1} - t_i}{t_{j-1} - t_i} \right) \\ & + \frac{(t_j - t_i)^2}{(t_{j+1} - t_j)^2} \left(\frac{\mu_{j-1} - 2\mu_j + \mu_{j+1}}{2} \right) \ln \left(\frac{t_{j+1} - t_i}{t_{j-1} - t_i} \right) \\ = & \frac{2}{(t_{j+1} - t_{j-1})^2} \left[\mu_{j-1} \left\{ (t_{j+1} - t_i)(t_j - t_i) \cdot \ln \left(\frac{t_{j+1} - t_i}{t_{j-1} - t_i} \right) - (t_{j+1} - t_i)(t_{j+1} - t_{j-1}) \right\} \right. \\ & + \mu_j \left\{ 2(t_{j+1} - t_{j-1})(t_j - t_i) - 2(t_{j+1} - t_i)(t_{j-1} - t_i) \right\} \ln \left(\frac{t_{j+1} - t_i}{t_{j-1} - t_i} \right) \\ & \left. + \mu_{j+1} \left\{ (t_{j-1} - t_i)(t_j - t_i) \ln \left(\frac{t_{j+1} - t_i}{t_{j-1} - t_i} \right) - (t_{j-1} - t_i)(t_{j+1} - t_{j-1}) \right\} \right] \end{aligned} \tag{3.12}$$

Before substituting this approximation for $\int_{t_{j-1}}^{t_{j+1}} \frac{\mu(t)}{t-t_i} dt$ into

(3.3) it is expedient to make a slight change in the numbering. In this, the boundary L is first partitioned into n segments such that every corner point of L is at the end of a section. We denote these points by the complex coordinates $t_0, t_2, t_4, \dots, t_{2j-2}, t_{2j}, \dots, t_{2n-2}, t_{2n}$, where $t_0 = t_{2n}$ since L is of course closed. The mid points of each segment are required as node points as well, and with this notation, they are denoted by $t_1, t_3, t_5, t_{2j-1}, t_{2j+1}, \dots, t_{2n-3}, t_{2n-1}$. We note that $t_{2j-1} = \frac{1}{2}(t_{2j-2} + t_{2j})$, $j = 1(1)n$.

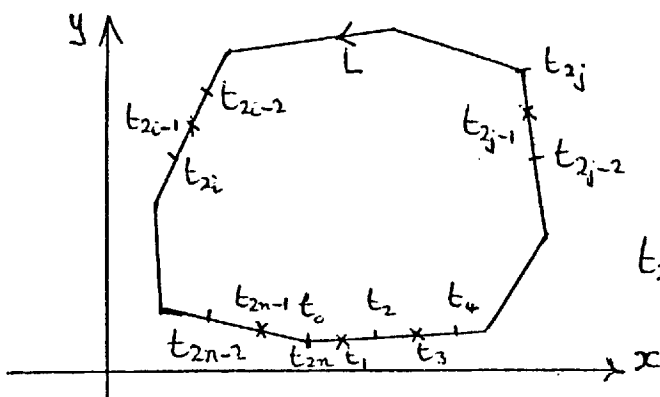


Fig. 41

$$t_{2j} = x_{2j} + iy_{2j}$$

The j th trio of points contains nodes t_{2j-2} , t_{2j-1} and t_{2j} , $j=1(1)n$ and replacing $\mu(t)$ by a sequence of quadratics gives rise to the approximation

$$\int_{t_{2j-2}}^{t_{2j}} \frac{\mu(t)}{t-t_i} dt = \frac{2}{(t_{2j}-t_{2j-2})^2} \{ E\mu_{2j-2} + F\mu_{2j-1} + G\mu_{2j} \}, \quad (3.13)$$

$i = 0(1)2n-1$

where $E = (t_{2j}-t_i)(t_{2j-1}-t_i) \rho_n \left(\frac{t_{2j}-t_i}{t_{2j-2}-t_i} \right) - (t_{2j}-t_i)(t_{2j}-t_{2j-2})$,

$$F = 2(t_{2j}-t_{2j-2})(t_{2j-1}-t_i) - 2(t_{2j}-t_i)(t_{2j-2}-t_i) \rho_n \left(\frac{t_{2j}-t_i}{t_{2j-2}-t_i} \right),$$

and $G = (t_{2j-2}-t_i)(t_{2j-1}-t_i) \rho_n \left(\frac{t_{2j}-t_i}{t_{2j-2}-t_i} \right) - (t_{2j-2}-t_i)(t_{2j}-t_{2j-2})$.

Now we obtain two versions of (3.3) according to whether the t_i node is taken at the end of a quadratic segment or as a mid point:-

$$(2\pi - \alpha_{2i-2})\mu(t_{2i-2}) + \text{Im} \sum_{\substack{j=1 \\ j \neq i-1, i}}^n \frac{2}{(t_{2j}-t_{2j-2})^2} \left\{ E\mu(t_{2j-2}) + F\mu(t_{2j-1}) + G\mu(t_{2j}) \right\}$$

$= 2\pi f(t_{2i-2}) \quad (3.14)$

and

$$\pi\mu(t_{2i-1}) + \text{Im} \sum_{\substack{j=1 \\ j \neq i}}^n \frac{2}{(t_{2j}-t_{2j-2})^2} \left\{ E\mu(t_{2j-2}) + F\mu(t_{2j-1}) + G\mu(t_{2j}) \right\} \quad (3.15)$$

$= 2\pi f(t_{2i-1})$

It should be noted that in (3.14), the coefficient values for E , F and G are now adjusted so that t_i is replaced by t_{2i-2} , while in (3.15), t_i is similarly replaced by t_{2i-1} .

Referring now to the three discretised forms of the integral equation, (3.4), (3.8) and (3.14), (3.15), sets of linear equations for the determination of the approximate solution, $\tilde{\mu}$, at the nodal points concerned can be generated by taking $i=0(1)n-1$ in (3.4) and (3.8), and by taking $i=1(1)n$ in each of (3.14) and (3.15). These sets of linear

equations may be solved by the method of Gaussian elimination. In the practical examples the results of which are given in Chapter IV, the well-known torsion problem of plane elasticity was used. In this problem the boundary data $f(t_i) = \frac{1}{2} \{x_i^2 + y_i^2\}$ where $t_i = x_i + iy_i$.

At this point in the thesis we make a distinction between the situation in which the polygon L is convex or otherwise, when it would possess at least one re-entrant vertex. If the arguments presented are narrowed to the former case then it will be shown that the numerical solutions obtained through each of the approximations A, B and C are completely reliable. In fact we can effectively deal with the questions posed on page 78 concerning the existence and convergence of $\tilde{\mu}(t_i)$, $i=0(1)n-1$. The author is of the opinion that such detailed analysis has not been presented elsewhere. However should L not be convex the same arguments unfortunately do not apply. In the case of approximation A, J. Benveniste [15] has shown that the numerical solution converges when L is polygonal with re-entrant corners not excluded. It is possible his methods can be extended to cover B and C as well, but not simply. We note that the error analysis of Anselone [27] and of Noble [23] cannot immediately be applied because the operators we use in potential theory problems for polygonal regions are not compact (completely continuous).

Consequently we shall proceed with the analysis of the numerical solutions in the situation where L is a convex polygon. It will now be shown in the following section that the coefficient matrix in the linear algebra is weakly diagonally dominant for each of the cases A, B and C.

Investigation of the Linear Algebra

§ 3.3 Approximation A:

Taking the equations generated by (3.4), the i^{th} row of the resulting linear equations produces a diagonal coefficient $2\pi - \alpha_i$ and off-diagonal coefficients from the terms $\sum_{\substack{j=0 \\ j \neq i-1, i}}^{n-1} \frac{1}{2} (\tilde{\mu}_j + \tilde{\mu}_{j+1}) \theta_j^{(i)}$.

For simplicity and without loss in generality we can take $i=0$, at which node we assume a corner angle α_0 , $0 < \alpha_0 \leq \pi$ since L is convex. Then subject to the usual anti-clockwise-positive rotation around L of the field point t , we have that for all j , $\theta_j^{(0)} \geq 0$. (This would no longer be true when L has re-entrant segments).

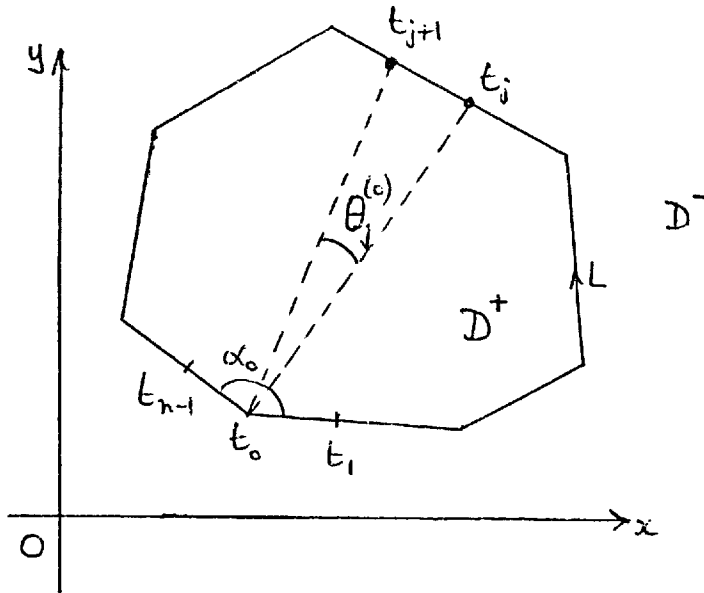


Fig. 42

The equations (3.4) may be written in the matrix form $K_A \tilde{\mu} = \underline{f}$ where $\tilde{\mu} = [\tilde{\mu}_0, \tilde{\mu}_1, \dots, \tilde{\mu}_{n-1}]^T$, $\underline{f} = [2\pi f(t_0), 2\pi f(t_1), \dots, 2\pi f(t_{n-1})]^T$ and K_A is the $(n \times n)$ coefficient matrix whose typical element k_{ij} may be read from (3.4). With $i=0$ then by reference to Fig.42 we easily see that

$$k_{0,0} = 2\pi - \alpha_0$$

$$k_{0,1} = \frac{1}{2} \theta_1^{(0)} \quad k_{0,2} = \frac{1}{2} (\theta_1^{(0)} + \theta_2^{(0)}), \quad k_{0,3} = \frac{1}{2} (\theta_2^{(0)} + \theta_3^{(0)}),$$

$$k_{0,j} = \frac{1}{2} (\theta_{j-1}^{(0)} + \theta_j^{(0)}), \quad \dots, \quad k_{0,n-1} = \frac{1}{2} \theta_{n-2}^{(0)}$$

(In the case of certain polygons, it is evident that some of these $\theta_j^{(0)}$ are zero, for instance possibly $\theta_1^{(0)}$ and $\theta_{n-2}^{(0)}$).

$$\begin{aligned} \text{Consider } \sum_{j=1}^{n-1} |k_{0,j}| &= \left| \frac{1}{2} \theta_1^{(0)} \right| + \left| \frac{1}{2} (\theta_1^{(0)} + \theta_2^{(0)}) \right| + \dots + \left| \frac{1}{2} \theta_{n-2}^{(0)} \right| \\ &= \theta_1^{(0)} + \theta_2^{(0)} + \dots + \theta_{n-2}^{(0)} \quad \text{since each } \theta_j^{(0)} \geq 0. \end{aligned}$$

But this latter sum is equal to the internal angle α_0 at t_0 .

$$\text{Thus } |k_{0,0}| = 2\pi - \alpha_0$$

$$\text{and } \sum_{j=1}^{n-1} |k_{0,j}| = \alpha_0.$$

Thus when L is convex, $\alpha_0 \leq \pi$ and $2\pi - \alpha_0 \geq \alpha_0$ so that $|k_{0,0}| \geq \sum_{j=1}^{n-1} |k_{0,j}|$. But since we shall be placing node points at each corner point, of which there must be at least three (when the region D^+ is triangular), then this inequality will be a strict "greater than" for t_0 at corners whilst being "equality" when t_0 lies on a straight edge. The occurrence of strict diagonal dominance at certain rows of the coefficient matrix K_A is sufficient for us to claim that K_A is non-singular ([22] p.282 Ex.6). Hence K_A^{-1} exists and $\tilde{u}(t_j)$ can be evaluated.

Unfortunately when L is re-entrant, the diagonal dominance will be lost; for when t_0 lies at a re-entrant corner, α_0 will exceed π .

$$\text{i.e. } |k_{0,0}| = 2\pi - \alpha_0 < \pi$$

$$\text{while } \sum_{j=1}^{n-1} |k_{0,j}| \geq \alpha_0 \quad (\text{greater than corresponding to the occurrence of further re-entrant$$

situations around L).

Hence for at least one position of t_0 , $|k_{0,0}| < \sum_{j=1}^{n-1} |k_{0,j}|$, thus spoiling the nature of K_A .

Approximation B:

From (3.8) we have that the i^{th} row of the linear algebra produces a diagonal coefficient $2\pi - \alpha_i$ and off-diagonal coefficients from

within the term

$$\sum_{\substack{j=0 \\ j=i-1, i}}^{n-1} \text{Im} \left[\frac{\tilde{\mu}_j(t_{j+1}-t_i) - \tilde{\mu}_{j+1}(t_j-t_i)}{t_{j+1}-t_j} \cdot \ell_n \left(\frac{t_{j+1}-t_i}{t_j-t_i} \right) \right] \quad (3.16)$$

Without loss in generality it is again convenient to take $i=0$ and also to simplify the algebra, t_0 will be taken as origin of coordinates

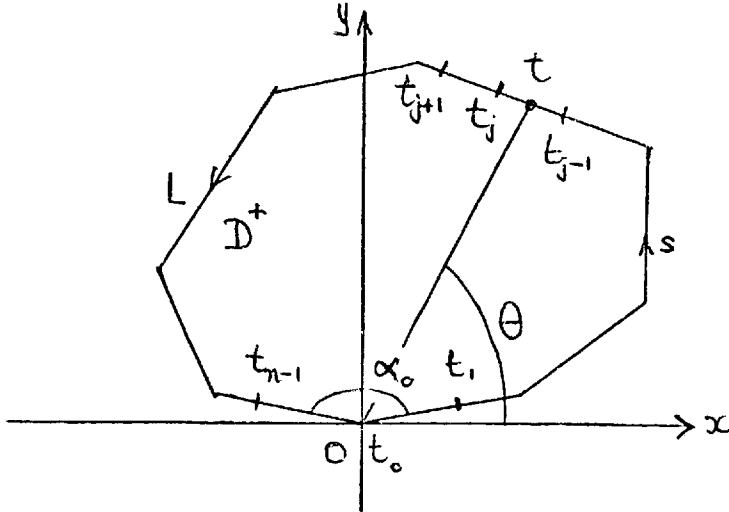


Fig. 43

Thus with (3.8) in matrix form as $K_B \underline{\tilde{\mu}} = \underline{f}$,

$$\underline{\tilde{\mu}} = [\tilde{\mu}_0, \tilde{\mu}_1, \dots, \tilde{\mu}_{n-1}]^T, \quad \underline{f} = [2\pi f(t_0), 2\pi f(t_1), \dots, 2\pi f(t_{n-1})]^T$$

and K_B the $(n \times n)$ coefficient matrix with elements k_{ij} , we are interested in the elements

$$k_{0,0}, k_{0,1}, k_{0,2}, \dots, k_{0,n-1}.$$

Clearly $k_{0,0} = 2\pi - \alpha_0$.

From (3.16), k_{0j} being the coefficient of $\tilde{\mu}_j$ will be

$$\text{Im} \left[\frac{t_{j+1}-t_0}{t_{j+1}-t_j} \cdot \ell_n \left(\frac{t_{j+1}-t_0}{t_j-t_0} \right) - \frac{(t_{j-1}-t_0)}{(t_j-t_{j-1})} \cdot \ell_n \left(\frac{t_{j-1}-t_0}{t_{j-1}-t_0} \right) \right],$$

or remembering that t_0 is taken as zero,

$$k_{0,j} = \text{Im} \left[\frac{t_{j+1}}{t_{j+1}-t_j} \cdot \ell_n \left(\frac{t_{j+1}}{t_j} \right) - \frac{t_{j-1}}{t_j-t_{j-1}} \cdot \ell_n \left(\frac{t_{j-1}}{t_{j-1}} \right) \right] \quad (3.17)$$

This expression applies for $j=2,3, \dots (n-2)$, but due to the special nature of the approximation around $t = t_0$ we have

$$k_{0,1} = \text{Im} \left[\frac{t_2}{t_2 - t_1} \cdot \ln \left(\frac{t_2}{t_1} \right) \right]$$

$$k_{0,n-1} = \text{Im} \left[\frac{-t_{n-2}}{t_{n-1} - t_{n-2}} \cdot \ln \left(\frac{t_{n-1}}{t_{n-2}} \right) \right]$$

Now to establish diagonal dominance it is necessary to compare $|k_{0,0}|$ with $\sum_{j=1}^{n-1} |k_{0,j}|$. Since $0 < \alpha_0 \leq \pi$, $|k_{0,0}| = k_{0,0} = 2\pi - \alpha_0$.

The coefficients k_{0j} stem from the linear interpolation approximation for $\mu(t)$ which gave rise to (3.8). Now it is possible to show that all the k_{0j} are non-negative and this proves to be the key in subsequently demonstrating diagonal dominance. Returning to (3.1) and remembering

that for the moment $t_i = 0$, then the integral term is $\frac{1}{2\pi} \oint_L \frac{\mu(t)}{t} dt$

$$= \frac{1}{2\pi} \oint_L \mu(t) \text{Im} \left(\frac{dt}{t} \right) = \frac{1}{2\pi} \oint_L \mu(t) \frac{d\theta}{ds} ds$$

$$= \frac{1}{2\pi} \sum_{j=1}^{n-2} \int_{s_j}^{s_{j+1}} \mu(t) \frac{d\theta}{ds} ds$$

where s_j is arc measurement at the node whose complex value is t_j ,

$$0 < s_j < S.$$

But with the substitution of a piecewise linear approximation for $\mu(t)$

it is easy to see that the coefficient k_{0j} is given by

$$k_{0j} = \frac{1}{2\pi} \left\{ \int_{s_{j-1}}^{s_j} \frac{d\theta}{ds} \left(\frac{s - s_{j-1}}{s_j - s_{j-1}} \right) ds + \int_{s_j}^{s_{j+1}} \frac{d\theta}{ds} \left(\frac{s_{j+1} - s}{s_{j+1} - s_j} \right) ds \right\}, j=2,3,\dots (n-2)$$

$$k_{0,1} = \frac{1}{2\pi} \int_{s_1}^{s_2} \frac{d\theta}{ds} \left(\frac{s_2 - s}{s_2 - s_1} \right) ds$$

(3.18)

$$\text{and } k_{0,n-1} = \frac{1}{2\pi} \int_{s_{n-2}}^{s_{n-1}} \frac{d\theta}{ds} \left(\frac{s - s_{n-2}}{s_{n-1} - s_{n-2}} \right) ds$$

Now all these k_{qj} are non-negative since

(i) for a convex polygon, $\frac{d\theta}{ds} \geq 0$, $s_1 \leq s \leq s_{n-1}$,

(ii) the quantities in brackets () in (3.18) are always non-negative. In fact of course these quantities are merely the "hat-functions" common in the literature [23], often written as

$$\Phi_j(s) = \begin{cases} \frac{s-s_{j-1}}{s_j-s_{j-1}}, & s_{j-1} \leq s \leq s_j \\ \frac{s_{j+1}-s}{s_{j+1}-s_j}, & s_j \leq s \leq s_{j+1} \end{cases}, \text{ zero elsewhere.}$$

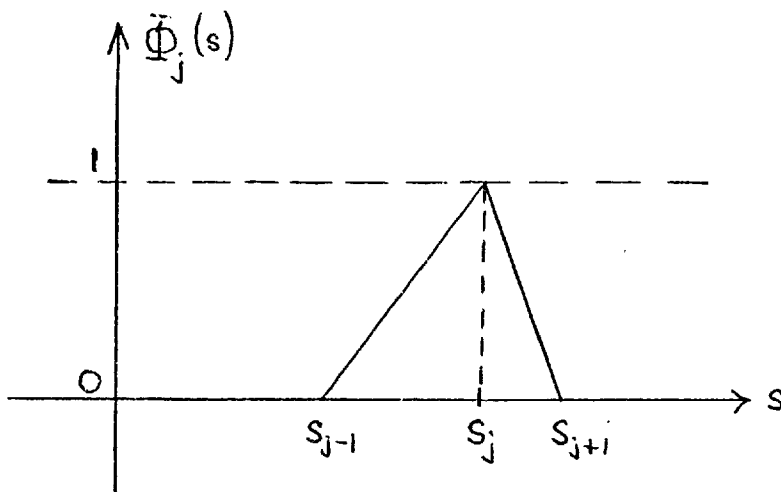


Fig. 44

i.e. each and every k_{qj} is the integral of the product of two non-negative quantities and so the $\{k_{qj}\}_{j=1(1)n-1}$ are non-negative. We can now return to the complex form for k_{qj} in (3.17) which proves to be more convenient to handle.

Having established the non-negativity of the $\{k_{qj}\}$, then the sum of the moduli of the off-diagonal terms

$$= \sum_{j=1}^{n-1} |k_{o,j}| = \sum_{j=1}^{n-1} k_{o,j}$$

$$\begin{aligned}
 &= \text{Im} \left[\frac{t_2}{t_2-t_1} \ell_n \left(\frac{t_2}{t_1} \right) \right] + \sum_{j=2}^{n-2} \text{Im} \left[\frac{t_{j+1}}{t_{j+1}-t_j} \ell_n \left(\frac{t_{j+1}}{t_j} \right) - \frac{t_{j-1}}{t_j-t_{j-1}} \ell_n \left(\frac{t_{j-1}}{t_{j-1}} \right) \right] \\
 &\qquad\qquad\qquad + \text{Im} \left[\frac{-t_{n-2}}{t_{n-1}-t_{n-2}} \ell_n \left(\frac{t_{n-1}}{t_{n-2}} \right) \right] \qquad\qquad\qquad (3.19)
 \end{aligned}$$

Picking out the term in $\ell_n t_j$ gives

$$\begin{aligned}
 &\ell_n t_j \left[\frac{t_j}{t_j-t_{j-1}} - \frac{t_{j+1}}{t_{j+1}-t_j} - \frac{t_{j-1}}{t_j-t_{j-1}} + \frac{t_j}{t_{j+1}-t_j} \right] \\
 &= \ell_n t_j \left[\frac{t_j-t_{j-1}}{t_j-t_{j-1}} - \frac{t_{j+1}-t_j}{t_{j+1}-t_j} \right] = 0.
 \end{aligned}$$

This cancelling of the term in $\ell_n t_j$ is valid for $j=2,3,\dots,n-2$ when all terms of (3.19) are incorporated, leaving

$$\begin{aligned}
 \sum_{j=1}^{n-1} |k_{oj}| &= \text{Im} \left[\frac{-t_2}{t_2-t_1} \ell_n t_1 + \frac{t_1}{t_2-t_1} \ell_n t_1 + \frac{t_{n-1}}{t_{n-1}-t_{n-2}} \ell_n t_{n-1} \frac{t_{n-2}}{t_{n-1}-t_{n-2}} \ell_n t_{n-1} \right] \\
 &= \text{Im} \left[-\ell_n t_1 + \ell_n t_{n-1} \right] = \text{Im} \ell_n \left(\frac{t_{n-1}}{t_1} \right) = \arg \left(\frac{t_{n-1}}{t_1} \right) . \\
 &= \alpha_o
 \end{aligned}$$

But $|k_{o,o}| = 2\pi - \alpha_o$ so that since $\alpha_o \leq \pi$ ($<$ at corner nodal points) then $|k_{o,o}| \geq \sum_{j=1}^{n-1} |k_{oj}|$.

Hence when L is convex we have a diagonally dominant coefficient matrix K_B the representation (3.8), and so similarly to K_A , we know that K_B is non-singular.

Approximation C:

In order to show the diagonal dominance of the matrix derived from (3.14) and (3.15), it will be sufficient to consider (3.14) alone since the analysis of (3.15) will be essentially the same, and as before, without loss of generality, we take $i=0$, and t_o at the origin. Then from (3.14) the off-diagonal terms come from

$$\text{Im} \sum_{j=2}^{n-1} \frac{2}{(t_{2j}-t_{2j-2})^2} \left\{ E \tilde{\mu}_{2j-2} + F \tilde{\mu}_{2j-1} + G \tilde{\mu}_{2j} \right\} \qquad\qquad\qquad (3.20)$$

where $E = t_{2j} t_{2j-1} \ell_n \left(\frac{t_{2j}}{t_{2j-2}} \right) - t_{2j} (t_{2j}-t_{2j-2})$,

$$F = 2(t_{2j} - t_{2j-2})t_{2j-1}^{-2} t_{2j} t_{2j-2} \rho_n \left(\frac{t_{2j}}{t_{2j-2}} \right)$$

and $G = t_{2j-2} t_{2j-1} \rho_n \left(\frac{t_{2j}}{t_{2j-2}} \right) - t_{2j-2} (t_{2j} - t_{2j-2})$

Once again, the required result follows easily once it is shown that the coefficients $\{k_{qj}\}$, $j = 1(1)2n-1$ of the matrix K_C (say) are all positive.

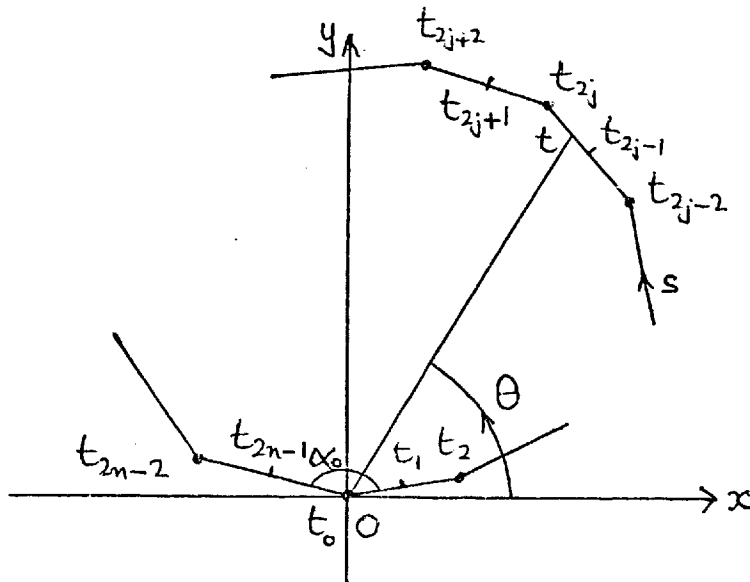


Fig. 45

Specially, we concentrate on $k_{o,2j}$ and $k_{o,2j+1}$ these being the coefficients of μ_{2j} and μ_{2j+1} in (3.14). Casting (3.14) back in terms of real valued expressions will give that $k_{o,2j}$ and $k_{o,2j+1}$ arise from the integrations

$$\int_{s_{2j-2}}^{s_{2j}} \mu(s) \frac{d\theta}{ds} ds + \int_{s_{2j}}^{s_{2j+2}} \mu(s) \frac{d\theta}{ds} ds \quad (3.21)$$

where s measures arc length round the polygon, $0 \leq s \leq S$, initiating at the origin, s_{2j} being arc value at the point on the polygon with complex coordinate t_{2j} . Under quadratic approximation $\mu(s)$ is replaced by quadratic functions along $[s_{2j-2}, s_{2j}]$ and $[s_{2j}, s_{2j+2}]$; and since the polygon is convex, then the kernel $\frac{d\theta}{ds}$ is non-negative for all values of s . In detail now we have that $k_{o,2j}$ is contributed to from both terms in (3.21) while $k_{o,2j+1}$ only from the second. The

piecewise quadratic on $[s_{2j}, s_{2j+2}]$, $s_{2j+1} = \frac{1}{2}(s_{2j} + s_{2j+2})$,

$$h_j = s_{2j+2} - s_{2j+1}$$

$$\text{is } \mu(s) = \frac{(s-s_{2j+1})(s-s_{2j+2})}{2h_j^2} \mu_{2j} + \frac{(s_{2j+2}-s)(s-s_{2j})}{h_j^2} \mu_{2j+1} + \frac{(s-s_{2j})(s-s_{2j+1})}{2h_j^2} \mu_{2j+2}$$

so that we easily obtain

$$\begin{aligned} k_{o,2j+1} &= \int_{s_{2j}}^{s_{2j+2}} \frac{d\theta}{ds} \times \frac{(s_{2j+2}-s)(s-s_{2j})}{h_j^2} ds \\ &= \int_0^S \frac{d\theta}{ds} \Psi_{2j+1}(s) ds \end{aligned} \quad (3.22)$$

$$\text{where } \Psi_{2j+1}(s) = \begin{cases} \frac{(s_{2j+2}-s)(s-s_{2j})}{h_j^2} & , \quad s_{2j} \leq s \leq s_{2j+2}, \\ 0 & , \quad \text{all other } s. \end{cases}$$

It is evident that $\Psi_{2j+1}(s)$ is non-negative on s_{2j}, s_{2j+2} .

Therefore the integrand in (3.22) is the product of two quantities both of which are non-negative, implying that $k_{o,2j+1} \geq 0$ as required.

The similar analysis for $k_{o,2j}$ is not so straight forward. This coefficient has contributions from both terms in (3.21) since the corresponding node links neighbouring piecewise quadratic approximations. However as the treatment of each side is similar it will be sufficient to consider the contribution to $k_{o,2j}$ from $[s_{2j}, s_{2j+2}]$. This part is given by

$$\begin{aligned} k_{o,2j} &= \int_{s_{2j}}^{s_{2j+2}} \frac{d\theta}{ds} \times \frac{(s-s_{2j+1})(s-s_{2j+2})}{2h_j^2} ds \\ &= \int_0^S \frac{d\theta}{ds} \Psi_{2j}^{(R)}(s) ds \end{aligned} \quad (3.23)$$

$$\text{where } \Psi_{2j}^{(R)}(s) = \begin{cases} \frac{(s-s_{2j+1})(s-s_{2j+2})}{2h_j^2} & , \quad s_{2j} \leq s \leq s_{2j+2}, \\ 0 & , \quad \text{all other } s. \end{cases}$$

The other contribution can be written in terms of a function $\Psi_{2j}^{(L)}(s)$ similarly defined.

Unfortunately neither $\Psi^{(L)}$ nor $\Psi^{(R)}$ are entirely non-negative quadratics:-

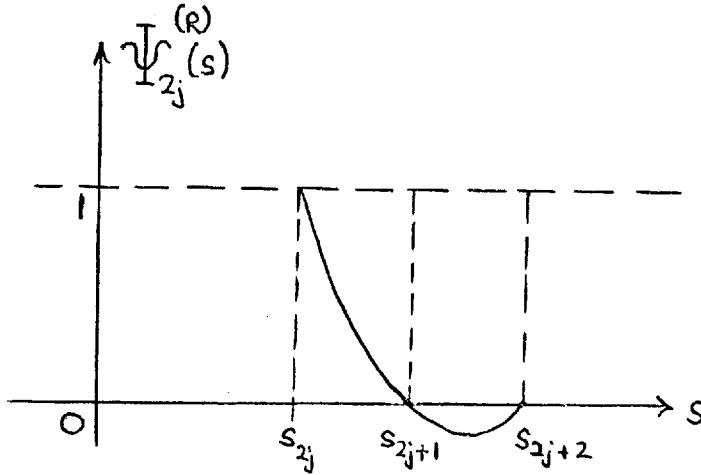


Fig. 46

Hence the investigation concerning the positivity or otherwise of $k_{o,2j}$ must depend on the relative behaviour of the two quantities in the integrand in (3.23), $\frac{d\theta}{ds}$ and $\Psi_{2j}^{(R)}(s)$. Although $\frac{d\theta}{ds}$ is known to be non-negative for all s on $[0, S]$ when the polygon is convex, its exact nature can be easily obtained from simple coordinate geometry.

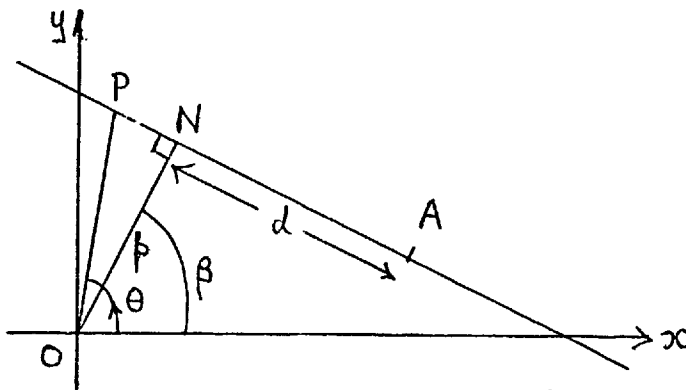


Fig. 47

Since it is the derivative $\frac{d\theta}{ds}$ that we require it will be permissible to measure s for convenience from some point A on a typical boundary line segment ANP (Fig.47), the equation of which is

$$x \cos \beta + y \sin \beta = p, \quad p > 0, \quad 0 \leq \beta \leq \pi.$$

Then if $AP = s$ and $AN = d$ we have

$$\begin{aligned}
 s-d &= p \tan (\theta - \beta) \\
 \frac{ds}{d\theta} &= p \sec^2 (\theta - \beta) = p \left\{ 1 + \frac{(s-d)^2}{p^2} \right\} \\
 \frac{d\theta}{ds} &= \frac{p}{p^2 + (s-d)^2} \tag{3.24}
 \end{aligned}$$

This relation gives that the maximum value of $\frac{d\theta}{ds}$ is $\frac{1}{p}$ and occurs for $s=d$ at the foot of the perpendicular N .

Hence consideration of (3.24) in relation to the behaviour of $\Psi_{2j}^{(R)}(s)$ (see Fig.46) gives that the minimum value of (3.23) will occur when $d = \frac{1}{2}(s_{2j+1} + s_{2j+2})$ i.e. the foot of the perpendicular to the boundary segment $[s_{2j}, s_{2j+2}]$ from the origin of coordinates O will be at the point with arc coordinate $\frac{1}{2}(s_{2j+1} + s_{2j+2})$.

In this case we are interested in

$$\int_0^{2h_j} \frac{p_j}{p_j^2 + (s - \frac{3}{2}h_j)^2} \times \frac{(s-h_j)(s-2h_j)}{2h_j^2} ds, \text{ where } p_j \text{ is the}$$

length of this perpendicular and for convenience of integration s is replaced by $s-s_{2j}$. On completing the integrations, this expression takes the value

$$\frac{p_j}{h_j} - \gamma \left\{ \frac{1}{2} \left(\frac{p_j}{h_j} \right)^2 + \frac{1}{8} \right\} \text{ where } \gamma = \tan^{-1} \left\{ \frac{\frac{h_j}{2} \frac{p_j}{h_j}}{1 - \frac{3}{4} \frac{h_j}{2} \frac{p_j}{h_j}} \right\} \tag{3.25}$$

is the angle subtended by the segment $[s_{2j}, s_{2j+2}]$ at O .

Now for any given convex polygonal boundary shape, the value of h_j can be made as small as is necessary in comparison to p_j by introducing more boundary nodes. Thus writing $q = \frac{h_j}{p_j}$, the sign of (3.25) can be investigated from the expansion in powers of q of

$$\begin{aligned}
 & \frac{1}{q} - \left(\frac{1}{8} + \frac{1}{2q^2}\right) \tan^{-1} \left(\frac{2q}{1 - \frac{3q^2}{4}} \right) \\
 &= \frac{1}{q} - \left(\frac{1}{8} + \frac{1}{2q^2}\right) \left\{ \left(\frac{2q}{1 - \frac{3q^2}{4}} \right) - \frac{1}{3} \left(\frac{2q}{1 - \frac{3q^2}{4}} \right)^3 \dots \right. \\
 &= \frac{1}{q} - \left(\frac{1}{8} + \frac{1}{2q^2}\right) \left\{ 2q \left(1 - \frac{3q^2}{4}\right)^{-1} - \frac{8q^3}{3} \left(1 - \frac{3q^2}{4}\right)^{-3} + o(q^5) \right\} \\
 &= \frac{1}{q} - \left(\frac{1}{8} + \frac{1}{2q^2}\right) \left(2q - \frac{7q^3}{6} + o(q^5)\right) \\
 &= \left(\frac{1}{q} - \frac{1}{q}\right) + \frac{1}{3} q + o(q^3) = \frac{1}{3} q + o(q^3) \tag{3.26}
 \end{aligned}$$

(3.26) shows that neglecting $q^3 = \left(\frac{h_j}{p_j}\right)^3$ then the value of the required integral is positive. Hence we claim that this contribution to $k_{o,2j}$ can be taken as positive provided that h_j is sufficiently small; and this can always be achieved through taking extra node points. In fact by direct calculation of (3.25) when $h_j = \frac{1}{2} p_j$, it can be verified that the result is positive. It is clear that the other contribution to $k_{o,2j}$ through consideration of the function $\Psi_{2j}^{(L)}(s)$ will behave in a similar manner and hence we proceed with the investigation of the diagonal dominance of the matrix K_C taking all its elements to be non-negative.

Taking the off-diagonal coefficients $\{k_{o,j}\}$, $j = 1(1)2n-1$, we have

$$\begin{aligned}
 \sum_{j=1}^{2n-1} |k_{o,j}| &= \sum_{j=1}^{2n-1} k_{o,j} \\
 &= \text{Im} \sum_{j=2}^{n-1} \frac{2}{(t_{2j} - t_{2j-2})^2} (E + F + G) \text{ from (3.20)}
 \end{aligned}$$

by putting $\tilde{\mu}_j = 1$, $j = 2(1)2n-2$,

$$= \text{Im} \sum_{j=2}^{n-1} \left\{ \frac{2}{(t_{2j} - t_{2j-2})^2} \left[t_{2j} t_{2j-1} \ell_n \left(\frac{t_{2j}}{t_{2j-2}} \right) - t_{2j} (t_{2j} - t_{2j-2}) \right] \right\}$$

$$\left. \begin{aligned} &+ 2(t_{2j} - t_{2j-2}) t_{2j-1} - 2t_{2j} t_{2j-2} \ell_n \left(\frac{t_{2j}}{t_{2j-2}} \right) \\ &+ t_{2j-2} t_{2j-1} \ell_n \left(\frac{t_{2j}}{t_{2j-2}} \right) - t_{2j-2} (t_{2j} - t_{2j-2}) \end{aligned} \right\} .$$

Making use of $t_{2j-1} = \frac{1}{2} (t_{2j-2} + t_{2j})$, this simplifies to

$$\begin{aligned} & \operatorname{Im} \sum_{j=2}^{n-1} \frac{2}{(t_{2j} - t_{2j-2})^2} \left\{ \frac{(t_{2j} + t_{2j-2})^2}{2} \ell_n \left(\frac{t_{2j}}{t_{2j-2}} \right) - 2t_{2j} t_{2j-2} \ell_n \left(\frac{t_{2j}}{t_{2j-2}} \right) \right\} \\ &= \operatorname{Im} \sum_{j=2}^{n-1} \frac{2}{(t_{2j} - t_{2j-2})^2} \cdot \frac{(t_{2j} - t_{2j-2})^2}{2} \cdot \ell_n \left(\frac{t_{2j}}{t_{2j-2}} \right) \\ &= \operatorname{Im} \sum_{j=2}^{n-1} \ell_n \left(\frac{t_{2j}}{t_{2j-2}} \right) = \operatorname{Im} (\ell_n t_{2n-2} - \ell_n t_2) \\ &= \alpha_0 \text{ (see fig.45)} \end{aligned}$$

But the diagonal term = $2\pi - \alpha_{2i-2}$ (by (3.14))

= $2\pi - \alpha_0$ in this case, and so the diagonal

coefficient is greater than or equal to the sum of the moduli of the diagonal coefficients; equality being achieved when t_0 lies on a straight portion of boundary, but inequality must occur at least three times for various t_0 . This establishes the diagonal dominance of K_C similar to K_A and K_B .

To summarise, when the polygon is convex, the discrete solution $\tilde{u}(t_i)$ can always be calculated since each of K_A , K_B and K_C is non-singular. For non-convex polygons this claim cannot be made since for at least one nodal position, one row of the matrix will not be diagonally dominant.

3.4 Convergence

Having constructed three different ways of approximating solutions of (3.3), we now consider whether the computed density function $\tilde{\mu}$ calculated at points on the boundary L will converge to the theoretical solution as the number of boundary nodes increases

i.e. whether
$$\lim_{n \rightarrow \infty} |\mu(t_i) - \tilde{\mu}(t_i)| = 0,$$

for each $i=1,2,\dots,n$.

The analysis will be similar in all three cases but for clarity we shall examine in detail approximation A first. This means a comparison must be made between the values $\mu(t_i)$ satisfying equation (3.3):-

$$(2\pi - \alpha_i) \mu(t_i) + \text{Im} \sum_{\substack{j=0 \\ j \neq i-1, i}}^{n-1} \int_{t_j}^{t_{j+1}} \frac{\mu(t)}{t-t_i} dt = 2\pi f(t_i) \quad (3.27)$$

and the values $\tilde{\mu}(t_i)$ satisfying the approximate form

$$(2\pi - \alpha_i) \tilde{\mu}(t_i) + \text{Im} \sum_{\substack{j=0 \\ j \neq i-1, i}}^{n-1} \frac{1}{2} \{ \tilde{\mu}(t_j) + \tilde{\mu}(t_{j+1}) \} \int_{t_j}^{t_{j+1}} \frac{dt}{t-t_i} = 2\pi f(t_i) \quad (3.28)$$

obtained from (3.4) by re-expressing it in complex form.

Now (3.27) can be written in the form

$$\begin{aligned} & (2\pi - \alpha_i) \mu(t_i) + \text{Im} \sum_{\substack{j=0 \\ j \neq i-1, i}}^{n-1} \frac{1}{2} \{ \mu(t_j) + \mu(t_{j+1}) \} \int_{t_j}^{t_{j+1}} \frac{dt}{t-t_i} \\ & = 2\pi f(t_i) + \text{Im} \sum_{\substack{j=0 \\ j \neq i-1, i}}^{n-1} \left[\frac{1}{2} \{ \mu(t_j) + \mu(t_{j+1}) \} \int_{t_j}^{t_{j+1}} \frac{dt}{t-t_i} - \int_{t_j}^{t_{j+1}} \frac{\mu(t)}{t-t_i} dt \right] \end{aligned}$$

where the imaginary part of the expression in square brackets here represents the local truncation error for approximation A when integration along $[t_j, t_{j+1}]$ is replaced by quadrature. Representing the expression by r_{ij} and then the aggregate $\text{Im} \sum_{\substack{j=0 \\ j \neq i-1, i}}^{n-1} r_{ij}$ by r_i ,

we now have

$$(2\pi - \alpha_i) \mu(t_i) + \text{Im} \sum_{\substack{j=0 \\ j \neq i-1, i}}^{n-1} \frac{1}{2} \{ \mu(t_j) + \mu(t_{j+1}) \} \int_{t_j}^{t_{j+1}} \frac{dt}{t-t_i} = 2\pi f(t_i) + r_i \quad (3.29)$$

Subtracting (3.29) and (3.28) gives

$$(2\pi - \alpha_i) e(t_i) + \text{Im} \sum_{\substack{j=0 \\ j \neq i-1, i}}^{n-1} \frac{1}{2} \{ e(t_j) + e(t_{j+1}) \} \int_{t_j}^{t_{j+1}} \frac{dt}{t-t_i} = r_i \quad (3.30)$$

where $e(t_i) = \mu(t_i) - \tilde{\mu}(t_i)$.

But with $i=0(1)n-1$, (3.30) is a set of n linear equations for the

determination of the error vector \underline{e} with components $e(t_i) = \mu(t_i) - \tilde{\mu}(t_i)$.

Moreover the coefficient matrix of the set ^{is} the same as that in (3.4)

itself, proven earlier to be weakly diagonally dominant with non-negative elements. Thus in matrix form (3.30) becomes

$$K_A \underline{e} = \underline{r}$$

where \underline{r} is the vector

whose i^{th} component is given by r_i .

To evaluate r_i consider first the contribution r_{ij} due to the single boundary segment $[t_j, t_{j+1}]$. For convenience let the segment be taken as the interval $[-h, h]$ of the x axis on the Oxy plane. Thus t_j is assigned to $-h$, t_{j+1} to $+h$ and we take t_i as the remote complex point z , (Fig.48). Introduce the notation $R_A[\mu(t)]$ to represent the operation

$$\text{Im} \left\{ - \int_{-h}^h \frac{\mu(t)}{t-z} dt + \frac{1}{2} (\mu(-h) + \mu(h)) \int_{-h}^h \frac{dt}{t-z} \right\}.$$

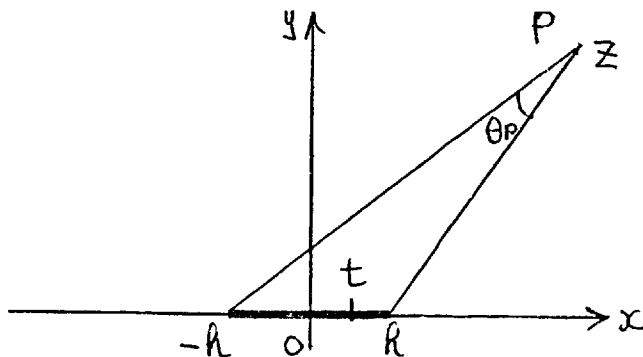


Fig. 48

Then the evaluation of $R_A[\mu(t)]$ will enable the local truncation error for approximation A to be measured.

Now we note that (3.27) applies generally for all t_i on L. Thus for an internodal boundary point with complex coordinate

$\tau = x(s) + iy(s)$, we have

$$\pi \mu(\tau) + \text{Im} \sum_{j=0}^{n-1} \int_{t_j}^{t_{j+1}} \frac{\mu(t)}{t-\tau} dt = 2\pi f(\tau), \quad (3.31)$$

where the summation omits the boundary segment containing τ . If we assume the boundary function f is differentiable at an internodal point, then (3.31) can be differentiated along the direction s of the boundary to give

$$\begin{aligned} \pi \mu'(\tau) \{x'(s) + iy'(s)\} + \text{Im} \sum_{j=0}^{n-1} \int_{t_j}^{t_{j+1}} \frac{\mu(t)}{(t-\tau)^2} \{x'(s) + iy'(s)\} dt \\ = 2\pi f'(\tau) \{x'(s) + iy'(s)\}. \end{aligned}$$

Thus $\mu'(\tau)$ exists and, in fact, assuming f is sufficiently differentiable, further differentiation will give the existence of $\mu''(\tau)$ and $\mu'''(\tau)$ for all points τ on the interior of a boundary segment. It is further assumed that these derivatives remain bounded as τ approaches a corner point of L from either side.

Returning to the evaluation of $R_A[\mu(t)]$, the first mean value theorem may then be applied to give

$$\mu(t) = \mu(0) + t\mu'(\tau), \quad 0 < \tau(t) < t. \quad (\text{Fig.48})$$

Thus since R_A is a linear operator we have

$$\begin{aligned} R_A[\mu(t)] &= R_A[\mu(0)] + R_A[t\mu'(\tau)] \\ &= R_A[t\mu'(\tau)] \quad \text{since } R_A \text{ is exact when used on a} \end{aligned}$$

constant.

$$\begin{aligned} \therefore R_A[\mu(t)] &= \text{Im} \left[- \int_{-h}^h \frac{t \mu'(\tau)}{t-z} dt + \frac{1}{2} \{ -h \mu'(\tau(-h)) + h \mu'(\tau(h)) \} \int_{-h}^h \frac{dt}{t-z} \right] \\ &= - \int_{-h}^h t \mu'(\tau) \text{Im} \left(\frac{1}{t-z} \right) dt - \frac{1}{2} h \mu'(\tau(-h)) \int_{-h}^h \text{Im} \left(\frac{1}{t-z} \right) dt \\ &\quad + \frac{1}{2} h \mu'(\tau(h)) \int_{-h}^h \text{Im} \left(\frac{1}{t-z} \right) dt . \end{aligned}$$

Now by direct integration $\int_{-h}^h \text{Im} \left(\frac{1}{t-z} \right) dt = \theta_p$ (see Fig.48).

Hence if $M'_h = \max_{(-h,h)} |\mu'(t)|$, then

$$|R_A(\mu(t))| \leq h M'_h \theta_p + \frac{1}{2} h M'_h \theta_p + \frac{1}{2} h M'_h \theta_p = 2 h M'_h \theta_p . \quad (3.32)$$

Returning to the term r_i , this is now easily bounded since it is the sum of $(n-2)$ terms of type (3.32).

Let $M' = \sup_j M'_h$ and $H = \max_j |t_{j+1} - t_j|$ where $h_j = |t_{j+1} - t_j|$;

$$\begin{aligned} \text{then } |r_i| &\leq M'H \times (\text{total angle subtended at node } t_i) \\ &= M'H \alpha_i \end{aligned}$$

and this quantity can be made as small as desired by increasing n and so decreasing H . Now although this analysis just described applies only to approximation A, it is simple to carry across the ideas to approximations B and C as well. In the case of B we are comparing the exact equation (3.27) with the approximate form (3.8):-

$$(2\pi - \alpha_i) \tilde{\mu}(t_i) + \text{Im} \sum_{\substack{j=0 \\ j \neq i-1, i}}^{n-1} \left\{ \frac{\tilde{\mu}(t_j)(t_{j+1} - t_i) - \tilde{\mu}(t_{j+1})(t_j - t_i)}{t_{j+1} - t_j} \ell_n \left(\frac{t_{j+1} - t_i}{t_j - t_i} \right) \right\} = 2\pi f(t_i)$$

By similar manipulations to those above we shall arrive at the equation for the error which is the counterpart of (3.30),

$$(2\pi - \alpha_i) e(t_i) + \text{Im} \sum_{\substack{j=0 \\ j \neq i-1, i}}^{n-1} \left\{ \frac{e(t_j)(t_{j+1}-t_i) - e(t_{j+1})(t_j-t_i)}{t_{j+1} - t_j} \ell_n \left(\frac{t_{j+1}-t_i}{t_j-t_i} \right) \right\} = \text{Im} \sum_{\substack{j=0 \\ j \neq i-1, i}}^{n-1} r_{ij},$$

(3.33)

where $r_{ij} = \frac{\mu_j(t_{j+1}-t_i) - \mu_{j+1}(t_j-t_i)}{t_{j+1} - t_j} \ell_n \left(\frac{t_{j+1}-t_i}{t_j-t_i} \right) - \int_{t_j}^{t_{j+1}} \frac{\mu(t)}{t-t_i} dt .$

But again with $i = O(1)n-1$, (3.33) is a set of linear equations for the determination of $e_i = \mu_i - \tilde{\mu}_i$ having the matrix form $K_B e = \underline{r}$, the coefficient matrix K_B being identical with that in (3.8), proven earlier to be weakly diagonally dominant with positive elements.

Hence the only problem is concerned with evaluating the truncation error $\text{Im} \sum_{\substack{j=0 \\ j=i-1, i}}^{n-1} r_{ij}$. This is best done by again arranging for the

interval $[t_j, t_{j+1}]$ to coincide with the interval $[-h, h]$ of the x axis, and defining

$$R_B[\mu(t)] = \text{Im} \left[\int_{-h}^h \frac{(h-t)\mu(-h) + (h+t)\mu(h)}{2h} \frac{dt}{t-z} - \int_{-h}^h \frac{\mu(t)}{t-z} dt \right],$$

recalling that the first integral was evaluated as in (3.8).

We write $R_B[\mu(t)] = \text{Im} \left[- \int_{-h}^h \frac{\mu(t)}{t-z} dt + \{ U\mu(-h) + V\mu(h) \} \right]$ (3.34)

where $U = \frac{1}{2h} \int_{-h}^h \frac{h-t}{t-z} dt$ and $V = \frac{1}{2h} \int_{-h}^h \frac{h+t}{t-z} dt .$

Now using Taylor's theorem to expand $\mu(t)$ we have

$$\mu(t) = \mu(0) + t\mu'(0) + \frac{1}{2}t^2\mu''(\tau) , \quad \tau = \tau(t) < t, \quad \text{the}$$

existence of μ'' justified from differentiating (3.31). Also there is no error when (3.34) is applied to a linear function, so

$$\begin{aligned}
 R_B[\mu(t)] &= R_B[\mu(0)] + R_B[t\mu'(0)] + R_B\left[\frac{1}{2}t^2\mu''(\tau)\right] \\
 &= R_B\left[\frac{1}{2}t^2\mu''(\tau)\right] \\
 &= \text{Im}\left[-\int_{-h}^h \frac{\frac{1}{2}t^2\mu''(\tau)}{t-z} dt + U.\frac{1}{2}h^2\mu''(\tau(-h)) + V.\frac{1}{2}h^2\mu''(\tau(h))\right] \\
 &= -\int_{-h}^h \frac{1}{2}t^2\mu''(\tau) \text{Im}\left(\frac{1}{t-z}\right) dt + \frac{1}{2}h^2\mu''(\tau(-h)) \text{Im}(U) \\
 &\qquad\qquad\qquad + \frac{1}{2}h^2\mu''(\tau(h)) \text{Im}(V) \quad (\text{see Fig.48})
 \end{aligned}$$

Now let $M_h'' = \max_{(-h,h)} |\mu''(t)|$.

Then $\left| R_B[\mu(t)] \right| \leq \frac{1}{2}h^2 M_h'' \theta_p + \frac{1}{2}h^2 M_h'' \left| \text{Im}(U) \right| + \frac{1}{2}h^2 M_h'' \left| \text{Im}(V) \right|$

But $\left| \text{Im}(U) \right| = \left| \frac{1}{2h} \int_{-h}^h (h-t) \text{Im}\left(\frac{1}{t-z}\right) dt \right| = \frac{1}{2h} \int_{-h}^h (h-t) \text{Im}\left(\frac{1}{t-z}\right) dt$ since

on $[-h, h]$, $h \gg t$ and $\text{Im}\left(\frac{1}{t-z}\right)$ is positive taking z in the upper half plane. (Fig.48)

Similarly $\left| \text{Im}(V) \right| = \left| \frac{1}{2h} \int_{-h}^h (h+t) \text{Im}\left(\frac{1}{t-z}\right) dt \right|$ so that

$$\left| \text{Im}(V) \right| = \frac{1}{2h} \int_{-h}^h (h+t) \text{Im}\left(\frac{1}{t-z}\right) dt .$$

$$\therefore \left| \text{Im}(U) \right| + \left| \text{Im}(V) \right| = \frac{1}{2h} \int_{-h}^h 2h \text{Im}\left(\frac{1}{t-z}\right) dt = \theta_p$$

$$\therefore R_B[\mu(t)] \leq \frac{1}{2}h^2 M_h'' \theta_p = M_h'' h^2 \theta_p \quad (3.35)$$

Finally we can bound $\text{Im} \sum_{\substack{j=0 \\ j \neq i-1, i}}^{n-1} r_{ij} = r_i$ since it is the sum

of $(n-2)$ terms such as (3.35). Taking $M'' = \sup_j M_h''$ and H as

before, we have

$$\begin{aligned}
 \left| r_i \right| &\leq M'' H^2 \alpha_i \quad (\text{total angle subtended at node } t_i) \\
 &= M'' H^2 \alpha_i
 \end{aligned}$$

This quantity can be made as small as desired by increasing n and thus decreasing H .

Finally, for the quadratic approximation C, we are comparing (3.27) with (3.14), (3.15). Although the algebra looks more formidable, the nature of (3.14) and (3.15) has been investigated so that it suffices to comment that by similar manipulation prior to (3.30) and (3.33) we arrive at the error equation

$$K_C \underline{e} = \underline{r} \tag{3.36}$$

where $\underline{e} = (e_1, e_2, \dots, e_i, \dots, e_{2n})^T$, $e_i = e(t_i) = \mu(t_i) - \tilde{\mu}(t_i)$.

K_C is the matrix resulting from the quadratic interpolation, shown earlier to be weakly diagonally dominant,

$$\underline{r} = (r_1, r_2, \dots, r_{2n})^T \text{ where } r_i = \text{Im} \sum_{j=1}^{2n} r_{ij} = \sum_{j=1}^{2n} \text{Im}(r_{ij})$$

and $\text{Im}(r_{ij})$ is the truncation error resulting from the replacement

$$\text{of } \int_{t_{2j-2}}^{t_{2j}} \frac{\mu(t)}{t-t_i} dt \text{ by } \frac{2}{(t_{2j}-t_{2j-2})^2} \left\{ E \mu_{2j-2} + F \mu_{2j-1} + G \mu_{2j} \right\}$$

as given in (3.13).

Calculation of this truncation error is again handled by taking the j^{th} boundary segment t_{2j-2}, t_{2j} to be on the real x axis, $-h \leq x \leq h$. Then t_i is taken as the remote complex point z . Referring to Fig. 48, $\mu(t)$ is replaced by the quadratic function interpolating $\mu(ih)$, $i=-1, 0, 1$. It is easily seen that

$$\mu(t) = \frac{t(t-h)}{2h^2} \mu(-h) + \frac{(h^2-t^2)}{h^2} \mu(0) + \frac{t(t+h)}{2h^2} \mu(h)$$

$$\text{and hence } \text{Im} \int_{-h}^h \frac{\mu(t)}{t-z} dt = \text{Im} \left[\int_{-h}^h \left\{ \frac{t(t-h)}{2h^2} \mu(-h) + \frac{(h^2-t^2)}{h^2} \mu(0) + \frac{t(t+h)}{2h^2} \mu(h) \right\} \frac{dt}{t-z} \right]$$

$$= \text{Im} \frac{1}{2h^2} \left[\mu(-h) \int_{-h}^h \frac{t(t-h)}{t-z} dt + \mu(0) \int_{-h}^h \frac{2(h^2-t^2)}{t-z} dt + \mu(h) \int_{-h}^h \frac{t(t+h)}{t-z} dt \right]$$

which we denote for simplicity as $\text{Im} \frac{1}{2h^2} \left[U \mu(-h) + V \mu(0) + W \mu(h) \right]$.

Following earlier notations the truncation error is

$$R_C[\mu(t)] = \text{Im} \left[- \int_{-h}^h \frac{\mu(t)}{t-z} dt + \frac{1}{2h^2} \{ U\mu(-h) + V\mu(0) + W\mu(h) \} \right] \quad (3.37)$$

But (3.37) measures truncation error in the case where μ is approximated by a quadratic and so is zero when $\mu(t)$ is quadratic.

Further on $[-h, h]$ we can write

$$\mu(t) = \mu(0) + t\mu'(0) + \frac{1}{2}t^2\mu''(0) + \frac{1}{6}t^3\mu'''(\tau), \quad 0 < \tau(t) < t,$$

the existence of μ''' following from differentiating (3.31) and the assumption that the boundary function f is three times differentiable at internodal points.

$$\begin{aligned} R_C[\mu(t)] &= R_C \left[\mu(0) + t\mu'(0) + \frac{1}{2}t^2\mu''(0) \right] + R_C \left[\frac{1}{6}t^3\mu'''(\tau) \right] \\ &= R_C \left[\frac{1}{6}t^3\mu'''(\tau) \right] \\ &= \text{Im} \left[\int_{-h}^h - \frac{\frac{1}{6}t^3\mu'''(\tau)}{t-z} dt + \frac{U}{2h^2} \cdot \frac{1}{6}h^3\mu'''(\tau(-h)) + \frac{V}{2h^2} \cdot 0 + \frac{W}{2h^2} \cdot \frac{1}{6}h^3\mu'''(\tau(h)) \right] \\ &= \int_{-h}^h - \frac{1}{6}t^3\mu'''(\tau) \text{Im} \left(\frac{1}{t-z} \right) dt + \frac{1}{12}h\mu'''(\tau(-h)) \cdot \text{Im}(U) + \frac{1}{12}h\mu'''(\tau(h)) \cdot \text{Im}(W) \end{aligned}$$

Now let $M_h''' = \max_{(-h, h)} |\mu'''(t)|$

$$\left| R_C[\mu(t)] \right| \leq \frac{1}{6}h^3 M_h''' \theta_p + \frac{hM_h'''}{12} \left| \text{Im}(U) \right| + \frac{hM_h'''}{12} \left| \text{Im}(W) \right| \quad (\text{Fig.48})$$

$$\text{But } \left| \text{Im}(U) \right| + \left| \text{Im}(W) \right| = \left| \text{Im} \int_{-h}^h \frac{t(t-h)}{t-z} dt \right| + \left| \text{Im} \int_{-h}^h \frac{t(t+h)}{t-z} dt \right|$$

$$= \left| \int_{-h}^h t(t-h) \text{Im} \left(\frac{1}{t-z} \right) dt \right| + \left| \int_{-h}^h t(t+h) \text{Im} \left(\frac{1}{t-z} \right) dt \right|$$

$$< 2h^2 \int_{-h}^h \left| \text{Im} \left(\frac{1}{t-z} \right) \right| dt + 2h^2 \int_{-h}^h \left| \text{Im} \left(\frac{1}{t-z} \right) \right| dt$$

$$= 4h^2 \theta_p$$

$$\left| R_C[\mu(t)] \right| \leq \frac{1}{6} h^3 M_h''' \theta_p + \frac{1}{12} h M_h''' 4h^2 \theta_p = \frac{1}{2} h^3 M_h''' \theta_p \quad (3.38)$$

Hence finally with r_i being the sum of $(2n)$ such terms it is clear that $|r_i| \leq \frac{1}{2} H^3 M''' \alpha_i$,

where $M''' = \sup_j M_{h_j}'''$, $2H$ the greatest step width and α_i the

total angle subtended at the node t_i .

As before this quantity can be made as small as required by increasing the number of node points n so that $H \rightarrow 0$.

To complete the argument we must now show that $\underline{e} \rightarrow 0$ as $n \rightarrow \infty$.

In all three approximations we have essentially the same equation for the error vector, namely $\underline{K}\underline{e} = \underline{r}$ where we can take the matrix K , representing K_A, K_B and K_C in the form

$$\begin{pmatrix} 2\pi - \alpha_0 & \alpha_{01} & \alpha_{02} & \dots & \alpha_{0,n-1} \\ \alpha_{10} & 2\pi - \alpha_1 & \alpha_{12} & \dots & \alpha_{1,n-1} \\ \alpha_{20} & \alpha_{21} & 2\pi - \alpha_2 & \dots & \alpha_{2,n-1} \\ \cdot & \cdot & \cdot & \cdot & \cdot \\ \cdot & \cdot & \cdot & \cdot & \cdot \\ \alpha_{n-1,0} & \alpha_{n-1,1} & \alpha_{n-1,2} & \dots & 2\pi - \alpha_{n-1} \end{pmatrix}$$

$$0 < \alpha_i \leq \pi, \quad \sum_{\substack{j=0 \\ (j \neq i)}}^{n-1} |\alpha_{ij}| = \sum_{\substack{j=0 \\ (j=i)}}^{n-1} \alpha_{ij} = \alpha_i, \quad i = 0(1)n-1.$$

since all α_{ij} are non-negative. (In approximation C the count is carried to $2n$, but this will not affect the general argument). Also since we are now concerned with the behaviour of K, \underline{e} and \underline{r} as n increases it is convenient to write the error equation as

$$K_n \underline{e}_n = \underline{r}_n \quad (3.39)$$

We know that K_n has an inverse for all n , but the question remains whether the norm of this inverse is bounded as $n \rightarrow \infty$. If this is so then writing

$$\underline{e}_n = K_n^{-1} r_n$$

and taking some appropriate norm gives

$$\| \underline{e}_n \| = \| K_n^{-1} r_n \| \leq \| K_n^{-1} \| \cdot \| r_n \| \quad (3.40)$$

To investigate the required bound on K_n^{-1} we recall first the standard theorem on bounded linear operators ([24]pp.233) that "if \mathcal{L} is a bounded linear operator mapping a normed space X into a normed space Y , then a necessary and sufficient condition for \mathcal{L}^{-1} to exist and be a bounded linear operator in Y_1 , the range of \mathcal{L} , is that there exists a constant $m > 0$ such that for all elements $x \in X, \|x\| = 1$,

$$\| \mathcal{L} x \| \geq m, \text{ in which case } \| \mathcal{L}^{-1} \| \leq \frac{1}{m}."$$

In our situation, K_n is a bounded linear operator mapping R_n into itself. Moreover taking the maximum norm defined by

$$\| \underline{x} \| = \| \underline{x} \|_{\infty} = \max_i |x_i|, \text{ where } \underline{x} = (x_0, x_1, \dots, x_{n-1}) \in R_n$$

$$\text{and } \| K_n \| = \| K_n \|_{\infty} = \max_i \sum_{j=0}^{n-1} |k_{ij}|, \text{ the maximum absolute row}$$

sum, then we see from the nature of K_n that

$$\| K_n \|_{\infty} = 2\pi, \text{ independent of the increase in } n.$$

Now consider the quantity $\| K_n \underline{x} \|_{\infty}$ where $\| \underline{x} \|_{\infty} = 1$. From the form of K_n we see that

$$\begin{aligned} \| K_n \underline{x} \|_{\infty} = \max_i & \left| \alpha_{i0} x_0 + \alpha_{i,1} x_1 + \dots + \alpha_{i,i-1} x_{i-1} \right. \\ & \left. + (2\pi - \alpha_i) x_i + \alpha_{i,i+1} x_{i+1} + \dots + \alpha_{i,n-1} x_{n-1} \right| \quad (3.41) \end{aligned}$$

The values of this expression are to be investigated over all possible \underline{x} such that $\|\underline{x}\|_\infty = 1$. Thus it is maximised by taking, without loss in generality, $x_i = +1$ and α_i as the minimum corner interior angle which we denote by α . Then with regard to the above theorem, the required value of the constant m will be achieved by considering the $\min_{\underline{x}} \left\| K_n \underline{x} \right\|_\infty$; and this occurs by taking $x_0 = x_1 = \dots = x_{i-1} = x_{i+1} = \dots = x_{n-1} = -1$ in (3.41) so that

$$\begin{aligned} & \min_{\underline{x}} \max_i \left| \alpha_{i,0} x_0 + \dots + (2\pi - \alpha_i) x_i + \dots + \alpha_{i,n-1} x_{n-1} \right| \\ &= 2\pi - \alpha - (\alpha_{i,0} + \alpha_{i,1} + \dots + \alpha_{i,i-1} + \alpha_{i,i+1} + \dots + \alpha_{i,n-1}) \\ &= 2\pi - 2\alpha = 2\beta \quad (\text{where } \beta \text{ is the greatest exterior angle} \\ & \text{of the polygon}). \end{aligned}$$

Thus $\left\| K_n \underline{x} \right\|_\infty \geq 2\beta$ and so $\left\| K_n^{-1} \right\| \leq \frac{1}{2\beta}$. Returning to (3.40) we now have, using the maximum norm, that

$$\left\| \underline{e}_n \right\|_\infty \leq \frac{1}{2\beta} \left\| \underline{r}_n \right\|_\infty \tag{3.42}$$

But $\left\| \underline{r}_n \right\|_\infty = \max_{0 \leq i \leq n-1} |r_i|$ where we recall from the truncation error analysis that for approximation A, $|r_i| \leq M'H\alpha_i$, for approximation B, $|r_i| \leq M''H^2\alpha_i$ and for approximation C, $|r_i| \leq \frac{1}{2}M'''H^3\alpha_i$ where α_i is the interior angle of the polygon at the node t_i .

$$\begin{aligned} \text{Thus for approximation A, } & \left\| \underline{e}_n \right\|_\infty \leq \frac{1}{2\beta} M'H\pi, \\ \text{approximation B, } & \left\| \underline{e}_n \right\|_\infty \leq \frac{1}{2\beta} M''H^2\pi \\ \text{and approximation C, } & \left\| \underline{e}_n \right\|_\infty \leq \frac{1}{2\beta} \frac{1}{2}M'''H^3\pi. \end{aligned} \tag{3.43}$$

As n increases, H will decrease as required and we conclude that $\left\| \underline{e}_n \right\|_\infty \rightarrow 0$ as $n \rightarrow \infty$ for each of the cases A, B and C. Thus the convergence of $\tilde{\mu}(t_i)$ to $\mu(t_i)$ is established.

§ 3.5 Error in Calculation of internal potential function $u(x,y)$

The ultimate aim of the proposed numerical methods is to calculate reliable approximate values of the potential function $u(x,y)$ at internal points $\in D^+$; and having analysed the behaviour of the approximations $\tilde{\mu}(t)$ to the boundary density $\mu(t)$ we are now in a position to examine the reliability of the subsequent calculation of the internal potential. Denoting the calculated quantity by $\tilde{u}(x,y)$ and the exact by $u(x,y)$ then we are interested in obtaining some measure of the error between the two quantities

$$\text{i.e. } |u(x,y) - \tilde{u}(x,y)|, \quad (x,y) \in D^+.$$

Now in order to evaluate $\tilde{u}(x,y)$, we merely return to (1.17) or its equivalent and write

$$\tilde{u}(x,y) = \frac{1}{2\pi} \oint_L \tilde{\mu}(s) d\theta, \quad 0 \leq s \leq S, \quad (3.44)$$

(see Fig.11). Having completed the earlier calculations given by the various approximations for $\tilde{\mu}(s)$, then the integral in (3.44) can be evaluated by "filling in" values of $\tilde{\mu}$ at points on the boundary L of the polygon between nodal points according to whether approximation A,B, or C has been pursued. We can then write from (3.44)

$$\tilde{u}(x,y) = \frac{1}{2\pi} \sum_{j=0}^{n-1} \int_{s_j}^{s_{j+1}} \tilde{\mu}(s) d\theta \quad (3.45)$$

where a typical integration along the straight boundary segment between nodes at s_j and s_{j+1} can be carried out exactly as appropriate to the three approximations.

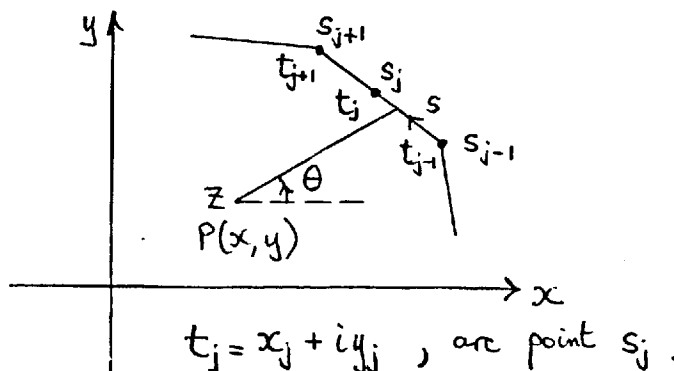


Fig. 49

i.e. for A, where μ was approximated by a piecewise constant,

$$\text{we have } \int_{s_j}^{s_{j+1}} \tilde{\mu}(s) d\theta = \frac{1}{2} \{ \tilde{\mu}(s_j) + \tilde{\mu}(s_{j+1}) \} \theta_j$$

where θ_j is the angle subtended at P by the segment $[s_j, s_{j+1}]$;

for B, where μ was approximated by a piecewise linear function

we have, following the work providing (3.7) in terms of complex points on Oxy, $z = x+iy$, that

$$\int_{s_j}^{s_{j+1}} \tilde{\mu}(s) d\theta = \text{Im} \left[\frac{\tilde{\mu}(t_j)(t_{j+1}-z) - \tilde{\mu}(t_{j+1})(t_j-z)}{t_{j+1} - t_j} \ell_n \left(\frac{t_{j+1}-z}{t_j-z} \right) \right];$$

and for C, where μ was approximated over say $s_{j-1} < s_j < s_{j+1}$

by a piecewise quadratic function, we have following the work prior

to (3.12) that

$$\int_{s_{j-1}}^{s_{j+1}} \tilde{\mu}(s) d\theta = \text{Im} \left[\frac{2}{(t_{j+1}-t_{j-1})^2} \{ E \tilde{\mu}(t_{j-1}) + F \tilde{\mu}(t_j) + G \tilde{\mu}(t_{j+1}) \} \right]$$

where $E = (t_{j+1}-z)(t_j-z) \ell_n \left(\frac{t_{j+1}-z}{t_{j-1}-z} \right) - (t_{j+1}-z)(t_{j+1}-t_{j-1})$,

$$F = 2(t_{j+1}-t_{j-1})(t_j-z) - 2(t_{j+1}-z)(t_{j-1}-z) \ell_n \left(\frac{t_{j+1}-z}{t_{j-1}-z} \right)$$

and $G = (t_{j-1}-z)(t_j-z) \ell_n \left(\frac{t_{j+1}-z}{t_{j-1}-z} \right) - (t_{j-1}-z)(t_{j+1}-t_{j-1})$.

Now it is known that any function of the form $\text{Im} \int_{t_j}^{t_{j+1}} \frac{\tilde{\mu}(t)}{t-z} dt$, (3.46)

where $\tilde{\mu}(t)$ satisfies very general conditions, gives rise to a harmonic function for all z in Oxy, z not on the contour. Further, the sum of a number of such functions being also harmonic, we have that $\tilde{u}(x,y)$ calculated from (3.45) by any of our approximations will be harmonic.

Thus both $u(x,y)$ and $\tilde{u}(x,y)$ are harmonic for any $(x,y) \in D^+$ and hence their difference $u - \tilde{u}$ is also harmonic. By the 'Maximum Principle' ([3] page 255) for two-dimensional harmonic functions,

$\max_{(x,y)} |u(x,y) - \tilde{u}(x,y)|$ will occur for some (x,y) on L . But $u(x,y)$ and $\tilde{u}(x,y)$ coincide at nodal points so that this gives the useful result that the maximum error between $u(x,y)$ and the calculated $\tilde{u}(x,y)$ can be estimated numerically by merely examining the difference $u - \tilde{u}$ at points on the boundary between nodes.

For instance we may refer to the exact equation (3.3), which for a point t_i , not a nodal point, so that $\alpha_i = \pi$, can be written as

$$u(t_i) = \frac{1}{2} \mu(t_i) + \frac{1}{2\pi} \operatorname{Im} \sum_{\substack{j=0 \\ j \neq i-1, i}}^{n-1} \int_{t_j}^{t_{j+1}} \frac{\mu(t)}{t-t_i} dt$$

For simplicity, let us take t_i between t_0 and t_1 so that

$$u(t_i) = \frac{1}{2} \mu(t_i) + \frac{1}{2\pi} \operatorname{Im} \sum_{j=1}^{n-1} \int_{t_j}^{t_{j+1}} \frac{\mu(t)}{t-t_i} dt \quad (3.47)$$

Again bearing in mind that the calculated density function $\tilde{\mu}(t)$ gives rise to the harmonic function $\tilde{u}(x,y)$ in (3.44) it follows that

$$\tilde{u}(t_i) = \frac{1}{2} \tilde{\mu}(t_i) + \frac{1}{2\pi} \operatorname{Im} \sum_{j=1}^{n-1} \int_{t_j}^{t_{j+1}} \frac{\tilde{\mu}(t)}{t-t_i} dt \quad (3.48)$$

where the integral term in (3.48) is variously calculated for $\tilde{\mu}$ being now generated for all boundary t as piecewise constant, linear or quadratic.

$$u(t_i) - \tilde{u}(t_i) = \frac{1}{2} \{ \mu_i - \tilde{\mu}_i \} + \frac{1}{2\pi} \operatorname{Im} \sum_{j=1}^{n-1} \int_{t_j}^{t_{j+1}} \frac{\mu(t) - \tilde{\mu}(t)}{t-t_i} dt. \quad (3.49)$$

But we had earlier for the density error vector $e_n = \underline{\mu} - \underline{\tilde{\mu}}$
 $= (\mu_0 - \tilde{\mu}_0, \mu_1 - \tilde{\mu}_1, \dots, \mu_{n-1} - \tilde{\mu}_{n-1})^T$ that $e_i = \mu_i - \tilde{\mu}_i \rightarrow 0$ for

all i as $n \rightarrow \infty$.

However in (3.49), t_i is not a node point, so we cannot immediately replace $\mu(t) - \tilde{\mu}(t)$. But on any interval of the boundary $[t_j, t_{j+1}]$ in the case of approximations B and C we have the difference between two continuous functions $\mu(t)$ and $\tilde{\mu}(t)$. This difference must also be continuous at any intermediate point t , so we may write

$$\mu(t) - \tilde{\mu}(t) = \mu(t_j) - \tilde{\mu}(t_j) + h_j \{ \mu'(\tau_j) - \tilde{\mu}'(\tau_j) \} \quad (3.50)$$

where if $h = |t_{j+1} - t_j|$ then $0 < h_j < h$ and $\tau_j = \tau_j(h_j)$.

(We already have existence of μ' from differentiating (3.31) and $\tilde{\mu}'$ exists being the derivative of a polynomial).

But (3.43) will imply that $|\mu(t_j) - \tilde{\mu}(t_j)| \leq kH^p$, $p = 2, 3$, k a positive constant equal to $\frac{M''\pi}{2\beta}$ in approximately B and $\frac{M'''\pi}{4\beta}$ in C,

and so we have

$$|\mu(t) - \tilde{\mu}(t)| \leq |\mu(t_j) - \tilde{\mu}(t_j)| + h_j |\mu'(\tau_j) - \tilde{\mu}'(\tau_j)|$$

$\leq kH^p + HM$ where as before H is the maximum step width and M is taken as $\max_{\text{all } j} |\mu'(\tau_j) - \tilde{\mu}'(\tau_j)|$.

Hence in (3.49) we now have

$$\begin{aligned} |u(t_i) - \tilde{u}(t_i)| &\leq \frac{1}{2} |\mu(t_i) - \tilde{\mu}(t_i)| + \frac{1}{2\pi} \sum_{j=1}^{n-1} \int_{t_j}^{t_{j+1}} |\mu(t) - \tilde{\mu}(t)| \operatorname{Im} \left(\frac{dt}{t-t_i} \right) \\ &\leq \frac{1}{2} kH^p + \frac{1}{2} HM + \frac{1}{2\pi} (kH^p + HM) \pi \\ &= kH^p + HM \end{aligned} \quad (3.51)$$

For approximations B and C, as the maximum step width H is decreased, then $|u(t_i) - \tilde{u}(t_i)|$ can be made as small as we please as is required.

For approximation A we proceed a little more warily since $\tilde{\mu}(t)$ being a piecewise constant is not continuous at nodal points. We have that

$$\mu(t) - \tilde{\mu}(t) = \mu(t) - \frac{1}{2} \{ \tilde{\mu}(t_j) + \tilde{\mu}(t_{j+1}) \} \quad \text{for intermediate } t.$$

But $\mu(t)$ is a continuous function and so we may write by applying the mean value theorem

$$\mu(t) = \mu(t_j) + h_j \mu'(\tau_j)$$

and also $\mu(t) = \mu(t_{j+1}) - (h - h_j) \mu'(\tau_{j+1})$. Adding these equations gives

$$\mu(t) = \frac{1}{2} \{ \mu(t_j) + \mu(t_{j+1}) \} + \frac{1}{2} h_j \mu'(\tau_j) - \frac{1}{2} (h - h_j) \mu'(\tau_{j+1}) \quad (3.52)$$

Hence finally $\mu(t) - \tilde{\mu}(t) = \frac{1}{2} (\mu_j - \tilde{\mu}_j) + \frac{1}{2} (\mu_{j+1} - \tilde{\mu}_{j+1}) + \frac{1}{2} h_j \mu'(\tau_j) - \frac{1}{2} (h - h_j) \mu'(\tau_{j+1})$

i.e. $|\mu(t) - \tilde{\mu}(t)| \leq \frac{1}{2\beta} M'H\pi + \frac{1}{2} HM' + \frac{1}{2} HM' , M'$ as previously defined.
 $= HM' + \frac{\pi}{2\beta} HM'$

Thus returning to (3.49) this gives for approximation A that

$$\begin{aligned} |u(t) - \tilde{u}(t_i)| &\leq \frac{1}{2} HM' (1 + \frac{\pi}{2\beta}) + \frac{1}{2\pi} \sum_{j=1}^{n-1} \int_{t_j}^{t_{j+1}} |\mu(t) - \tilde{\mu}(t)| \operatorname{Im}(\frac{dt}{t-t_i}) \\ &\leq \frac{1}{2} HM' (1 + \frac{\pi}{2\beta}) + \frac{1}{2\pi} \times HM' (1 + \frac{\pi}{2\beta}) \pi \\ &= HM' (1 + \frac{\pi}{2\beta}) \end{aligned} \quad (3.53)$$

But again as H is decreased this expression for $|u(t) - \tilde{u}(t_i)|$ can be made as small as we please so that overall we have achieved the desired aim of showing that for increasing discretisation refinement on the boundary, then

$$\tilde{u}(x,y) \rightarrow u(x,y) , \text{ all } P(x,y) \in D^+$$

in the case of all of our approximations.

Chapter IV

In this chapter we give numerical results obtained through applying the methods described in Chapter III. This means that (3.4), (3.8) and (3.14) and (3.15) are used to generate sets of linear equations which are then solved for $\tilde{\mu}(t_i)$ by the use of computer programs. Finally further computer programs are used to enable $\tilde{u}(x,y)$ to be generated. Tables of values of $\tilde{\mu}$ and \tilde{u} are given at the end.

As stated earlier, the well known torsion problem in elasticity has been used to provide the example considered. Hence in each of the representations the boundary data $f(t_i)$ is taken as $\frac{1}{2}(x_i^2 + y_i^2)$ where $t_i = x_i + iy_i$. The polygonal boundary L is taken to be rectangular, of size 2 units \times 1 unit, this being a suitable shape for trial since the analytic solution is available in the form of an infinite series. Comparison can then be made between the analytic solution, $u(x,y)$, and the various approximate solutions $\tilde{u}(x,y)$.

To simplify the computation and make use of symmetries, the position of L is as given in Fig.50. This means that four-fold symmetry is exhibited for a (2×1) rectangle, so that if (\bar{x}, \bar{y}) are coordinates of a typical boundary point then

$$\tilde{\mu}(\bar{x}, \bar{y}) = \tilde{\mu}(-\bar{x}, \bar{y}) = \tilde{\mu}(\bar{x}, -\bar{y}) = \tilde{\mu}(-\bar{x}, -\bar{y}).$$

Also for any point (x,y) in D^+ , we have

$$\tilde{u}(x,y) = \tilde{u}(-x,y) = \tilde{u}(x,-y) = \tilde{u}(-x,-y).$$

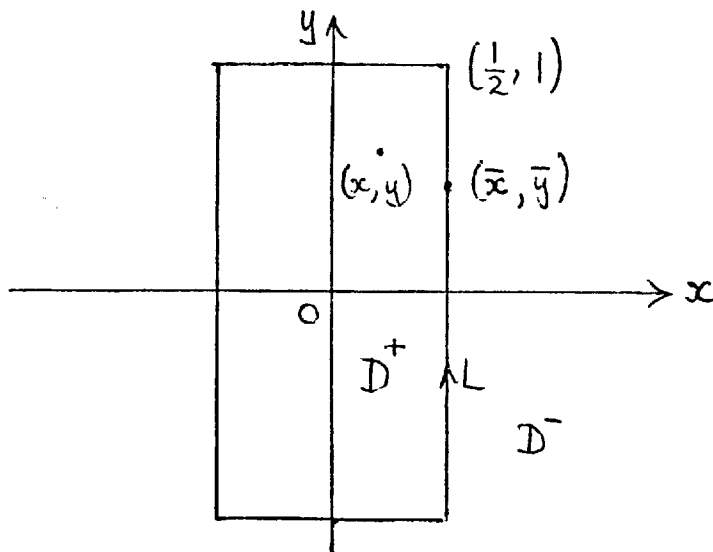


Fig 50

This four-fold symmetry has been incorporated into the computer programs. Hence although we require a discretisation of L around its entire length we can in fact work solely with the quadrant $x \geq 0, y \geq 0$. Node points have now to be placed on L , and a flexible system is required so that the number of node points can be easily increased without the necessity for a new computer program each time. Also the nodes do not need to be at equally spaced intervals (apart from the requirement in approximation C) and it is possible to arrange for them to be clustered more densely if desirable around a corner point of L .

A typical situation is shown in Fig.51:-

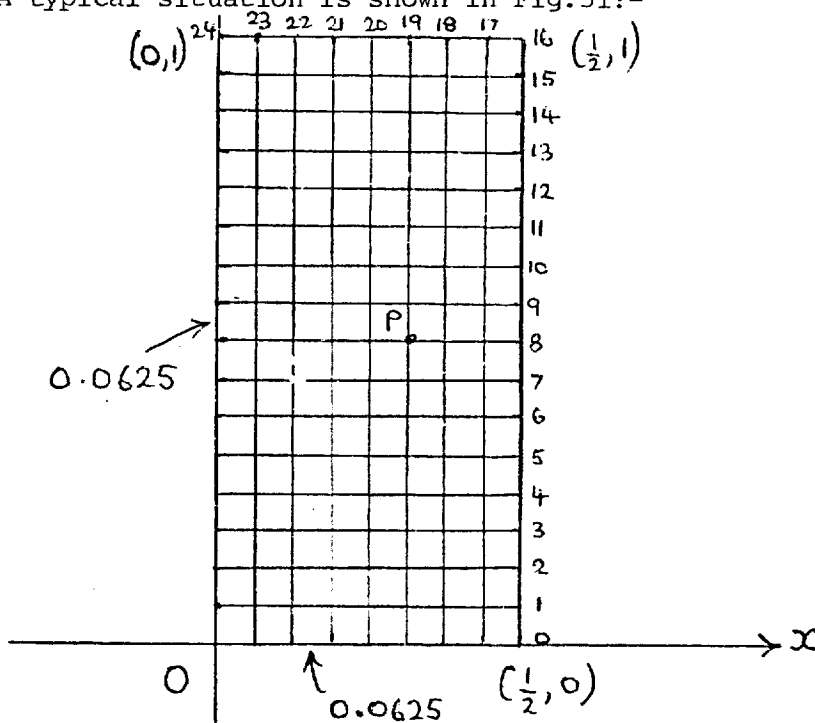


Fig. 51

In this case nodes are spaced equally at distance $\frac{1}{16} = 0.0625$. Thus around the quarter rectangle there is a total of 25 nodes, numbered as shown from 0 to 24. The values $\tilde{\mu}_0, \tilde{\mu}_1, \dots, \tilde{\mu}_{24}$ are found by solving a set of 25 linear equations. Bearing in mind the four-fold symmetry, this is equivalent to placing a total of 96 nodes around the entire boundary L .

The mesh shown in the interior D^+ of the rectangle occurs naturally as a suitable framework for points at which $\tilde{u}(x,y)$ can be calculated.

Thus in Fig.51, an array of size (8 x 16) can be set up to hold calculated values for $\tilde{u}(x,y)$ in each of the approximations A,B, and C.

As mentioned at the beginning of this chapter, comparisons are possible with the analytic solution of this problem. This is so since the classical problem "solve $\nabla^2 u = 0$ within D^+ such that $u(x,y)$ continues onto L as $\frac{1}{2}(x^2 + y^2)$ " may be solved by the methods of "separation of variables of a partial differential equation" and the use of Fourier series. The solution may be expressed in the form

$$u(x,y) = \frac{1}{2}(x^2 - y^2 + 2) + \frac{32}{\pi^3} \sum_{n=0}^{\infty} \frac{(-1)^{n+1}}{(2n+1)^3} \frac{\cosh(2n+1) \pi x/2}{\cosh(2n+1) \pi/4} \cos(2n+1) \frac{\pi y}{2} \quad (4.1)$$

This series can be summed for given input of (x,y) by suitable computer program.

Although we can make direct comparisons between the values of $\tilde{u}(x,y)$ and $u(x,y)$ and the reliability of the numerical methods then assessed, no similar comparison is possible for the calculated boundary density $\tilde{\mu}(t_i)$. For the Dirichlet problem in the case of a region with a circular or elliptic boundary, exact solutions are available for $\mu(t)$, see [5] and [18]. But in general, including the case here, we have no analytic expression available. This calculation of an intermediate quantity $\tilde{\mu}$ is one of the main draw-backs of casting the interior Dirichlet problem in terms of the double layer potential since the double layer density μ is not of any physical interest.

Surveying the integral equation formulations described in Chapter I, let us consider the alternative choices available.

1. The single layer formulation gave rise to the integral equation (1.6) for the determination of the single layer density $\sigma(s)$, followed by the evaluation of $\tilde{u}(x,y)$ from (1.5). Here $\sigma(s)$ is the solution of a Fredholm equation of the first kind with logarithmic kernel. As

with $\mu(s)$ the calculation of $\sigma(s)$ is of minimal interest in solving the interior Dirichlet problem. The discretisation of (1.6) will lead to a problem in linear algebra for the determination of $\alpha(s_i)$. This alternative has been used chiefly by Jaswon and Symm [12] in which it is proved that (1.6) has a solution for smooth boundary contour L apart from an exceptional contour which can be avoided by scaling. Assuming this theory can be extended to polygonal contours, then on discretising (1.6), the resulting matrix does not possess the convenient form of that found through use of the double-layer. A further numerical difficulty is presented by the logarithmic kernel which requires the evaluation of improper integrals. No such difficulty occurs for the kernel of the double layer formulation as explained in (3.3).

2. The other alternative is the use of Green's boundary formulas. In this case the solution of the Dirichlet problem is obtained through the use of the integral equations (1.38), (1.39) and (1.37). It is convenient to list them here again

$$(1.38): \oint_L \frac{\partial u}{\partial n} \cdot \ell_n\left(\frac{1}{r}\right) ds = \oint_L f(s) d\theta, \quad o \in D^-$$

$$(1.39): \oint_L \frac{\partial u}{\partial n} \cdot \ell_n\left(\frac{1}{r}\right) ds = \oint_L f(s) d\theta - \alpha_o f(s_o), \quad o \in L$$

$$\text{and (1.37): } u(x,y) = \frac{1}{2\pi} \oint_L \left\{ f(s) d\theta - \frac{\partial u}{\partial n} \cdot \ell_n\left(\frac{1}{r}\right) ds \right\}, \quad (x,y) \in D^+$$

where o is the pivot point.

Clearly an outstanding advantage of this formulation is the absence of any density function, the calculations yielding approximations to the normal derivative $\frac{\partial u}{\partial n}$. Either (1.38) or (1.39) may be used as Fredholm integral equations of the first kind. Having obtained $\frac{\partial u}{\partial n}$, it would then be substituted into (1.37) and the generation of the

internal potential $u(x,y)$ completed. The differing positions of O mean that the evaluation of $\oint f(s)d\theta$ is completed separately for each of (1.38), (1.39) and (1.37). We may refer in passing to the paper by P.Swartztrauber [25] where an integral equation method is used derived from Cauchy's integral formula. However as explained in Chapter I of this thesis, equations (1.59), (1.60) etc., this is equivalent to Green's Boundary Formula and essentially no new formulation is obtained.

Now it is clear that since the kernel of (1.39) is identical with that of (1.6) then the discretisation of (1.39) will lead to the same matrix. Thus the same comments on the difficulties in the numerical linear algebra apply again. Also allowance must be made for discontinuity in $\frac{\partial u}{\partial n}$ at corner points.

With regard to (1.38), we have a different situation, inspite of the apparently identical kernel $Q_n(\frac{1}{r})$. The placing of the pivot O in D^- removes worries concerning the calculation of $Q_n(\frac{1}{r})$ since in this new situation r is never zero. This formulation of the Dirichlet problem, ostensibly the simplest and most concise of all, has almost completely escaped attention of most workers in this field. It may be found as far as the author is aware in only one source, namely the book by V.Kupradze [13]. The existence of a solution $\frac{\partial u}{\partial n}$, provided that L is smooth, is established by Kupradze in [13], page 253. There seems no doubt this can be extended to a polygonal contour. With regard to obtaining a numerical solution by carrying out the usual boundary discretisations there is the added facility of being able to place the collocation points anywhere throughout D^- . Some analysis is given by Kupradze (p.254) in which it is shown that the resulting linear equations can be solved provided the points are taken on a contour lying in D^- that is concentric with L and sufficiently close to it. This accords with results obtained by one

of the author's undergraduate project students [26] in which it was found that the solution of the torsion problem for a rectangular region through the application of (1.38) was inaccurate unless the concentric contour was moved up close to L . It is clear that as this external contour moves up into coincidence with L then the integral equation formulation (1.39) will be recovered.

Results Section

In TABLE 1, calculated values of the boundary density $\tilde{\mu}$ are listed for each of the three approximations A,B and C. In TABLE 2, the resulting potential $\tilde{u}(x,y)$ is displayed at selected points within the rectangular region. At each point four values are listed corresponding to approximations C,B,A and the analytic solutions respectively. Each value is quoted correct to six decimal places. In TABLE 3, the errors have been calculated and listed at the same selected points as in TABLE 2. Both the raw error, $\tilde{u}(x,y) - u(x,y)$, and the percentage error are given, as explained in the key to TABLE 3.

It will be noticed that the results are generally satisfactory with a small percentage error when any of approximations A,B or C is applied. An error pattern is also established throughout the rectangular region with the exception of the part lying near to the corner point. This pattern shows the reward expected by the greater sophistication of approximation C over approximation B and also that of B over approximation A. In fact it is clear from the data in TABLE 3 that the respective errors, E_A, E_B, E_C to six decimal places, fall naturally into the pattern

$$E_A : E_B : E_C = 2 : 1 : 0 .$$

This satisfactory state of affairs is rather spoilt as we examine the approximate potential values obtained close to the corner point. To get an idea of the fluctuations, the results are quoted in TABLE 4 for a number of interior points close to the corner. It can be seen from examination of TABLE 5 that the general error pattern suggested above collapses. Some of the approximate solutions $\tilde{u}(x,y)$ fall below the exact $u(x,y)$ for the first time and although approximation C is generally the most accurate, this is not always the case.

As discussed in Chapter 3, the positioning of the original boundary nodes can always be adjusted. We do not require equal spacing between

them save only that in approximation C, a mid point node has to be used. Hence it is possible to cluster the nodes more closely near to corner points as appropriate on the assumption that greater refinement near to a corner will lead to more accurate results. In the case of the rectangle, effectively one corner only has to be considered, with the nodes placed more closely along each arm enclosing the angle.

Three different node clusters were tried leading to new calculations for $\tilde{\mu}$ in each case. The derivation of new positions for nodal points was incorporated into the computer programs written for the application of approximation C. Thus new data is available for $\tilde{u}(x,y)$ based upon the quadratic variation in $\tilde{\mu}(t)$ around the boundary. For each of the clusters tried there were still in fact only 25 distinct nodal points.

The results obtained from this refinement are displayed in TABLES 6-10. It is clear from the results for this example that a mild clustering of nodes is preferable, this being listed as "1st cluster" with corresponding calculations of the double-layer density and final interior potential denoted by $\tilde{\mu}_C^I$ and $\tilde{u}(x,y)_C^I$ respectively.

One further table is incorporated, giving data generated in an attempt to check the conclusions drawn from the 'Maximum Principle' outlined in Chapter III on page 113. This establishes that the greatest error $|u - \tilde{u}|$ will occur at points on the boundary L of the rectangle. It is seen from the end of Chapter III that as the distance between the node points decreases that then this maximum error can be made as small as we please. Hence we may attempt to find $\max_Q |u(t_Q) - \tilde{u}(t_Q)|$ where t_Q is some point on L, not a node point. The theory will not tell us where absolute maximum is obtained, but it would seem sensible for the calculations to be performed at points mid way between nodes. The attendant results are given in TABLE 11, and were computed only with

respect to approximation C, the node points being equally spaced, at interval 0.0625 as before, around the rectangle. The table gives values of $u(t_i)$ and $\tilde{u}(t_i)$ where it is worth recalling that $u(t_i) = \frac{1}{2}(x_i^2 + y_i^2)$ and, from (3.48),

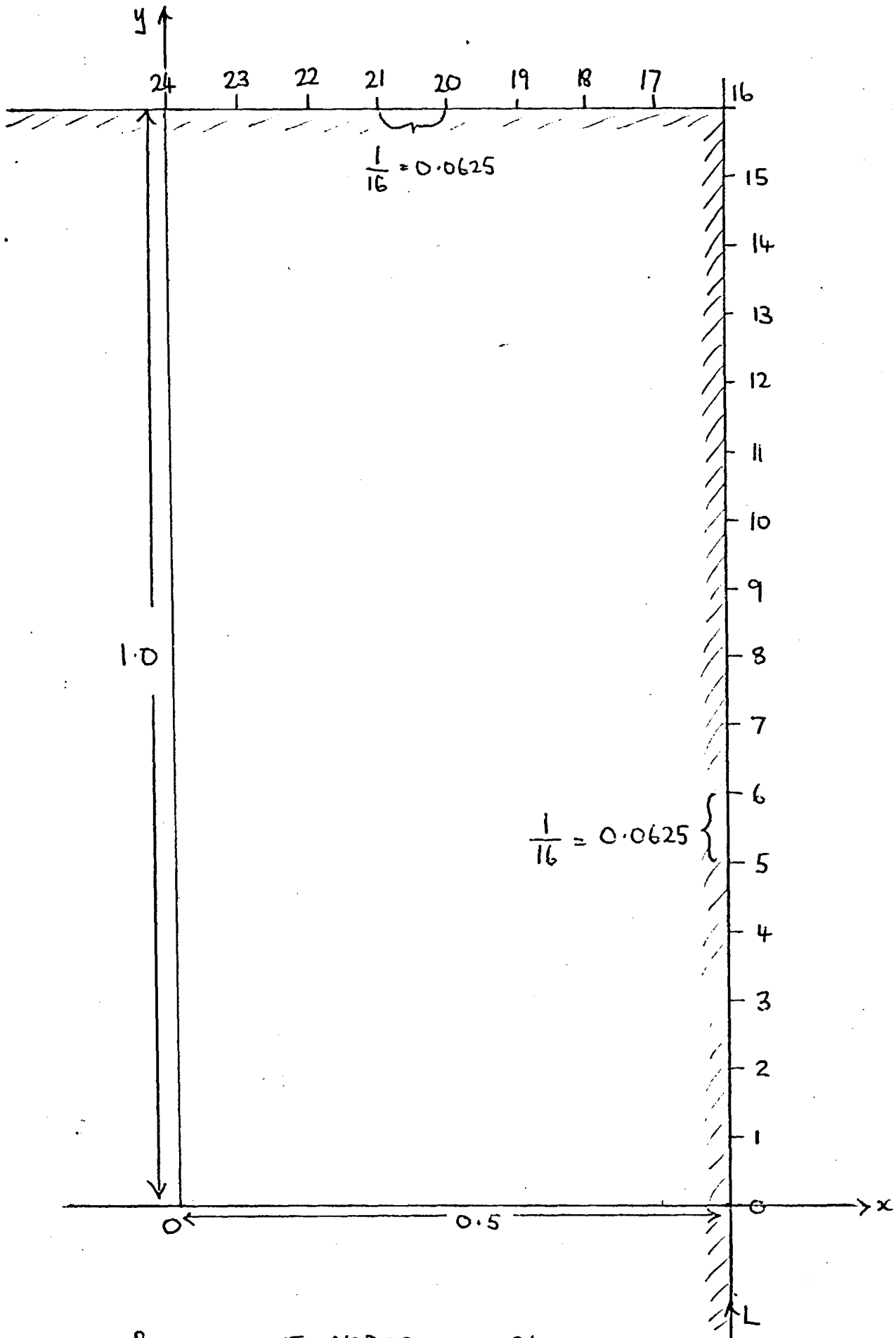
$$\tilde{u}(t_i) = \frac{1}{2} \tilde{\mu}(t_i) + \frac{1}{2\pi} \operatorname{Im} \sum_{\substack{j=0 \\ j \neq i-1, i}}^{n-1} \int_{t_j}^{t_{j+1}} \frac{\tilde{\mu}(t)}{t-t_i} dt ,$$

$\tilde{\mu}$ being interpolated at t_i from its quadratic nature in the case of the first term in this expression.

From TABLE 11 we see the worst situation at the point denoted by (ix) at which the % error can be calculated as 0.58 % .

Conclusion

This thesis attempts to show the complete reliability in posing the interior Dirichlet problem for convex polygonal regions in terms of double layer potentials leading to a Fredholm integral equation of the second kind. The error analysis developed has shown that complete faith may be placed in the resulting numerical solutions attempted. Although the solution of two dimensional 'potential' problems is more popularly considered nowadays through the Green boundary formulas, nevertheless it must be recognised that the traditional double-layer method will produce a completely sound theoretical basis which can be translated into an equally reliable approximate form.



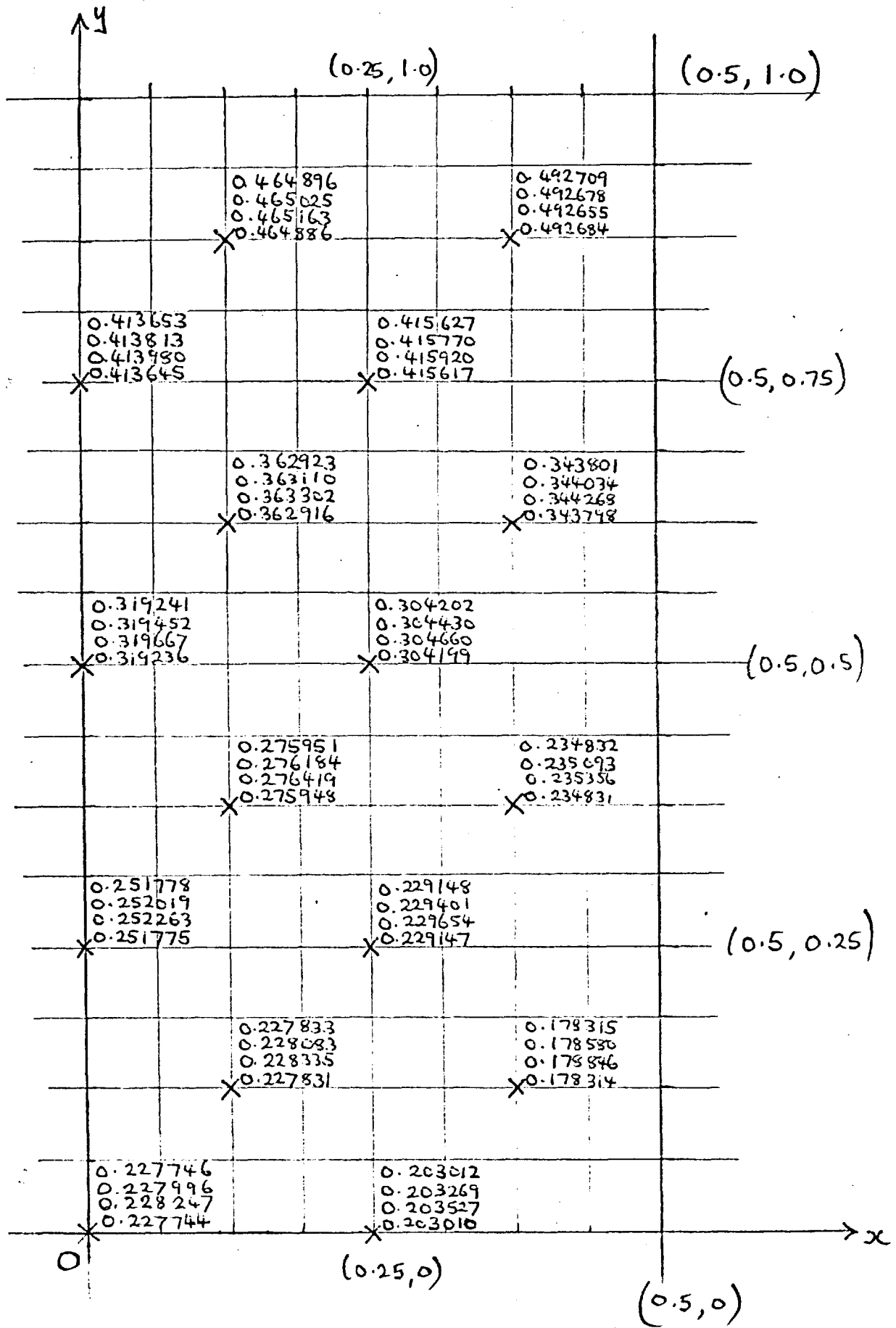
POSITION OF NODES 0 → 24

AT EQUALLY SPACED POINTS ON BOUNDARY.

(REF. TABLE 1)

NODE COORDINATES		NODE LABEL	$\tilde{\mu}_A$ (APPROX. A)	$\tilde{\mu}_B$ (APPROX. B)	$\tilde{\mu}_C$ (APPROX. C)
0.5000	0	0	-0.155299	-0.154879	-0.155164
0.5000	0.0625	1	-0.152024	-0.151604	-0.151890
0.5000	0.1250	2	-0.142190	-0.141769	-0.142061
0.5000	0.1875	3	-0.125775	-0.125353	-0.125653
0.5000	0.2500	4	-0.102742	-0.102317	-0.102631
0.5000	0.3125	5	-0.073040	-0.072612	-0.072943
0.5000	0.3750	6	-0.036607	-0.036174	-0.036528
0.5000	0.4375	7	+0.006629	+0.007068	+0.006686
0.5000	0.5000	8	0.056746	0.057193	0.056774
0.5000	0.5625	9	0.113823	0.114281	0.113815
0.5000	0.6250	10	0.177935	0.178407	0.177831
0.5000	0.6875	11	0.249145	0.249633	0.249031
0.5000	0.7500	12	0.327500	0.328024	0.327306
0.5000	0.8125	13	0.413037	0.413615	0.412732
0.5000	0.8750	14	0.505853	0.506551	0.505438
0.5000	0.9375	15	0.606459	0.607671	0.606217
0.5000	1.0000	16	0.726511	0.726490	0.726619
0.4375	1.0000	17	0.766283	0.762966	0.764202
0.3750	1.0000	18	0.759914	0.758317	0.759461
0.3125	1.0000	19	0.746593	0.745514	0.746575
0.2500	1.0000	20	0.731975	0.731142	0.732144
0.1875	1.0000	21	0.718305	0.718106	0.719070
0.1250	1.0000	22	0.708581	0.707959	0.708898
0.0625	1.0000	23	0.702153	0.701572	0.702496
0	1.0000	24	0.699964	0.699396	0.700316

1. TABLE OF $\tilde{\mu}(x, y)$



2. TABLE

OF $\tilde{u}(x,y)$

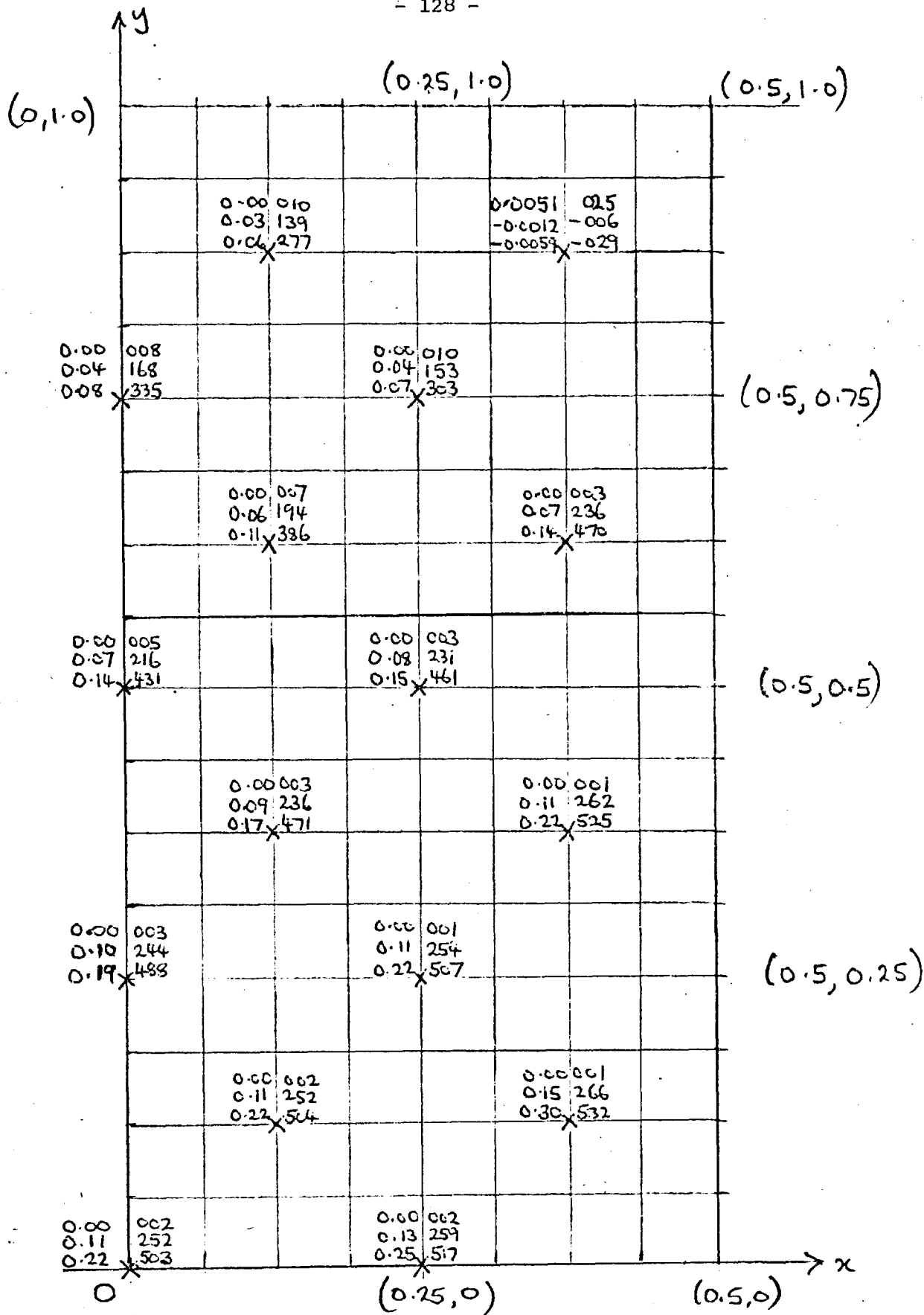
KEY:

APPROX. C	$\tilde{u}(x,y)_C$
APPROX. B	$\tilde{u}(x,y)_B$
APPROX. A	$\tilde{u}(x,y)_A$
ANALYTIC	$u(x,y)$

GRID

$$\frac{1}{16} \times \frac{1}{16}$$

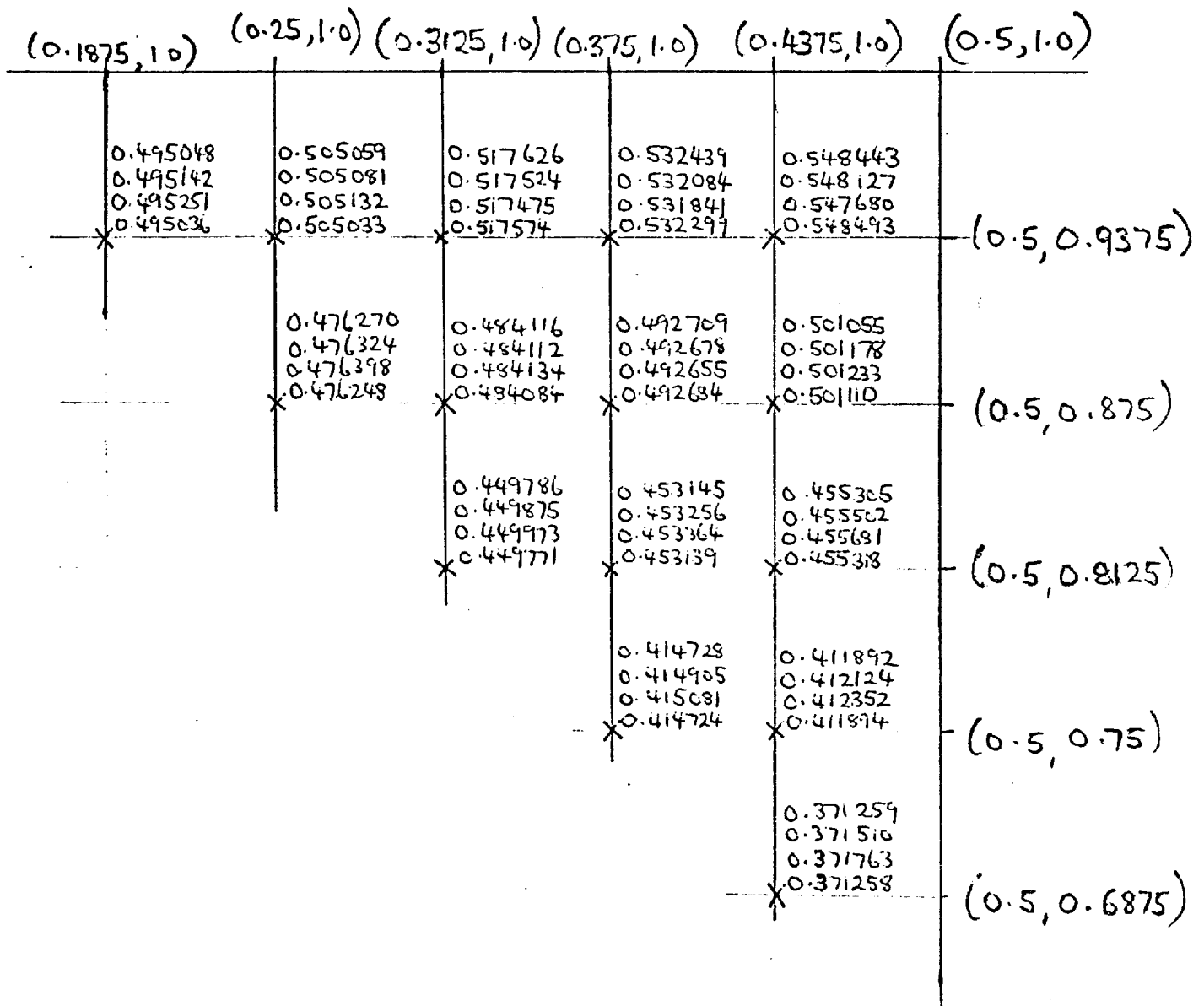
$$= 0.0625 \times 0.0625$$



KEY:

% ERROR, APPROX. C	$[\tilde{u}(x,y)_C - u(x,y)] \times 10^6$
% ERROR, APPROX. B	$[\tilde{u}(x,y)_B - u(x,y)] \times 10^6$
% ERROR, APPROX. A	$[\tilde{u}(x,y)_A - u(x,y)] \times 10^6$

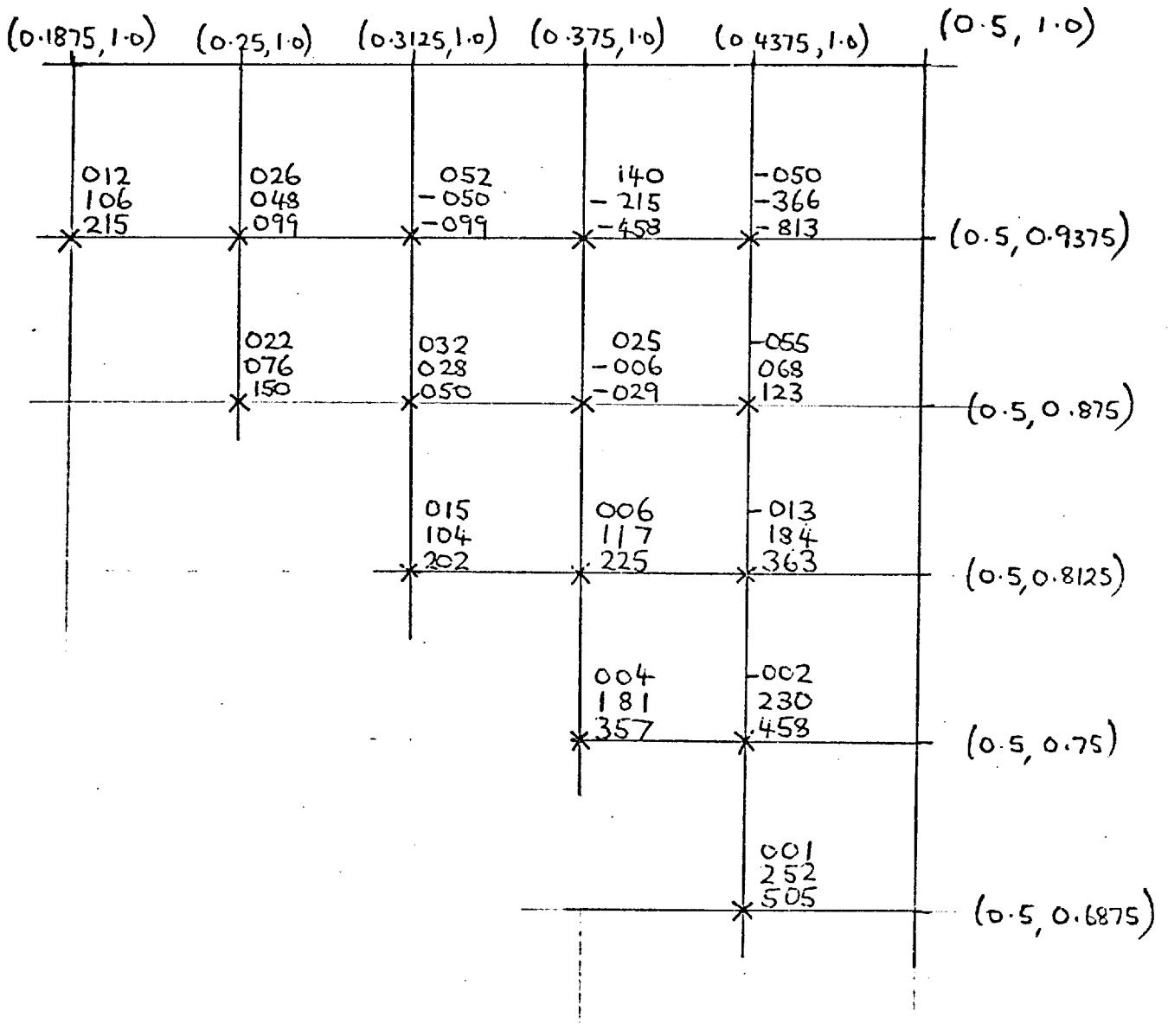
3. TABLE OF ERRORS IN $\tilde{u}(x,y)$ ← X →



4. TABLE OF
 $\tilde{u}(x, y)$,
 (x, y) CLOSE TO
 CORNER

KEY :

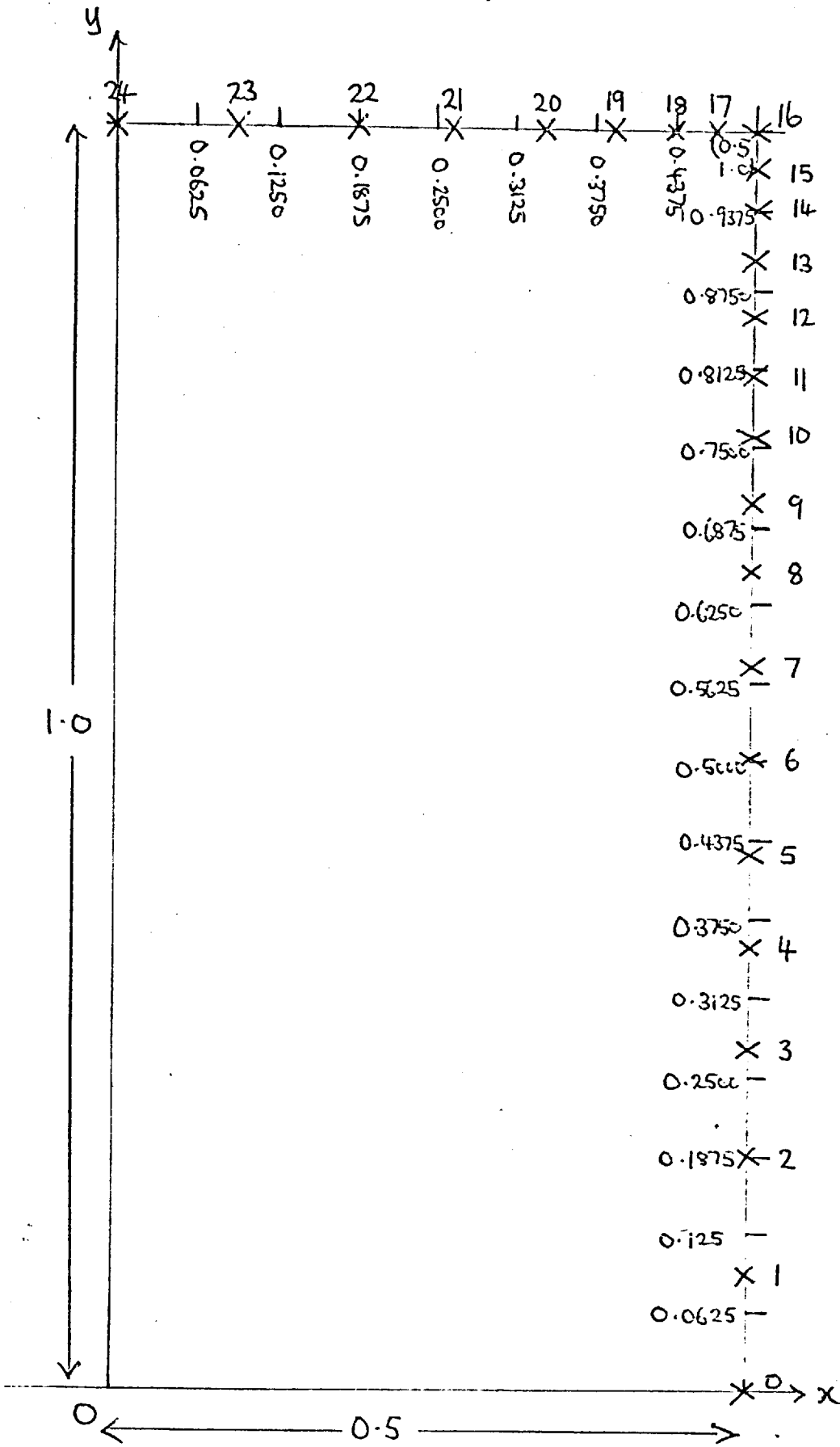
APPROX. C	$\tilde{u}(x, y)_C$
APPROX. B	$\tilde{u}(x, y)_B$
APPROX. A	$\tilde{u}(x, y)_A$
ANALYTIC	$u(x, y)$



5. TABLE OF
 ERRORS IN
 $\tilde{u}(x, y)$

KEY

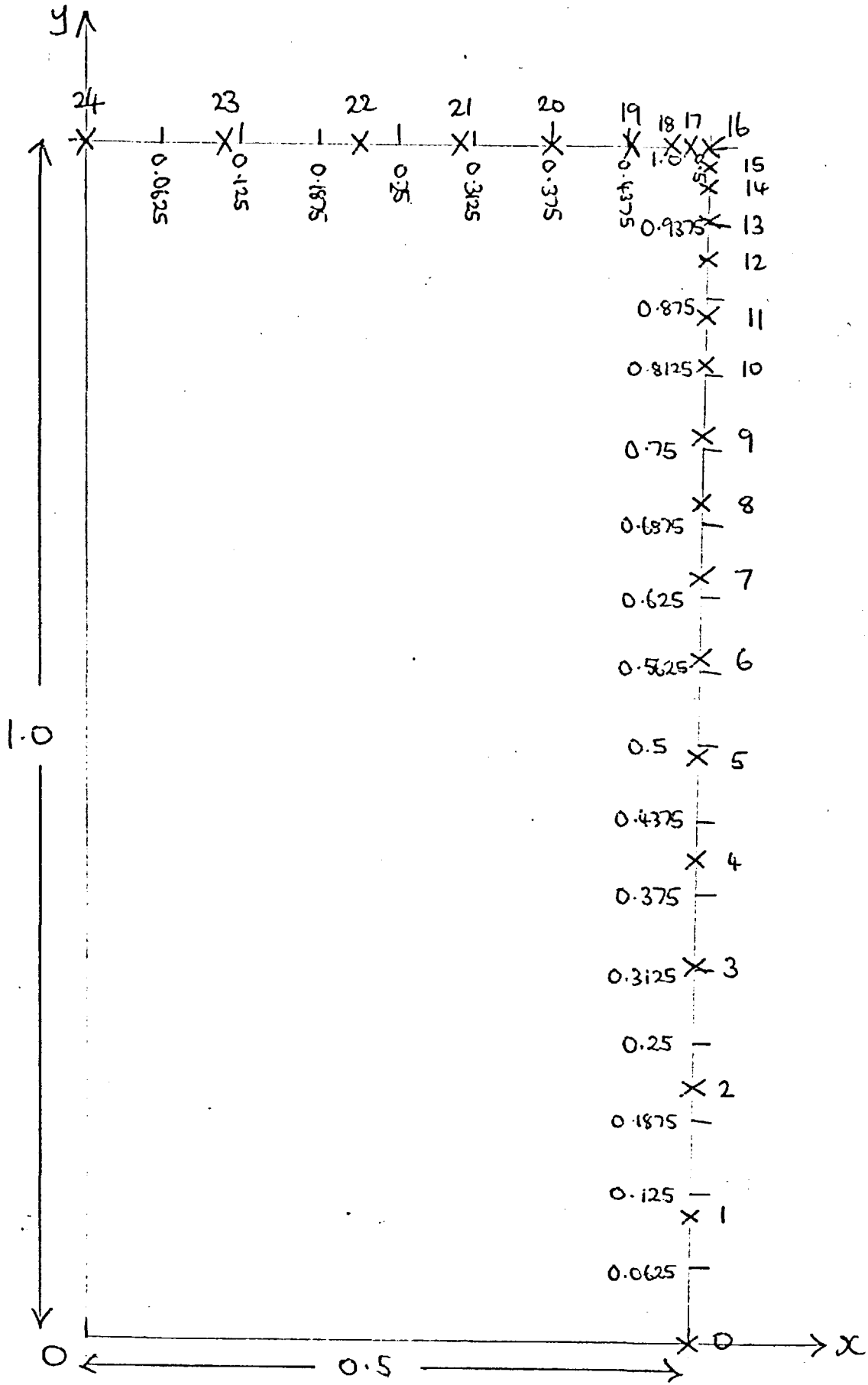
$[\tilde{u}(x, y)_C - u(x, y)] \times 10^6$
$[\tilde{u}(x, y)_B - u(x, y)] \times 10^6$
$[\tilde{u}(x, y)_A - u(x, y)] \times 10^6$



POSITION OF NODES 0 → 24 FOR 1ST CLUSTER
(REF TABLE 6)

NODE COORDINATES		NODE LABEL	DENSITY $\tilde{\mu}_c^I$
x	y		
0.50000	0	0	-0.155373
0.50000	0.09375	1	-0.148007
0.50000	0.18750	2	-0.125868
0.50000	0.27232	3	-0.093018
0.50000	0.35714	4	-0.047855
0.50000	0.43304	5	-0.003125
0.50000	0.50893	6	+0.064230
0.50000	0.57589	7	0.126661
0.50000	0.64286	8	0.197163
0.50000	0.70089	9	0.264842
0.50000	0.75893	10	0.338650
0.50000	0.80803	11	0.405895
0.50000	0.85714	12	0.477553
0.50000	0.90732	13	0.539553
0.50000	0.93750	14	0.604968
0.50000	0.96875	15	0.659353
0.50000	1.00000	16	0.726653
0.46875	1.00000	17	0.758914
0.43750	1.00000	18	0.765136
0.38542	1.00000	19	0.761780
0.33333	1.00000	20	0.751805
0.26042	1.00000	21	0.734975
0.18750	1.00000	22	0.719485
0.09375	1.00000	23	0.705574
0	1.00000	24	0.700692

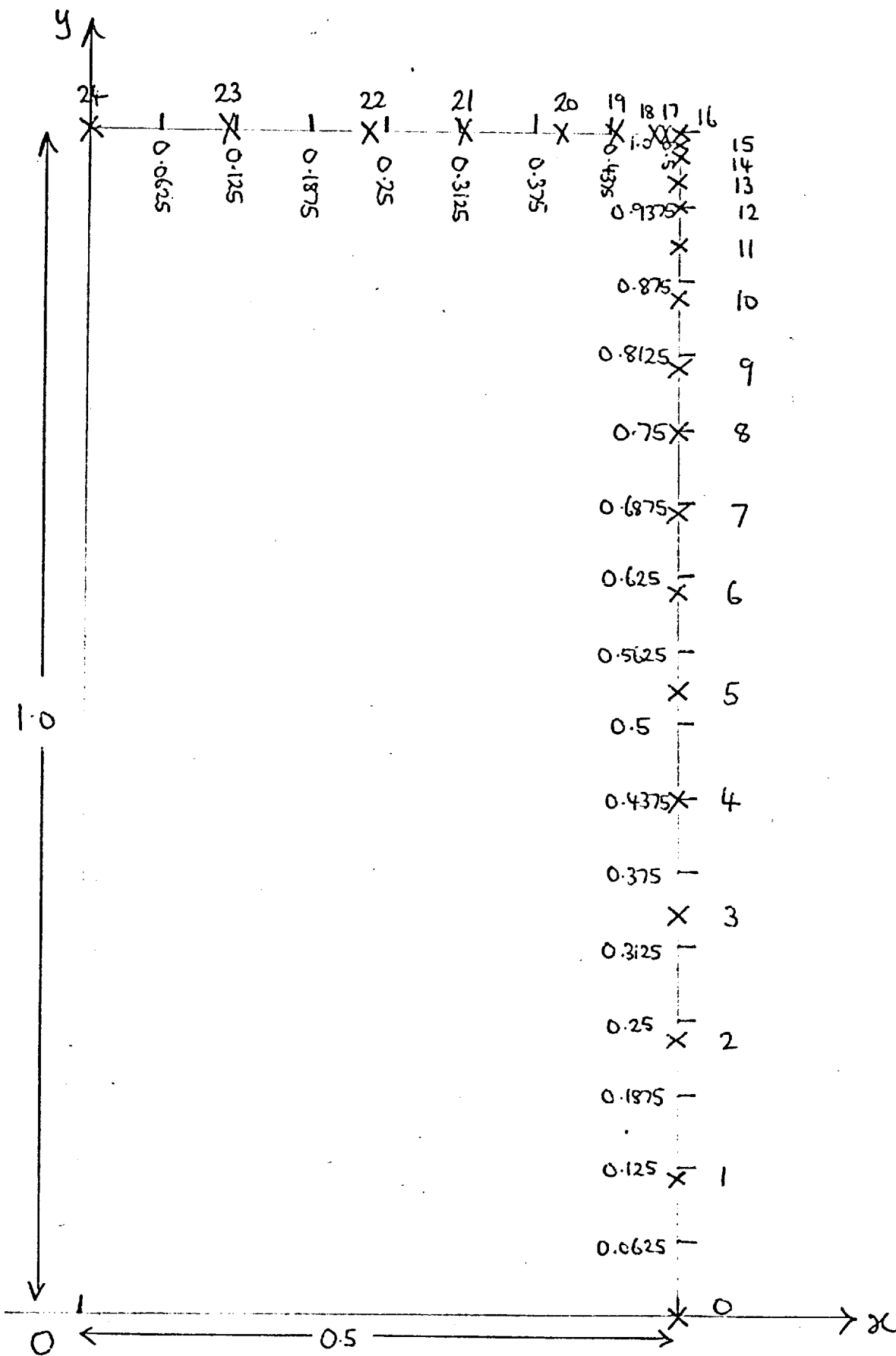
6. TABLE OF $\tilde{\mu}(x, y)$:
1st CLUSTER



POSN. OF NODES 0 → 24 FOR 2ND CLUSTER
(REF. TABLE 7)

NODE COORDINATES		NODE LABEL	DENSITY $\tilde{\mu}_c^{\text{II}}$
x	y		
0.50000	0	0	-0.155447
0.50000	0.10938	1	-0.145419
0.50000	0.21875	2	-0.115266
0.50000	0.31473	3	-0.072066
0.50000	0.41071	4	-0.013000
0.50000	0.49330	5	+0.050724
0.50000	0.57589	6	0.126561
0.50000	0.64509	7	0.199542
0.50000	0.71429	8	0.281204
0.50000	0.77009	9	0.353402
0.50000	0.82589	10	0.431265
0.50000	0.86830	11	0.494250
0.50000	0.91071	12	0.560653
0.50000	0.93973	13	0.608324
0.50000	0.96875	14	0.658658
0.50000	0.98437	15	0.688114
0.50000	1.00000	16	0.726666
0.48437	1.00000	17	0.750782
0.46875	1.00000	18	0.759514
0.42188	1.00000	19	0.765650
0.37500	1.00000	20	0.760359
0.29688	1.00000	21	0.743656
0.21875	1.00000	22	0.725916
0.10938	1.00000	23	0.707454
0	1.00000	24	0.700333

7. TABLE OF $\tilde{\mu}(x, y)$:
2ND CLUSTER



POSN. OF NODES 0 → 24 FOR 3RD CLUSTER
(REF TABLE 8)

NODE COORDINATES		NODE LABEL	DENSITY $\tilde{\mu}_c^{III}$
x	y		
0.50000	0	0	-0.155464
0.50000	0.11719	1	-0.143952
0.50000	0.23438	2	-0.109322
0.50000	0.33594	3	-0.060408
0.50000	0.43750	4	+0.006332
0.50000	0.52344	5	0.076961
0.50000	0.60938	6	0.160771
0.50000	0.67969	7	0.239261
0.50000	0.75000	8	0.326730
0.50000	0.80469	9	0.400977
0.50000	0.85938	10	0.480674
0.50000	0.89844	11	0.541015
0.50000	0.93750	12	0.604519
0.50000	0.96094	13	0.644638
0.50000	0.98438	14	0.687799
0.50000	0.99219	15	0.704097
0.50000	1.00000	16	0.726670
0.49219	1.00000	17	0.743424
0.48438	1.00000	18	0.751125
0.44010	1.00000	19	0.765479
0.39583	1.00000	20	0.763565
0.31510	1.00000	21	0.747949
0.23438	1.00000	22	0.729327
0.11719	1.00000	23	0.708453
0	1.00000	24	0.700869

8. TABLE OF $\tilde{\mu}(x, y)$:
3RD CLUSTER

$(0.1875, 1.0)$	$(0.25, 1.0)$	$(0.3125, 1.0)$	$(0.375, 1.0)$	$(0.4375, 1.0)$	$(0.5, 1.0)$
0.495012 0.495024 0.495040 0.495048 X 0.495036	0.505048 0.505047 0.505036 0.505059 X 0.505033	0.517566 0.517555 0.517567 0.517626 X 0.517574	0.532261 0.532282 0.532301 0.532439 X 0.532299	0.548461 0.548462 0.548484 0.548443 X 0.548493	(0.5, 0.9375)
	0.476246 0.476247 0.476248 0.476270 X 0.476248	0.484076 0.484077 0.484083 0.484116 X 0.484084	0.492669 0.492673 0.492681 0.492709 X 0.492684	0.501096 0.501100 0.501103 0.501055 X 0.501110	(0.5, 0.875)
		0.449766 0.449767 0.449770 0.449786 X 0.449771	0.453132 0.453134 0.453137 0.453145 X 0.453139	0.455312 0.455313 0.455315 0.455305 X 0.455318	(0.5, 0.8125)
			0.414721 0.414722 0.414724 0.414728 X 0.414724	0.411891 0.411892 0.411893 0.411892 X 0.411894	(0.5, 0.75)
				0.371255 0.371258 0.371258 0.371259 X 0.371258	(0.5, 0.6875)

9. TABLE OF
 $\tilde{u}(x, y)$,
 (x, y) CLOSE TO
 CORNER

KEY

APPROX. C	3RD CLUSTER	$\tilde{u}(x, y)_C^{III}$
APPROX. C	2ND CLUSTER	$\tilde{u}(x, y)_C^{II}$
APPROX. C	1ST CLUSTER	$\tilde{u}(x, y)_C^I$
APPROX. C	EQUAL SPACE	$\tilde{u}(x, y)_C$
ANALYTIC		$u(x, y)$

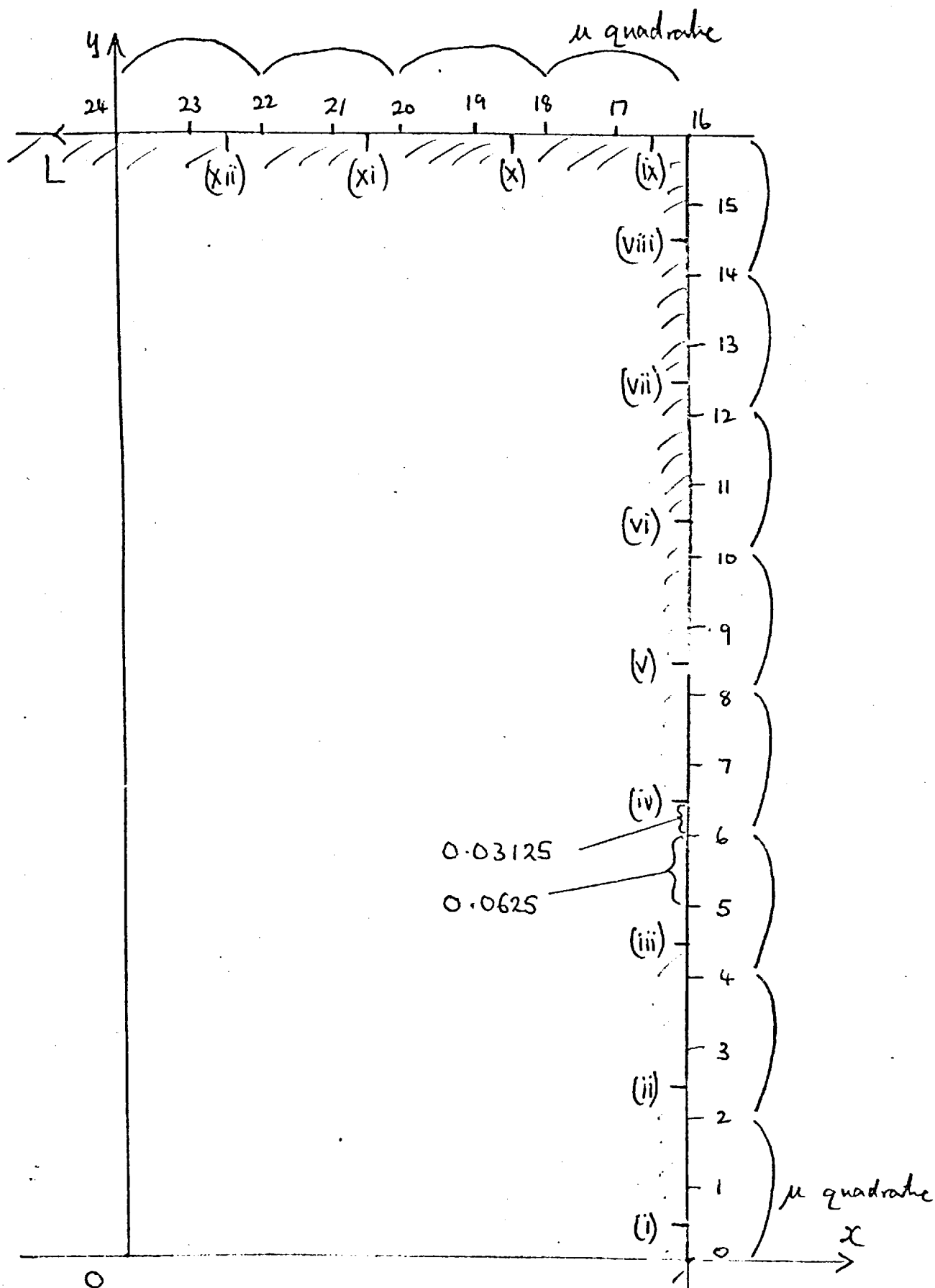
(0.1875, 1.0)	(0.25, 1.0)	(0.3125, 1.0)	(0.375, 1.0)	(0.4375, 1.0)	(0.5, 1.0)
- 024 - 012 004 ✓ X 012	015 014 003 ✓ X 026	- 008 - 019 - 007 ✓ X 052	- 038 - 017 002 ✓ X 140	- 032 - 031 - 009 ✓ - 050	(0.5, 0.9375)
	- 002 - 001 060 ✓ X 022	- 008 - 007 - 001 ✓ X 032	- 015 - 011 - 003 ✓ X 025	- 014 - 010 - 007 ✓ X 055	(0.5, 0.875)
		- 005 - 004 - 001 ✓ X 015	- 007 - 005 - 002 ✓ X 006	- 006 - 005 - 003 ✓ X 013	(0.5, 0.8125)
			- 003 - 002 000 ✓ X 004	- 003 - 002 - 001 ✓ - 002	(0.5, 0.75)
				000 000 000 ✓ X 001	(0.5, 0.6875)

10. TABLE OF ERRORS IN $\tilde{u}(x, y)$

KEY.

$[\tilde{u}(x, y)_c^{III} - u(x, y)] \times 10^6$
$[\tilde{u}(x, y)_c^{II} - u(x, y)] \times 10^6$
$[\tilde{u}(x, y)_c^I - u(x, y)] \times 10^6$
$[\tilde{u}(x, y)_c - u(x, y)] \times 10^6$

✓ = OPTIMUM RESULT



POSITION OF NODES $0 \rightarrow 24$
 and POSITION OF POINTS ON L AT WHICH $\tilde{u}(x,y)$ IS CALCULATED (i) \rightarrow (xii)

(i) Exact 0.125488
 Approximate 0.125488
 |Error| zero

(ii) Exact 0.137207
 Approximate 0.137206
 |Error| 1.0×10^{-6}

(iii) Exact 0.164551
 Approximate 0.164549
 |Error| 2.0×10^{-6}

(iv) Exact 0.207520
 Approximate 0.207517
 |Error| 3.0×10^{-6}

(v) Exact 0.266113
 Approximate 0.266111
 |Error| 2.0×10^{-6}

(vi) Exact 0.340332
 Approximate 0.340331
 |Error| 1.0×10^{-6}

(vii) Exact 0.430176
 Approximate 0.430170
 |Error| 6×10^{-6}

(viii) Exact 0.535645
 Approximate 0.534991
 |Error| 654.0×10^{-6}

(ix) Exact 0.609863
 Approximate 0.606337
 |Error| 3526.0×10^{-6}

(x) Exact 0.559082
 Approximate 0.558946
 |Error| 136.0×10^{-6}

(xi) Exact 0.523926
 Approximate 0.523888
 |Error| 38.0×10^{-6}

(xii) Exact 0.504396
 Approximate 0.504384
 |Error| 12×10^{-6}

II. TABLE OF MAXIMUM ERRORS $|u(t_i) - \tilde{u}(t_i)|$

- [1] V.C.A. Ferraro "Electromagnetic Theory", Athlone Press, 1954.
- [2] O.D. Kellogg "Foundations of Potential Theory",
Dover Publications Ltd., 1953.
- [3] R.Courant and D.Hilbert "Methods of Mathematical Physics" Vol.II,
Wiley Interscience Publishers, 1965.
- [4] T.M.Apostol "Mathematical Analysis" Addison Wesley, 1957.
- [5] S.G.Mikhlin "Integral Equations" Pergamon Press, 1963.
- [6] N.I.Muskhelishvili "Singular Integral Equations" Noordhoff,
Holland, 1953.
- [7] L.M.Milne-Thomson "Plane Elastic Systems", Springer-Verlag, 1960.
- [8] E.Hille "Analytic Function Theory", Blaisdell New York, 1959.
- [9] B.L.Moiseiwitsch "Integral Equations" Longman Mathematical Texts, 1977.
- [10] W.V.Lovitt "Linear Integral Equations", Dover Publications Ltd. 1950.
- [11] F.Riesz and B.Sz.-Nagy "Functional Analysis" Ungar Publishing Co.
New York, 1971.
- [12] { M.A.Jaswon 1963 Proc.Roy.Soc. A(275) (pp.23-32)
G.T.Symm 1963 Proc.Roy.Soc. A(275) (pp.33-46)
- [13] V.D.Kupradze "Potential Methods in the Theory of Elasticity"
Israel Program for Scientific Translations, Jerusalem, 1965.
- [14] J.Radon. 1919 Akad. Wiss. Wien, (128) (pp.1123-1167).
- [15] J.Benveniste 1967 Siam.J.Appl.Maths.,Vol.15,No.3 (pp.558-568).
- [16] C.Neumann Leipzig, 1877.
- [17] E.Goursat "A Course in Mathematical Analysis" Vol.III, Part I,
Dover Publications Ltd., 1964
- [18] L.V.Kantorovich and V.I.Krylov "Approximate Methods of Higher
Analysis" Noordhoff, Holland 1964.
- [19] L.M.Delves and J.E.Walsh "Numerical Solution of Integral Equations",
Clarendon Press, Oxford, 1974.
- [20] G.T.Symm, 1973, N.P.L. Report NAC 31.
- [21] K.E.Atkinson, 1972, Siam.J.Numer.Anal. Vol.9,No.2 (pp.284-299).

- [22] P.Lancaster "Theory of Matrices", Academic Press, 1969.
- [23] B.Noble "Topics in Numerical Analysis" Ed. by J.J.H.Miller,
Academic Press, 1973.
- [24] B.Z.Vulikh "Introduction to Functional Analysis", Pergamon Press, 1963.
- [25] P.N.Swartztrauber, 1972, Siam.J.Numer.Anal.Vol.9, No.2, (pp.300-306).
- [26] D.Becker, Undergraduate Project, Mathematics Degree, Thames Polytechnic
1975.
- [27] P.M.Anselone "Collectively Compact Operator Approximation Theory",
Prentice Hall, 1971.